pmod wrc

WMO

International Pyrheliometer Comparison

IPC-XI

27. Sep - 15. Oct 2010
Davos, Switzerland

IOM report No. xx
WMO/TD No. xxxx
2011

WMO International Pyrheliometer Comparison
IPC-XI
27 September - 15 October 2010
Davos, Switzerland

Final Report

Wolfgang Finsterle

PMOD/WRC Internal Report, Davos, July 2011

Contents

Chapter 1 Organization and Procedures

1.1 Introduction

The 11^{th} International Pyrheliometer Comparison (IPC-XI) was held together with Regional Pyrheliometer Comparisons (RPCs) of all WMO Regional Associations (RA I to RA IV) from 27 September through 15 October 2010 at the Physikalisch-Meteorologisches Observatorium Davos/World Radiation Centre (PMOD/WRC) in Davos, Switzerland.

The results presented in this report are based on the measurements carried out during the three weeks assigned to the IPC-XI. The favorable weather conditions allowed to acquire a large number of calibration points for most participating instruments. Cloudy and overcast days were used for technical preparations and training of participants as well as for a the IPC-XI symposium and Course on Radiation Measurement. A Saharan Dust Event (SDE) affected the measurements during several days starting October 8^{th}. Analyzing the effect of the SDE on different types of instruments led to interesting findings which are summarized in dedicated section of this report.

1.2 Participation

Representatives from 17 Regional and 22 National Radiation Centers as well as 14 manufacturers and other institutions took part in the comparison. Additionally, two institutions who did not send a representative had their pyrheliometers operated by other participants, resulting in 88 participants operating 95 pyrheliometers from 42 countries. The six World Standard Group (WSG) and 24 additional pyrheliometers, including the new Cryogenic Solar Absolute Radiometer (CSAR), were operated by the WRC staff. A representative of WMO was attending during the first couple of days of IPC-XI.

Table 1.1: IPC-XI Participation: *World, Regional and National Radiation Centers*

Country	*Type*	*Institution*	*Operator(s)*	*Instrument(s)*
World Radiation Center				
Switzerland	WRC	Physikalisch-Meteorologisches Observatorium Davos/ World Radiation Center, Davos	W. Finsterle A. Fehlmann J. Gröbner W. Schmutz M. Suter C. Thomann C. Wehrli R. Winkler (NPL)	**PMO2** **PMO5** **CROM2L** **PAC3** **HF18748** **MK67814** CIMEL 0501657 31144E6 DARA A, B, C EPAC11402 CH1 970147 PMO6-0401 PMO6-79-122 PMO6-80022 AHF32455 CSAR PMO6-0101 PMO6-0401 PMO6-0801 PMO6-0803 PMO6-0810 PMO6-0811 PMO6-0812 PMO6-0813 PMO6-0814 PMO6-0815 PMO6-0816 PMO8-P01 SIAR-2A SIAR-2B
RA I				
Algeria	RRC	Office National de Météorologie, Tamanrasset	B. Ouchene	HF 29225
Kenya	NRC	Kenya Meteorological Dept., Nairobi	P. Sira	Å13444
Morocco	NRC	Meteo Maroc, Casablanca	M. Badrane	CH1 080004
Mozambique	NRC	National Inst. of Meteo, Maputo	A. M. Mandlate	Å26835 CH1 950086 31822E6

Table 1.1: (continued)

Country	*Type*	*Institution*	*Operator(s)*	*Instrument(s)*
Nigeria	RRC	Nigerian Meteorol. Agency, Abuja	I. D. Nnodu K. S. Muyiolu	Å 576
South Africa	NRC	CSIR, Pretoria, Gauteng	M. Lysko S. Mulaudzi	AHF 31117
Sudan	NRC	Sudan Meteorological Authority, Karthoum	Y. Odan	NIP 28330
RA II				
China	NRC	CMA, Beijing	Yang Yun Quan Jimei Luo Chang	PMO6-850406 AHF 36011
India	RRC	Central Radiation Laboratory, Pune, Maharashtra	R. J. Sharma	AHF 18742
Japan	RRC	JMA, Tokyo	O. Ijima	PMO6-0403 HF 32446
Philippines	NRC	Philippine Atmospheric, Geophys. and Astron. Services PAGASA, Diliman, Quezon City	V. Esquivel	Å12578
Thailand	NRC	Thai Meteorological Department, Bangkok	W. Subwat	HF 27796
RA III				
Argentina	RRC	Servicio Meteorologico Nacional, Buenos Aires	G. Carbajal Benitez	AHF 29225
Chile	RRC	Dirección Meteorológica Chile, Santiago	P. Mostraj	PMO6-850410
Colombia	NRC	IDEAM, Bogotá	F. J., Bernal Garcia	PMO6-79-123
Peru	RRC	SENAMHI, Lima	E. Villegas	Å18020
RA IV				
Canada	RRC	Environment Canada, Wilcox, Saskatchewan	O. Niebergall D. Halliwell I. Abboud	HF 18747 HF 20406 AHF 34320 AHF 34321
Mexico	RRC	Instituto de Geofísica, UNAM México	D. Riveros	HF 29223

Table 1.1: (continued)

Country	*Type*	*Institution*	*Operator(s)*	*Instrument(s)*
USA	RRC	NOAA/ESRL/GMD, Boulder	D. Nelson J. Michalsky J. Wendell G. Hodges	HF 28553 AHF 32448 AHF 30710 AHF 28553 TMI 67502
RA V				
Australia	RRC	Bureau of Meteorology, Melbourne	B. Forgan M. Milner	HF 27160 TMI 69137
RA VI				
Austria	NRC	ZAMG, Vienna	M. Mair	TMI 68025 CHP1 100245
Belgium	RRC	Royal Meteorological Institute, Uccle	A. Chevalier S. Dewitte S. Bali L. Gonzales P. Malcorps	CR09L CR09R
Croatia	NRC	Meteorological and Hydrological Service, Zagreb	K. Premec	CH1 940072 CHP1 100288
Czech Republic	NRC	Czech. Hydromet. Institute, Hradec Kralove	J. Pokorny	HF 30497
Estonia	NRC	Estonian MH Inst, Tallin	A. Kallis	PMO6-850405
France	RRC	Météo-France-Centre Radiométrique, Carpentras-Serres	J.-P. Morel	TMI 68016
Germany	RRC	DWD/MOL-RAO, Tauche -OT Lindenberg	K. Behrens	HF 27157 PMO6-5 PMO6-0405
Hungary	RRC	Hungarian Met. Service, Budapest	S. Varga-Fogarasi Z. Nagy	HF 19746
Israel	NRC	Israel Meteorological Service, Bet-Dagan	A. Baskis	HF 27162
Lithuania	NRC	Lithuanian HMS, Vilnius	D. Mikalajunas	PMO6-0804
Norway	NRC	Geophys. Inst, Bergen	J. A. Olseth	EPAC 13617
Poland	NRC	Institute of Meteorology and Water Management, Warsaw	B. Bogdañska	HF 30716
Romania	NRC	National Meteorological Administration, Bucharest	C. Oprea	Å702

Table 1.1: (continued)

Country	*Type*	*Institution*	*Operator(s)*	*Instrument(s)*
Russia	RRC WRDC	Voeikov MGO, St. Petersburg	A. Pavlov	Å212
Slovakia	NRC	Slovak Hydrometeorological Institute, Bratislava	M. Chmelik	Å13439
Spain	NRC	CIEMAT, Madrid	I. Rodriguez Outon	AHF 28486 PMO6-0301
Sweden	RRC	SMHI, Norrköping	T. Carlund J.-E. Karlsson	PMO6-811108 AWX 33393
The Netherlands	NRC	KNMI, De Bilt	W. Knap C. van Oort	HF 27159 CH1 020283
United Kingdom	NRC	Met Office, Exeter, Devon	P. Fishwick L. Green	TMI 67604 HF 31110

Table 1.2: IPC-XI Participation: *Various Institutions and Manufacturers*

Country	*Institution*	*Participant(s)*	*Instrument(s)*
China	CIOMP, Changchun, Jilin	Yu Peng Wang Xin Ye Dong Jun Yang	SIAR-1 SIAR-2c
Italy	European Commission JRC, Ispra, Varese	W. Zaaiman T. Sample A. Colli	PMO6-81109 PMO6-911204 21451E6 25738E6 CH1 060460 CH1 930018 TMI 68835
Russia	VNIIOFI, Moscow	S. Morozova M. Pavlovich V. Pavlovich	MAR-1-1 MAR-1-2 MAR-1-3
Sweden	SP Swedish National Testing and Research Institute, Borås	S. Källberg A. Andersson	HF 15744
Thailand	Solar Energy Research Lab., Silpakorn University, Muang, Nakhon Pathom	I. Masiri R. Wattan J. Somchit	AHF 32454

Table 1.2: (continued)

Country	*Institution*	*Participant(s)*	*Instrument(s)*
The Netherlands	EKO Instruments Europe B.V., Leiden	A. Los K. Hoogendijk E. Worrell A. Akihito	PMO6-850402 MS54-S07122 PMO6-0802 (for CRP Tudor, Luxembourg)
The Netherlands	Hukseflux Thermal Sensors, Delft	K. van den Bos J. Konings	DR018117 CP01P CP01T CP01U
The Netherlands	Kipp & Zonen BV, Delft	J. Mes I. Staupe	PMO6-cc 103 CH1 940068 CHP1 REF1
USA	ACRF, Billings OK	C. Webb	–
USA	ATLAS Weathering/DSET Laboratories, Phoenix AZ	E. Naranen	AHF 17142
USA	LASP, Boulder, CO	G. Kopp K. Heuermann	TIM-Witness
USA	NASA Langley, Hampton VA	F. Denn	AHF 31041 AHF 31105
USA	National Renewable Energy Lab., Golden CO	I. Reda T. Stoffel	AHF 23734 AHF 28968 AHF 29220 AHF 30713 TMI 68018
USA	The Eppley Laboratory Inc., Newport RI	J. R. Hickey T. Kirk	AHF 14915 AHF 27798 AHF 33396 (for AIST Japan)

1.3 Data Acquisition and Evaluation

The signals from the WSG instruments and additional WRC radiometers were acquired by a new data acquisition system based on 17 National Instruments PXI-4065 6.5-digit digital multimeters with NI PXI-2501 24-channel multiplexers. The system was controlled by a LabView application running on an industrial PC and operated flawlessly. The LabView application also triggered the timing signals as well as the initialization and readout of the data entry form for manually operated instruments (see below). The major operational advantage of this new system lies in the improved flexibility to add/remove instruments on the fly and to analyze data in near-real-time, allowing to quickly detect and fix potential problems with participating instruments, without loosing an entire day worth of measurements.

The participating instruments were operated with their standard pointing and data acquisition equipment, either manually or automated.

The data from the manually operated instruments were typed into a java based data entry form by the operator. WLAN connections were used to initialize the web interface and to dump its content to the central data acquisition computer at end of each measurement series. Participants could start the data entry form either on their own laptop computer or borrow one from the WRC. They were also required to keep written records as a backup copy of their data and to double-check for typing errors in the web interface.

The data from computer controlled instruments (synchronized to the timing of the IPC's measurement series) had to be written to ASCII files containing the instrument's serial number in the header and three columns for date, time, and irradiance, respectively. The ASCII files were then either up-loaded to a dedicated directory on the IPC-XI FTP site or handed to the WRC staff on a USB memory stick. All data were ingested into the data acquisition and evaluation system at the end of each measurement day.

1.3.1 Timing of the Measurements

The measurements were taken in series of 21 minutes with a basic cadence of 90 seconds. Voice announcements and acoustic signals were used to inform the participants about the sequence of operation. All automated data acquisition systems were synchronized to Central European Time (CET). A network time server and a large reference clock on the measuring field were set up for this purpose. The time until the next measurement was also indicated on the web interface for manual operators. The timing for the different types of instrument was as follows:

- Ångström pyrheliometers: Before the start and after the end of the run the zero of the instrument was established. Alternating right and left strip readings were performed, starting with the right hand strip exposed to the sun. The following readings were paired as L-R, R-L, etc., yielding a total of 12 irradiance values per run.

- PAC3: the run started with the shutter closed, after $60\ \mathrm{s}$ the electrical heater[1] was turned on for $40\ \mathrm{s}$ (this was introduced after IPC-III in order to have a well defined thermal state of the instrument independent of the operation sequence before the run). At $270\ \mathrm{s}$ the zero of the thermopile was read and the heater switched on for 180 seconds. At $450\ \mathrm{s}$ the heater voltage, current and thermopile was read, the heater turned off and the shutter opened. Starting at $540\ \mathrm{s}$ readings were taken every $90\ \mathrm{s}$ yielding 8 irradiance values per run. After the last reading the shutter was closed.

- HF- and TMI-type pyrheliometers: the run started with the shutter closed, after $90\ \mathrm{s}$ the thermopile zero was read and the electrical heater[1] turned on until at $180\ \mathrm{s}$ the voltage, current and thermopile were read. The heater was then switched off and the shutter opened. From $270\ \mathrm{s}$ onward the thermopile signal was recorded every $90\ \mathrm{s}$ yielding 11 irradiance values per run. Some automated instruments performed the electrical calibration in between the series and/or read the irradiance every 30 seconds, consequently providing up to 39 irradiance values per run.

[1] The heater voltage was manually selected before each run to match the expected level of solar irradiance.

- PMO-, SIAR- and CROM-type pyrheliometers: the run started with a reference phase (shutter closed) of $90\ \mathrm{s}$, followed by a measurement phase (shutter open) of $90\ \mathrm{s}$. This sequence was repeated for the next 18 minutes. A total of 6 open and 7 closed readings were taken yielding a total of 6 irradiance values during a run. PMO2 was read at twice that pace, with a reference phase of $45\ \mathrm{s}$ and a measurement phase of $45\ \mathrm{s}$, producing 13 irradiance values per run so that for all readings of the basic sequence a PMO2 irradiance was available.

- Normal Incidence Pyrheliometers (NIP, CH1, etc.): These pyrheliometers recorded 12 irradiance values every $90\ \mathrm{s}$ after an initial zero reading at 90 seconds. Some instruments omitted the initial zero reading, thus yielding 13 irradiance readings.

- Other pyrheliometers: Prototype instruments such as the CSAR, DARA or TIM-Witness were using various modes of operation which are specific to their design. They all share the principle of electrical substitution and were synchronized to the 90-seconds base cadence.

1.3.2 Data Evaluation

For each instrument the irradiance was obtained with the appropriate evaluation procedure as listed below. After each day a graphical print-out of the ratios to PMO2 was put on display in the "Data Center" room to be reviewed by the participants. This simple but effective measure of quality control revealed instrumental problems in several cases which subsequently could be fixed quickly.

"Quick-look" print-outs were also produced during the day when an instrument was suspected to malfunction.

The procedure used to calculate the irradiance S of each instrument type is described below. The notations are:

V_{th}	output of the thermopile
U_h, U_i	voltage across the heater (h) or across the standard resistor (i)
R_n	standard resistor
C_1	calibration factor
C_2	correction factor for lead heating
P	electrical power in the active cavities

- Ångström-pyrheliometers: the current through the right or left strip was measured as voltage drop across a standard resistor and the irradiance was obtained as:

$$S = C_1 \frac{U_i(\text{left}) U_i(\text{right})}{R_n^2}$$

  This corresponds to the geometric mean of the irradiances at the time of right and left readings. Thus, the ratio to WRR was calculated using the geometric mean of the WSG irradiances at the corresponding instances.

- PAC3, HF, and TMI type pyrheliometers: the irradiance was calculated from the thermopile output $V_{th}(\text{irrad})$ when the receiver was irradiated. The sensitivity was determined by the calibration during which the cavity was shaded and electrically heated and U_h and U_i were measured together with the corresponding thermopile output $V_{th}(\text{cal})$. Furthermore, the zero of the thermopile $V_{th}(\text{zero})$ was measured and subtracted from all thermopile readings.

$$S = C_1 \frac{V_{th}(\text{irrad}) - V_{th}(\text{zero})}{V_{th}(\text{cal}) - V_{th}(\text{zero})} \frac{U_i}{R_n} \left(U_h - \frac{U_i}{R_n} C_2 \right)$$

- PMO-, SIAR- and CROM-type pyrheliometers: the irradiance was obtained from P(closed) averaged from the closed values before and after the open reading P(open).

$$S = C_1(P(\text{closed}) - P(\text{open}))$$

The power calculation was done according to the prescription of the instrument type with

$$P = U_h^2 \qquad \text{or} \qquad P = U_h U_i \qquad \text{or} \qquad P = U_h \frac{U_i}{R_n}$$

The SIAR-type radiometers slightly deviate from this scheme in that they subtract the open power from the *preceding* closed power rather than the average of the preceding and successive closed reading.

- Normal Incidence Pyrheliometer (NIP, CH1, etc.): the thermopile reading was divided by the calibration factor after subtraction of the zero point reading[1].
- PMO2: As during preceding IPCs, PMO2 was used as the reference instrument for the daily summaries because it can be operated fast enough to provide an irradiance value every 90 seconds. The values of PMO2 were obtained with the algorithm for PMO-type pyrheliometers. At the end of the open phase, 6 readings were taken in rapid succession within about two seconds. The standard deviation of the 6 readings was used during the final evaluation as a quality control parameter to assess the atmospheric stability during each acquisition sequence (see Sect. 2.1).

1.3.3 Auxiliary Data

The meteorological parameters (air temperature, relative humidity, atmospheric pressure) were obtained from the MeteoSwiss' automated weather station SwissMetNet located at PMOD/WRC (see Sect. 4.2). Wind speed and direction sensors were set up at the south and west corners of the measuring field as well as by the WSG tracker.

A cloud sensor flagged all data points when clouds were within 15 degrees of the Sun. The flagged points were not used to evaluate Ångstrom type pyrheliometers.

Precision Filter Radiometers (PFR) were used to determine Aerosol Optical Depth (AOD) at four wavelengths (367.6 nm, 412.0 nm, 501.2 nm, and 862.4 nm, see Sect. 4.3).

The measurements and inversion results (mainly scattering phase functions) from the Aerosol Robotic Network (AERONET) Davos station (located at PMOD/WRC) were used to correct for aureole effects (circumsolar radiation) in cavity pyrheliometers according to their view-limiting geometry[2].

1.4 Approvement and Dissemination of the Results

According to Resolution 1 of CIMO-XI an Ad-hoc Group was established to discuss the preliminary results of the IPC-XI, based upon criteria defined by the WRC, evaluate the above reference and recommend the updating of the calibration factors of the participating instruments. It was chaired by the Bruce W. Forgan, (Australia, RA V) and composed as follows: Kolawole Muyiolu (Nigeria, RA I), Meena Lysko (South Africa, RA I), Rajendra Sharma (India, RA II), Pedro Mostraj Aquilera (Chile, RA III), David Halliwell (Canada, RA IV), Don Nelson (USA, RA IV), Thomas Carlund (Sweden, RA VI), Martin Mair (Austria, RA VI), Krunoslav Premec (Croatia, RA VI). The WRC was represented by Wolfgang Finsterle.

The procedures used to compute the new WRR factors of the WSG and participating instruments are explained in Section 2.2.

[1] Some operators assumed a vanishing zero signal. They did not perform zero readings.

[2] The WMO CIMO Guide (WMO-No. 8) definition for *direct solar radiation* explicitly *includes* an aureole component. As to the view-limiting geometry the CIMO Guide further recommends "[...] that the opening half-angle be 2.5° and the slope angle 1°". We therefore apply a correction to *reduce* the aureole effect to the recommended view-limiting geometry. For instruments which obey the CIMO recommendations this correction vanishes (c.f. Sect. 2.5).

Chapter 2 Measurements and Results

Measurements were taken on 14 days (2010 September 28, October 2, 3, 4, and 6 - 15). October 8^{th} and 12^{th} were the most productive days, each yielding 17 series' of 21 minutes duration. In total 164 series' were acquired. All data from September 28^{th} (1 series), October 2^{nd} (10 series'), 4^{th} (3 series'), and 6^{th} (15 series') were rejected due to bad or unstable weather conditions on those days. Of the remaining days all data points that satisfy the following data selection criteria were considered in the final evaluation.

2.1 Data Selection Criteria for the Final Evaluation

The Ad-hoc Group responsible for the approval of the final evaluation procedure (c.f. Sect. 1.4) agreed on the following criteria for the acceptance of IPC-XI data:

1. Any series or part there-of were the field of view of Angstrom pyrheliometers is obscured by local topographic features (e.g. mountain sides) shall not be considered as valid data.
2. That no measurements be used for Angstrom pyrheliometers if a cloud is within 15 degrees of the sun. No measurements will be used for the absolute cavity radiometers (field of view = 5 degrees) if a cloud is within 8 degrees of the sun.
3. That no measurements be used if the wind speed is greater than 2.5 m/s.
4. That no data be used if the 500 nm AOD is greater than 0.120.
5. That an individual point be excluded from the series if the variation of the 8 fast PMO2 measurements is greater than 0.5 Wm-2.
6. That a minimum of 150 acceptable data points be taken by PMO2 over a minimum of three days during the comparison period. $0.5\,\mathrm{Wm}^{-2}$.
7. That the minimum number of acceptable data points be 150 for the PMO2 taken over a minimum of three days during the comparison period.

2.2 Computation of the New WRR Factors

2.2.1 WSG Instruments

The WRR factor $WRR_{i,IPC}$ for the WSG instrument i, $i \in$ {PMO2, CROM2L, MK67814, HF18748, PAC3, PMO5}, by definition is the ratio of the WRR to the WSG instrument i averaged over the duration of the IPC:

$$WRR_{i,IPC-XI} = \left\langle \frac{WRR(t)}{WSG_i(t)} \right\rangle_t ,$$

where $WRR(t)$ and $WSG_i(t)$ are the reference irradiance and the irradiance measured by WSG instrument i at the time t, and $\langle x(t) \rangle_t$ denotes the temporal average of $x(t)$. The reference irradiance (WRR) is defined as the mean value of the simultaneous readings of at least four WSG instruments, multiplied by their corresponding WRR factors from the previous IPC. Because the ratios of PAC3 and

Table 2.1: New WRR-factors for the WSG instruments computed using PMO2, PMO5, CROM2L, and MK67814 and the IPC-X WRR-factors.

Instrument	*WRR factor IPC-X*	**WRR factor IPC-XI**	*Standard Uncertainty* $\frac{\sigma}{\sqrt{N-1}}$*[ppm]*	*# of points N*	*Change [ppm] IPC-XI - IPC-X*
PMO2	0.998618	**0.998623**	29	554	5
PMO5	0.998982	**0.999052**	22	554	70
CROM2L	1.002998	**1.003157**	21	544	159
MK67814	1.000708	**1.000458**	21	497	-250
PAC3	1.001116	**1.002117**	26	381	1000
HF18748	0.996274	**0.997138**	26	493	867

HF18748 with respect to the WRR suffered from inexplicable jumps during the past five years these two instruments were not used to compute the reference irradiance during IPC-XI. With $j \in$ {PMO2, CROM2L, MK67814, PMO5} we calculate the reference irradiance as

$$WRR(t) = \langle WSG_j(t) * WRR_{j,IPC-X} \rangle_j .$$

We thus get

$$WRR_{i,IPC-XI} = \left\langle \frac{\langle WSG_j(t) * WRR_{j,IPC-X} \rangle_j}{WSG_i(t)} \right\rangle_t ,$$

where $i \in$ {PMO2, CROM2L, MK67814, HF18748, PAC3, PMO5} and $j \in$ {PMO2, CROM2L, MK67814, PMO5}.

2.2.2 Participating Instruments

For each participating instrument k the new WRR factor is calculated according to

$$WRR_{k,IPC-XI} = \left\langle \frac{WRR(t)}{Irr_k(t)} \right\rangle_t ,$$

where $Irr_k(t)$ is the irradiance measured by the instrument k at the time t and $WRR(t)$ the coinstantaneous reference irradiance.

Temporal averaging is done by fitting a gaussian to the distribution of WRR-to-instrument ratios. Outliers are sucessively removed until the ratios are normally distributed with a probability higher than 90%, or until all ratios are within a certain range of their arithmetic mean value[1].

The new WRR factors for the WSG and all participating instruments are listed in Table 2.2.

2.3 Status of the WSG and Transfer of the WRR

The main objective of the periodic IPC's is the dissemination of the World Radiometric Reference (WRR) in order to ensure worldwide homogeneity of meteorological radiation measurements. The

[1] This threshold range ususally is ± 0.002 for cavity pyrheliometers. However, for most Ångströms, NIP's and some cavities a different range had to be chosen manually in order to make the most plausible selection of data points.

WRR is realized by the WSG which is frequently inter-compared at PMOD/WRC to detect possible deviations of individual radiometers with respect to the group average and to ensure the stability of the WRR. In addition to this internal stability check the stability of the WRR is assessed during IPCs by comparing the WSG to other pyrheliometers that have participated in previous IPC's.

Since IPC-X, which was held in 2005, two member instruments of the WSG failed in internal stability checks. The instrument HF18748 suffered from several sensitivity drops of up to -0.1%. The sensitivity of PAC3 also dropped sharply by $\sim 0.05\%$ in summer 2011. Non-intrusive checks of both instruments did not reveal any contamination in their cavities.

The WRR factors of the remaining four WSG instruments (PMO2, PMO5, CROM2L, MK67814) changed by less than ± 50 ppm per year. These instruments are considered stable over the past five years and were used to calculate the new WRR.

Table 2.2: The new WRR factors for the participating instruments

Instrument	C_1	C_2	**WRR Factor**	σ [ppm]	*N used*	*N tot*	*Country/ Owner*
0501657	7.50000	0.000	**1.014357**	10310	551	4382	WRC
080002	9.62000	0.000	**1.000254**	1668	547	4382	Spain
080004	10.2100	0.000	**1.007385**	4436	417	1389	Morocco
080015	7.80000	0.000	**0.997799**	1675	554	4217	Spain
0804	51397.2	0.000	**0.999914**	645	364	696	Lithuania
090090	8.10000	0.000	**1.003663**	1187	554	4217	Spain
21451E6	8.42000	0.000	**0.999193**	7691	453	2719	JRC Italy
25738E6	7.92000	0.000	**0.998843**	6621	453	2719	JRC Italy
28335	8.33000	0.000	**1.009038**	5364	424	1549	Sudan
31144E6	8.04000	0.000	**0.997184**	5636	554	4382	WRC
79-122	600.000	0.000	**0.999401**	638	540	982	WRC
79-123	601.610	0.000	**0.937200**	6131	344	531	Columbia
80022	597.875	0.000	**1.003082**	538	493	982	WRC
850402	24.0720	0.000	**1.003330**	1230	102	169	EKO The Netherlands
850405	24.1940	0.000	**1.000565**	1609	420	705	Estonia
850409	24.0780	0.000	**1.004183**	574	539	982	ESA/ESTEC The Netherlands
970147	11.1500	0.000	**0.996057**	1745	554	4382	WRC
A12578	4465.90	0.000	**1.008580**	4558	134	437	Philippines
A13439	4426.32	0.000	**1.001350**	1468	396	1208	Slovakia
A13444	6.21000	0.000	**1.036795**	3545	312	1172	Kenya
A18020	4647.26	0.000	**1.002650**	1468	323	905	Peru
A212	10556.0	0.000	**0.996482**	3117	258	616	Russia
A26839	8.11000	0.000	**1.007547**	2069	361	1149	Mozambique
A576	5885.13	0.000	**0.990369**	4001	382	1318	Nigeria
A702	6177.80	0.000	**0.998769**	4794	373	1209	Romania
AHF-AWX34320	1.00000	0.000	**0.992830**	845	442	4774	Canada
AHF-AWX34321	1.00000	0.000	**0.994550**	847	442	4774	Canada
AHF14915	20010.0	0.000	**0.999682**	920	392	5331	Eppley USA
AHF17142	19959.0	0.000	**0.998358**	909	397	4788	ATLAS-DSET USA
AHF18742	20089.3	0.066	**1.002281**	2277	361	1252	India
AHF23734	1.00000	0.000	**0.998281**	660	412	5549	NREL USA

Table 2.2: (continued)

Instrument	C_1	C_2	**WRR Factor**	σ [ppm]	*N used*	*N tot*	*Country/ Owner*
AHF27798	20020.0	0.000	**0.999018**	990	395	5331	Eppley USA
AHF28486	1.00000	0.000	**0.997308**	674	422	4899	Spain
AHF28553	19986.0	0.000	**0.996842**	932	463	8223	NOAA USA
AHF28968	19980.2	0.000	**0.997734**	657	420	5549	NREL USA
AHF29220	19999.0	0.000	**0.997691**	670	418	5549	NREL USA
AHF29223	19998.0	0.066	**0.997352**	741	384	1458	Mexico
AHF29225	20004.2	0.000	**0.996896**	1029	336	1240	Algeria
AHF30112	19936.7	0.000	**1.011725**	1972	74	546	Argentina
AHF30713	19989.0	0.000	**0.997548**	680	421	5549	NREL USA
AHF30716	20009.2	0.066	**0.997136**	657	360	1042	Poland
AHF31041	19999.2	0.000	**0.996286**	701	441	5162	NASA Langley USA
AHF31105	1.00000	0.000	**0.999964**	707	431	5123	NASA Langley USA
AHF31110	19989.0	0.066	**0.996431**	629	399	1268	UK
AHF31117	1.00000	0.000	**0.998861**	641	401	4091	South Africa
AHF32446	19986.9	0.000	**1.000046**	745	444	1694	Japan
AHF32455	20009.2	0.000	**1.000276**	595	401	6672	WRC
AHF33396	1.00000	0.000	**0.998079**	926	396	5330	AIST Japan
AHF36011	1.00000	0.000	**0.996933**	2198	367	1454	China
AHF36013	1.00000	0.000	**1.058115**	2327	384	9430	Thailand
AWX31114	1.00000	0.000	**1.001244**	891	462	8604	NOAA USA
AWX32448	1.00000	0.000	**0.999939**	1149	465	8616	NOAA USA
AWX33393	2.00090	0.000	**0.999362**	819	427	5715	Sweden
CH1020283	1.00000	0.000	**0.997677**	1426	516	1776	KNMI The Netherlands
CH1060460	10.0700	0.000	**1.002334**	2034	449	2759	JRC Italy
CH1930018	10.8500	0.000	**1.000748**	3256	453	2759	JRC Italy
CH1940068	10.3700	0.000	**0.997717**	955	147	1904	K&Z The Netherlands
CH1940072	10330.0	0.000	**1.007576**	2507	439	4940	Croatia
CH1950086	1.00000	0.000	**1.005036**	1316	329	5776	Mozambique
CHP100288	1.00000	0.000	**0.999634**	1924	434	4940	Croatia
CHP1100245	1.00000	0.000	**1.000486**	1413	449	5333	Austria
CHP1REF1	7.92000	0.000	**0.997956**	1900	179	2268	K&Z The Netherlands
CP01P	1.00000	0.000	**1.021933**	885	47	234	Hukseflux The Netherlands
CP01T	1.00000	0.000	**1.008928**	629	47	286	Hukseflux The Netherlands
CP01U	1.00000	0.000	**1.018302**	1772	49	286	Hukseflux The Netherlands
CR09L	12780.9	0.000	**0.998363**	882	220	407	Belgium
CROM2L	127.687	0.000	**1.003157**	449	544	892	WRC
CSAR	1.00000	0.000	**0.992123**	519	28	2811	WRC
DARAAREFB	1.00000	0.000	**1.004210**	843	143	1859	WRC
DARAAREFC	1.00000	0.000	**1.004358**	1260	141	1278	WRC

Table 2.2: (continued)

Instrument	C_1	C_2	**WRR Factor**	σ [ppm]	*N used*	*N tot*	*Country/ Owner*
DARABREFC	1.00000	0.000	**1.006060**	1330	214	2612	WRC
DARACREFB	1.00000	0.000	**1.004984**	1161	143	1859	WRC
DR018117	1.00000	0.000	**1.025037**	1550	49	286	Hukseflux The Netherlands
EPAC11402	10024.0	0.000	**1.000684**	2017	145	5099	WRC
EPAC13617	10046.9	0.064	**1.001243**	1448	385	1187	Norway
HF15744	20020.0	0.000	**0.998085**	708	303	1117	Sweden
HF18747	20014.0	0.000	**1.001865**	729	483	5125	Canada
HF18748	19989.0	0.070	**0.997138**	571	493	5058	WRC
HF19746	20013.8	0.066	**0.998886**	811	262	718	Hungary
HF20406	20038.0	0.000	**1.002435**	869	477	5086	Canada
HF27157	20037.6	0.000	**0.999647**	1469	394	1172	Germany
HF27159	20030.0	0.000	**1.000021**	950	514	1797	KNMI The Netherlands
HF27160	20030.0	0.000	**0.996467**	780	468	4517	Australia
HF27162	20020.0	0.066	**0.999212**	1050	345	1049	Israel
HF27796	19986.1	0.066	**0.997204**	1112	373	1221	Thailand
HF30497	19943.8	0.000	**0.999623**	641	438	4097	Czech Republic
MAR-1-2	35600.0	0.000	**1.000116**	1048	94	157	Russia
MAR-1-3	1.00000	0.000	**0.999991**	884	92	179	Russia
MK67814	10007.0	0.000	**1.000458**	465	497	5102	WRC
MS54-S07122	1.00000	0.000	**1.003003**	1008	94	10093	EKO The Netherlands
NIP31822E6	1.00000	0.000	**0.996873**	5200	349	5776	Mozambique
PAC3	9962.60	0.070	**1.002117**	509	381	3242	WRC
PMO2	600.163	0.000	**0.998623**	692	554	11364	WRC
PMO5	2565.14	0.000	**0.999052**	528	554	982	WRC
PMO6-0101-CERNY-PS	1.00000	0.000	**1.005155**	462	437	14068	WRC
PMO6-0101-CERNY-T	1.00000	0.000	**1.004938**	502	486	7473	WRC
PMO6-0301	51161.5	0.000	**1.000588**	820	426	1126	Spain
PMO6-0401D	50000.0	0.000	**1.020979**	477	312	1075	WRC
PMO6-0405	50926.8	0.000	**0.999684**	593	414	684	Germany
PMO6-0801D	1.00000	0.000	**1.137201**	1356	484	1514	WRC
PMO6-0802	50000.0	0.000	**1.001435**	34269	161	208	Luxemburg
PMO6-0803D	51221.0	0.000	**1.000364**	473	312	1077	WRC
PMO6-0810D	50000.0	0.000	**1.018938**	499	389	1392	WRC
PMO6-0811D	51037.6	0.000	**1.000835**	541	496	1481	WRC
PMO6-0812D	50642.6	0.000	**1.004392**	668	501	1484	WRC
PMO6-0814D	51084.6	0.000	**1.002749**	743	271	865	WRC
PMO6-0815D	50972.3	0.000	**1.001582**	548	458	1565	WRC
PMO6-0816D	51022.2	0.000	**1.015310**	8442	242	594	WRC
PMO6-5	50565.5	0.000	**0.999116**	725	419	690	Germany
PMO6-81109	23.9995	0.000	**0.998577**	709	426	2758	JRC Italy

Table 2.2: (continued)

Instrument	C_1	C_2	**WRR Factor**	σ [ppm]	*N used*	*N tot*	*Country/ Owner*
PMO6-850410	609.170	0.000	**0.990890**	1155	434	1558	Chile
PMO6-911204	24.1040	0.000	**0.999711**	1049	437	2758	JRC Italy
PMO6-CC0403	50489.5	0.000	**1.000160**	732	425	773	Japan
PMO6850406	24.0008	0.000	**1.000198**	876	323	664	China
PMO8-P01	1.00000	0.000	**0.994812**	6995	497	982	WRC
PMO811108	24.1010	0.000	**1.000657**	727	417	1890	Sweden
SIAR-1A	23.6313	0.000	**1.002401**	994	440	1505	China
SIAR-2A	1.00000	0.000	**0.991696**	737	495	2107	WRC
SIAR-2B	1.00000	0.000	**1.000286**	668	427	2107	WRC
SIAR-2C	1.00000	0.000	**0.999839**	1124	441	1505	China
TIM-WITNESS	1.00000	0.000	**0.997303**	1420	278	1114	LASP USA
TMI67502	1.00390	0.000	**0.999294**	1024	454	8145	NOAA USA
TMI67604	1.00520	0.000	**0.998226**	1343	440	1589	UK
TMI68016	10031.5	0.000	**0.999858**	758	462	4918	France
TMI68018	1.00460	0.000	**0.996804**	643	415	5549	NREL USA
TMI68025	1.00200	0.000	**0.998613**	921	436	5340	Austria
TMI68835	1.00000	0.000	**1.000980**	1049	436	4686	JRC Italy
TMI69137	10020.0	0.000	**1.001752**	841	467	4520	Australia

2.4 External stability check of the WSG

In Section 2.3 the stability of the WSG was checked by analyzing the trends of individual members of the WSG with respect to the group's average. Here we present an external assessment of the stability of the WSG with respect to all cavity radiometers which have participated in at least two IPCs since 1980 (c.f. Fig. 2.1). This analysis confirms the long-term stability of the WSG within the required uncertainty level of 0.3%. Compared to last IPC (IPC-X, 2005) the WRR factors of HF-type instruments changed by -151 ppm on average. For the "SlowRad" instruments the apparent change is $+316$ ppm. The statistical uncertainties (1-σ) of these averages are 340 ppm (HF) and 960 ppm ("SlowRad"), respectively. We thus conclude that the WSG has not significantly drifted over the past five years. For completeness the history of WRR factors since 1980 (IPC-V) is given in Table 2.3 for all participating instruments. Note that in this table the raw WRR factors are listed while normalized factors were used for assessing the stability of the WSG. Normalization was necessary because some instruments used different calibration factors at different times, which produces spurious changes in their WRR factors.

Table 2.3: The history of WRR factors. In this table the raw factors are listed. They depend on the calibration constant which was used which may have changed with time. In the WSG-stability analysis presented in Section 2.4 and Figure 2.1 these factors were re-normalized accordingly.

Instrument	*IPC-V*	*IPC-VI*	*IPC-VII*	*IPC-VIII*	*IPC-IX*	*IPC-X*	*IPC-XI*
A212	1.019121	0.999320	1.001542	1.001750	1.000650	1.003381	0.996482

A576	1.020130	1.005233	1.001071	1.000460	0.997370	1.000050	0.990369
A702				1.029100	1.003940	1.005965	0.998769
A12578				1.041370	1.005990	1.006532	1.008580
A13439				1.022990	1.002370	1.003291	1.001350
A13444			1.010458				1.036800
A18020		0.998700				1.004923	1.002650
CH1940072						1.005958	1.007580
N-28335				1.003039			1.009040
EPAC11402					0.999250	1.000560	1.000680
EPAC13617	1.003704	1.002801	0.999480				1.001240
HF15744	1.000640	1.000030	0.999650	0.999470	0.999160	0.998034	0.998085
HF18747	1.001964	0.999230	0.999930	1.000950	1.002140	1.002677	1.001870
HF19746	0.999520	0.999940	1.001603	0.999190	0.999660	0.998782	0.998886
HF20406				1.001370	1.003710	1.004066	1.002430
HF27157				1.000380	0.999020	0.998722	0.999647
HF27159			0.999271	0.998880		0.998004	1.000020
HF27162			1.000370	1.000960	1.000820	1.000180	0.999212
HF27796					0.996910	0.996979	0.997204
HF29223				0.997450	0.997470	0.996761	0.997352
AHF14915	0.998751	0.998421	0.999980	1.000460	1.000260	0.999640	0.999682
AHF17142	0.998801	0.997733	0.998901	0.998860	0.998930	0.999141	0.998358
AHF18742						1.003773	1.002280
AHF27160			0.997267	0.997090	0.996770	0.996910	0.996467
AHF27798			0.998363	0.998980	0.999880	0.999410	0.999018
AHF28553				0.997560	0.997330	0.996105	0.996842
AHF28968				0.998720	0.998660	0.997765	0.997734
AHF29220				0.998620	0.998460	0.997556	0.997691
AHF29225					0.997090	0.996105	0.996896
AHF30497					0.997740	0.999350	0.999623
AHF30713					0.998610	0.997512	0.997548
AHF30716					0.997450	0.997157	0.997136
AHF31041					0.998130	0.996294	0.996286
AHF31105						1.001649	0.999964
AHF31110					0.997890	0.997211	0.996431
AHF32446					0.999750	0.998873	1.000050
AHF32448					1.000310	0.999874	0.999939
AHF32455						0.999090	1.000280
AHF33396						0.997951	0.998079
AWX33393						0.997281	0.999362
TMI67502	0.999290	0.998471	1.000390	0.998660	0.999660	0.999480	0.999294
TMI67604	1.002376	1.000932	1.001402	1.002390	0.999280	0.998792	0.998226
TMI68016	1.001492	0.999830	1.001242	1.000500	0.997790	1.000090	0.999858
TMI68018			0.998692		0.998480	0.997138	0.996804
TMI68025			0.999460	0.999860	1.000060	0.998135	0.998613
TMI69137				1.002790	1.002300	1.001703	1.001750
MAR-1-2				0.999610		0.998702	1.000120
CROM9L					0.998570	0.999111	0.998363

PMO6-5	1.006756	1.000100	0.998602	0.997980	1.000530	0.999960	0.999116
PMO6-79-122			0.996890	0.999970	0.999860	1.000390	0.999401
PMO6-79-123					1.003400	1.000510	0.937200
PMO6-80022		1.000230	0.996890	0.996130	0.996990	0.997944	1.003080
PMO6-811108		0.999210	0.999970	1.000110	0.999970	0.998114	1.000660
PMO6-811109					0.999460	0.998412	0.998577
PMO6-850405				1.000370	0.999290	0.999191	1.000560
PMO6-850406					1.000320	0.999440	1.000200
PMO6-850410				1.001800	1.015280	0.987030	0.990890
PMO6-911204					1.000810	0.999011	0.999711
SIAR-1 (SIAR-1A)					0.999220	1.001924	1.002400
SIAR-2A						1.000623	0.991696
SIAR-2B						0.998620	1.000290
SIAR-2C						1.000087	0.999839

2.5 Saharan Dust Event (SDE)

During the night of October $7^{th}/8^{th}$ a dust cloud from the Sahara desert has been transported over Switzerland by high-altitude winds. The appearance of the dust particles is reflected in an excess of large particles ($> 1\mu\text{m}$) in the AERONET inversion results on the corresponding days (c.f. Fig. 2.2). The particle distribution significantly affects the scattering phase function (scattering angle) and thus changes the aureole radiation. Instruments with different view-limiting geometries see either more or less of this change. We use the view-limiting geometries from Table 2.4 together with the scattering phase functions (see Sect. 4.5), the Aerosol Optical Depth (AOD, see Sect. 4.3), and other scattering parameters (Sect. 4.4) to calculate the aureole correction with SMARTS (Gueymard, C. A., Solar Energy, 71(5), 2001) depending on the view-limiting geometry of each type of cavity radiometer[2]. The aureole correction is calculated with respect to the view-limiting geometry recommended by the CIMO Guide. Hence, all HF- and PMO6-type radiometers which follow the CIMO recommendations very closely do not need this correction, although we applied it for sake of consistency. On the other hand, on October 8^{th} the correction can be as large as -0.2% in the case of the SIAR. Also PMO2 and PMO5 require large corrections of -500 ppm and $+600$ ppm, respectively.

The correction factors for the WSG are plotted in Figure 2.3.

[2]Interestingly, the SDE effect is not very distinct in most Ångströms (c.f. Chap. 3.1). Probably because the *area* of sky at large angular distance from the sun is small in the elongated field-of-view. In other words, the it "radiation-weighted" effective field-of-view of Ångströms might not be too different the CIMO recommendations. Because of the smallness of the SDE effect and the difficulties to reduce the rectangular to a circualar view-limiting geometry we did not apply the SDE correction to Ångströms. In the case of thermopile instruments (NIPs, CH1s etc.) their level of accuracy does not warrant to apply the correction.

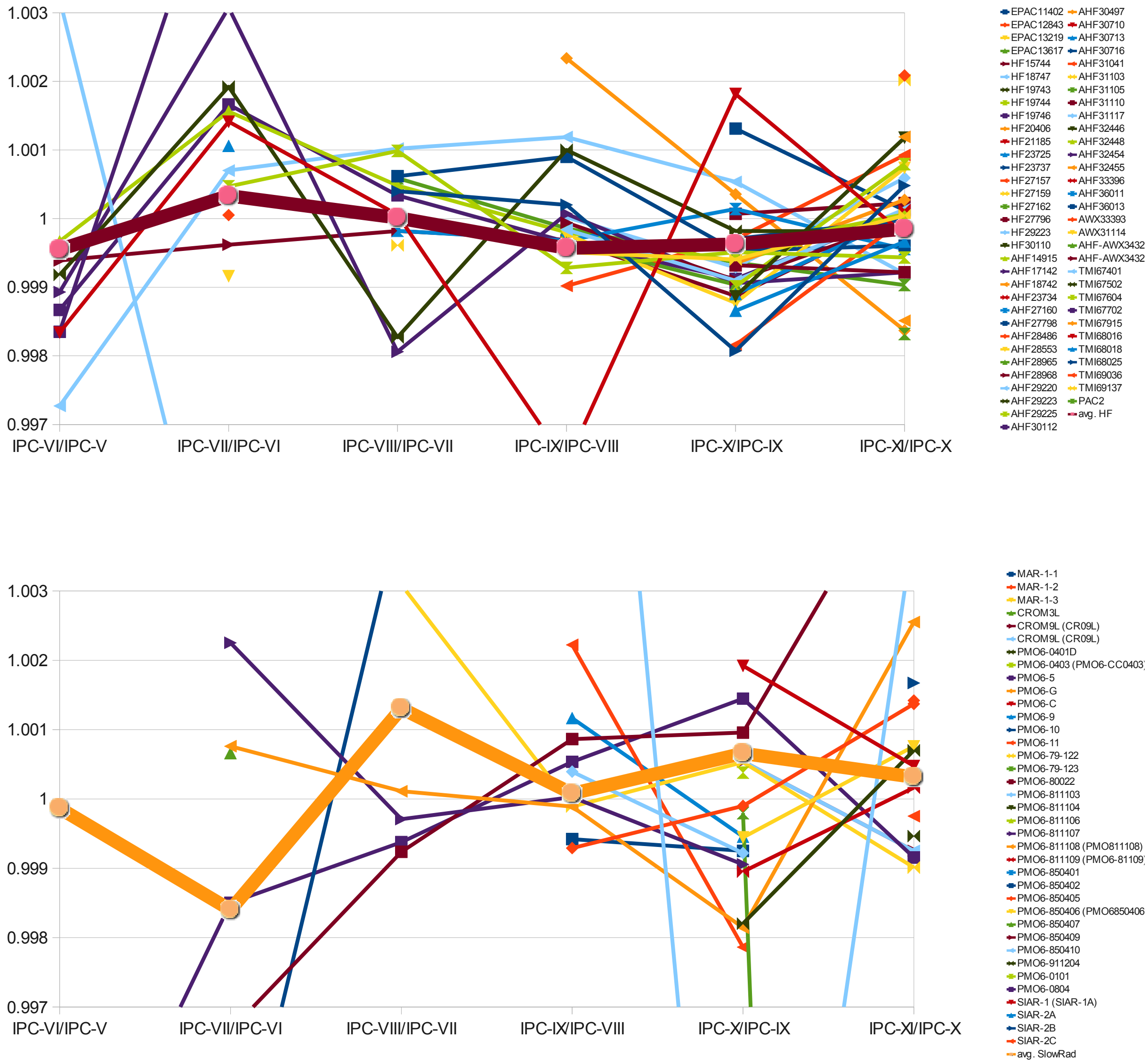

Figure 2.1: The historic development of the WRR factors of all cavity radiometers which have participated in at least two IPC's since 1980 (IPC-V). The top panel shows how the WRR factors of HF-type pyrheliometers (including PAC, EPAC, and TMI) changed between consecutive IPCs since 1980 (IPC-V). The same is shown on the bottom panel for "SlowRad"-type radiometers, i.e. radiometers with alternating open/closed measurements. Note that in this analysis all WRR factors are normalized to the calibration constant which was used at the time.

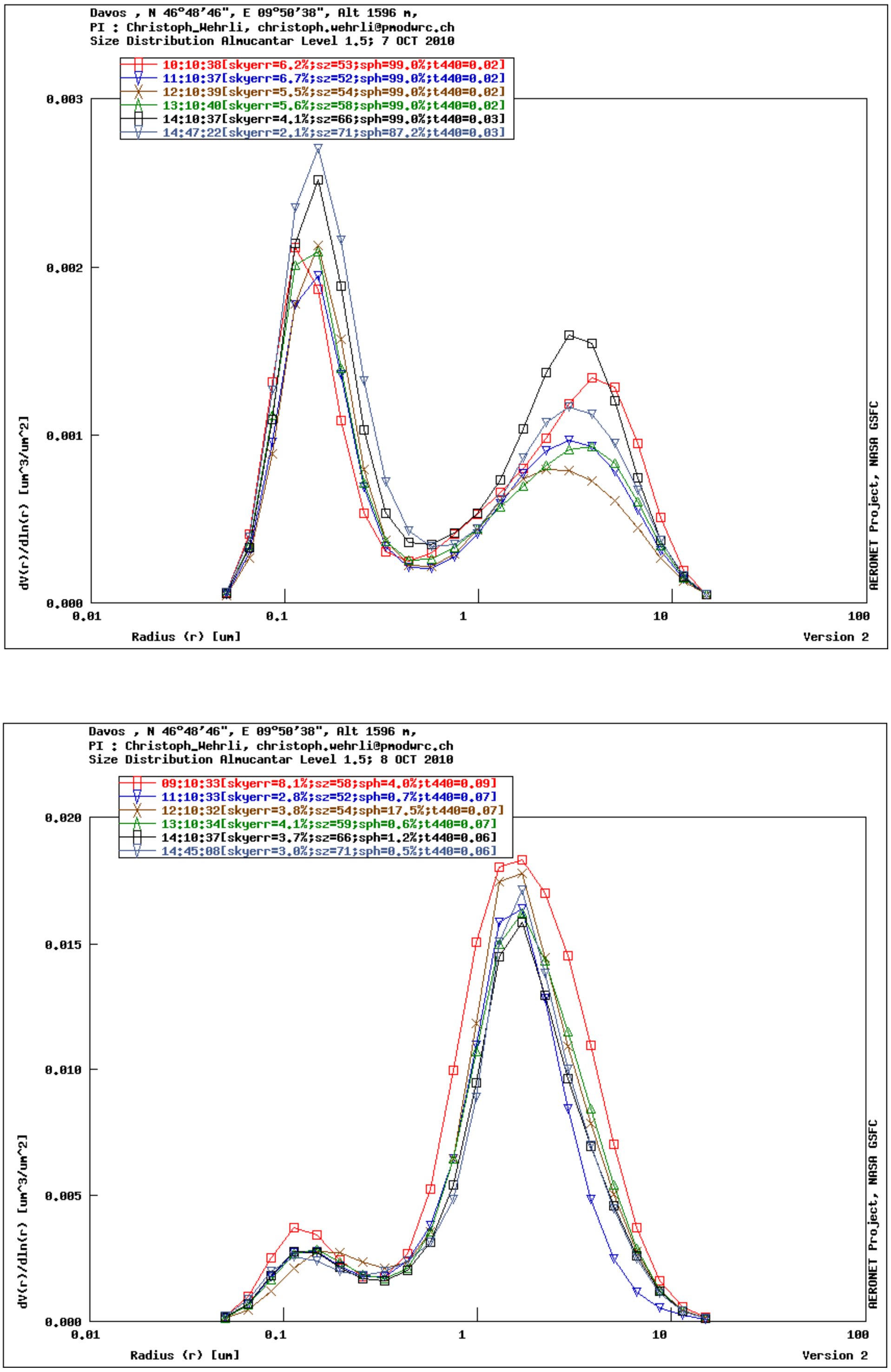

Figure 2.2: The size distribution of aerosol particles measured by the AERONET Davos station on October 7th (top panel) and 8th (bottom panel). The excess in large particles ($> 1\mu\mathrm{m}$) gradually normalizes during the following week. The size distribution significantly affects the scattering phase function and thus the aureole radiation.

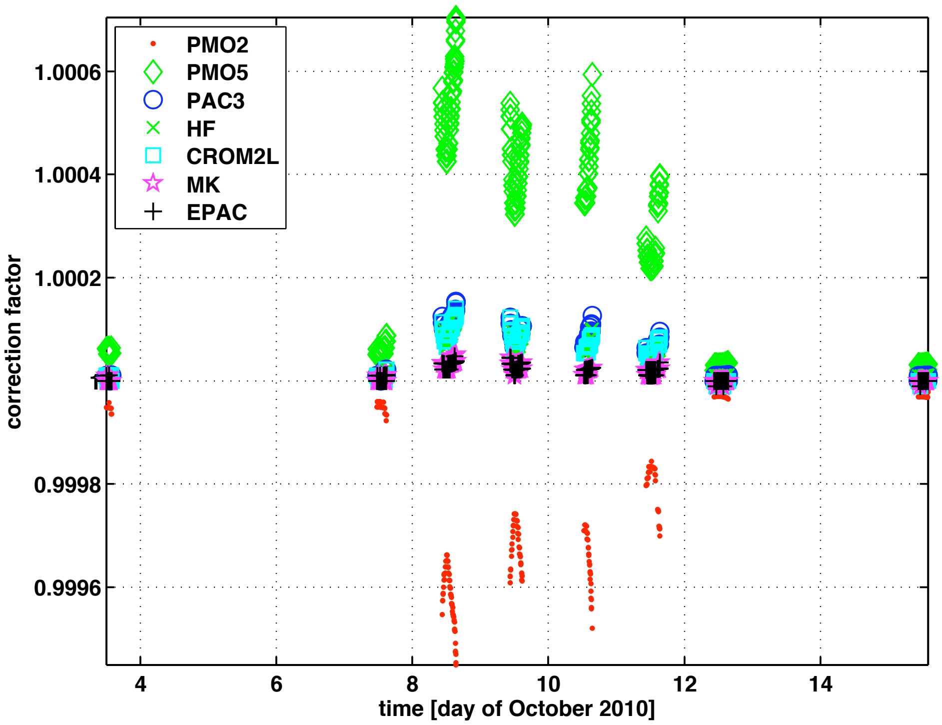

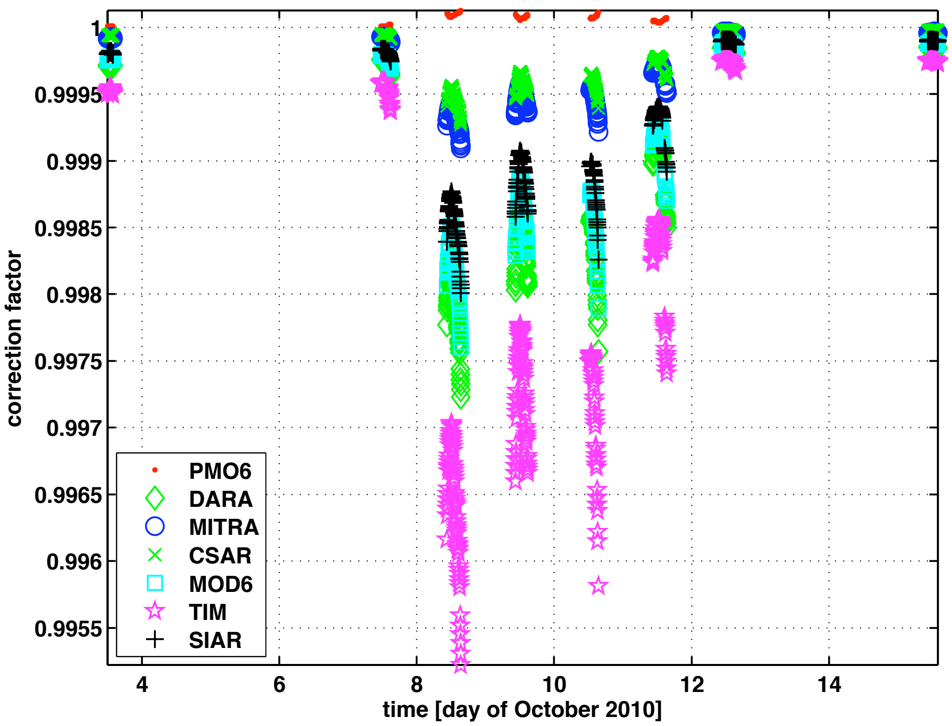

Figure 2.3: The aureole correction before and during the Saharan dust event depending on type fo instrument. The correction was applied to all cavity instruments. In the top panel the symbols for HF/AHF are hidden behind MK/TMI, CROM, and EPAC. (Calculations and graphics by André Fehlmann.)

Table 2.4: The view-limiting geometries for each type of instrument (all dimensions in mm).

Instrument (Type)	*front aperture radius*	*rear aperture radius*	*distance between apertures*
PMO2	3.6	2.5	75.0
PMO5	3.7	2.5	95.4
PMO6	4.2	2.5	98.5
PAC3	8.18	5.64	190.5
CROM2L	6.29	5.0	144.05
HF	5.81	3.99	134.7
TMI	8.2	5.56	187.6
SIAR	5.7	4.0	100.0

Chapter 3 Conclusions and Recommendations

Despite the partial failure of two WSG instruments (PAC3 and HF18748, c.f. Sect. 2.4) the WRR is considered stable within the limits required by the WMO-CIMO Guide. The new WRR factors are calculated based on the average readings of PMO2, PMO5, CROM2L, and MK67814. Compared to IPC-X most participating instruments show insignificant changes in their WRR factors, which confirms the stability of the WRR. The recommended WRR factors are listed in Table 2.2.

The flexibility offered by the new data acquisition system allowed for quick response in case of suspected problems with individual instruments. In serveral cases small stability issues of participating instruments could be identified and fixed with only minimal loss of observing time.

The Saharan Dust Event (SDE) which affected the measurements from October 8^{th} through 13^{th} revealed the susceptibility of direct solar irradiance measurements to atmospheric conditions and emphasized the importance to follow the recommendations concerning view-limiting geometry. While it was possible to compensate for the geometry-induced SDE effect the required auxiliary data (AOD, scattering phase function) and sophisticated models are not normally available at field sites. We thus strongly recommend the use of pyrheliometers which obey the CIMO recommendations for view-limiting geometry.

3.1 Graphical Representation of the Results

On the following pages are the data plots for each instrument. The deviation from WRR is plotted in percents. All the points which were used for the analysis (i.e. the points fulfilling the selection criteria listed in Sect. 2.1) have been plotted with a corresponding histogram on the side.

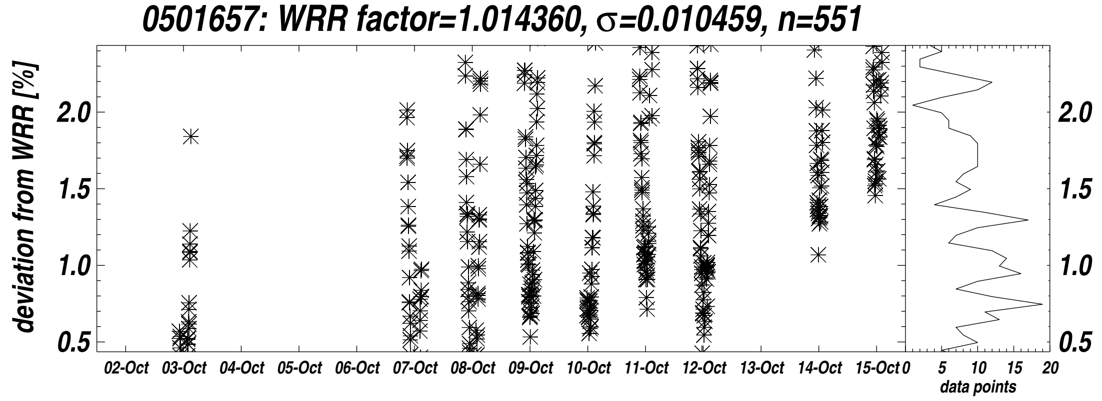
0501657: WRR factor=1.014360, σ=0.010459, n=551
deviation from WRR [%]
0.5 1.0 1.5 2.0
02-Oct 03-Oct 04-Oct 05-Oct 06-Oct 07-Oct 08-Oct 09-Oct 10-Oct 11-Oct 12-Oct 13-Oct 14-Oct 15-Oct
0 5 10 15 20
data points

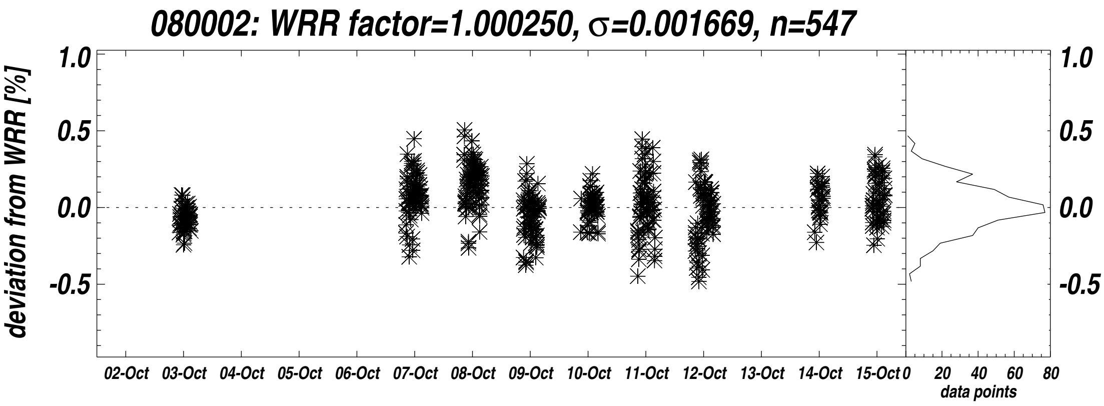
080002: WRR factor=1.000250, σ=0.001669, n=547
deviation from WRR [%]
-0.5 0.0 0.5 1.0
02-Oct 03-Oct 04-Oct 05-Oct 06-Oct 07-Oct 08-Oct 09-Oct 10-Oct 11-Oct 12-Oct 13-Oct 14-Oct 15-Oct
0 20 40 60 80
data points

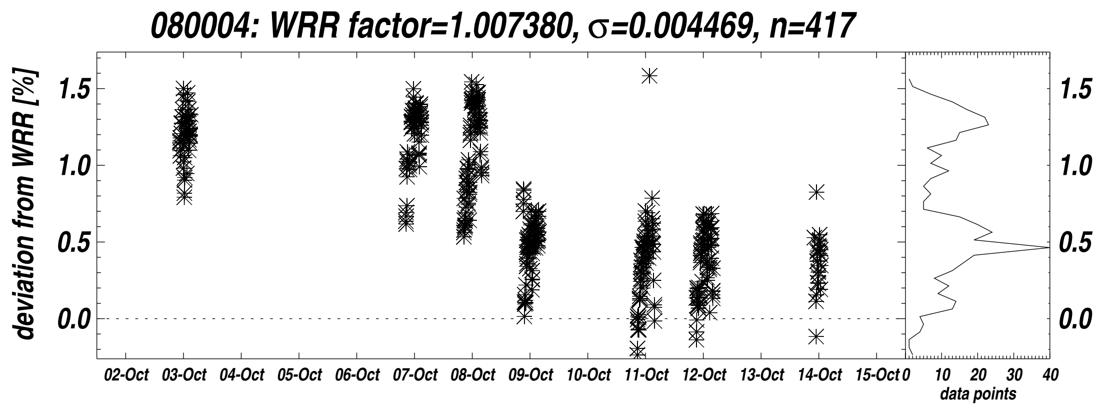
080004: WRR factor=1.007380, σ=0.004469, n=417
deviation from WRR [%]
0.0 0.5 1.0 1.5
02-Oct 03-Oct 04-Oct 05-Oct 06-Oct 07-Oct 08-Oct 09-Oct 10-Oct 11-Oct 12-Oct 13-Oct 14-Oct 15-Oct
0 10 20 30 40
data points

080015: WRR factor=0.997799, σ=0.001671, n=554

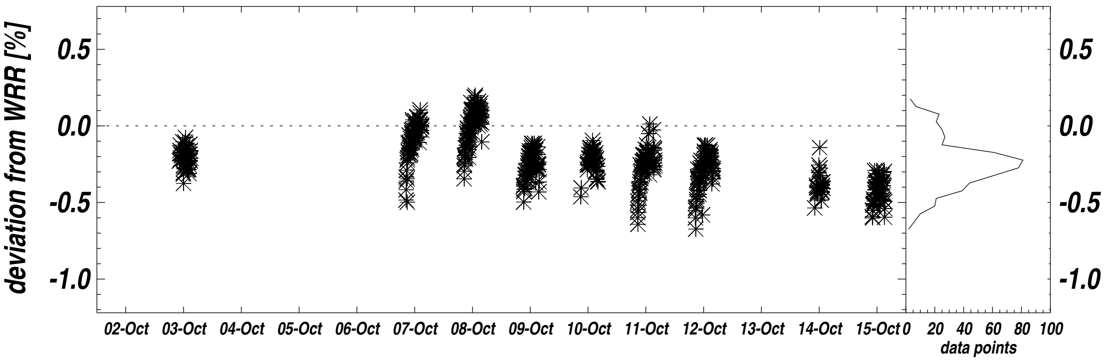

0804: WRR factor=0.999914, σ=0.000645, n=364

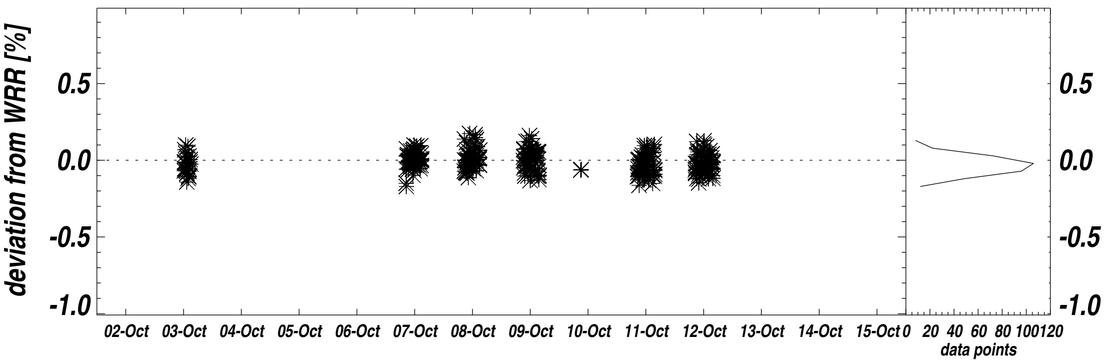

090090: WRR factor=1.003660, σ=0.001191, n=554

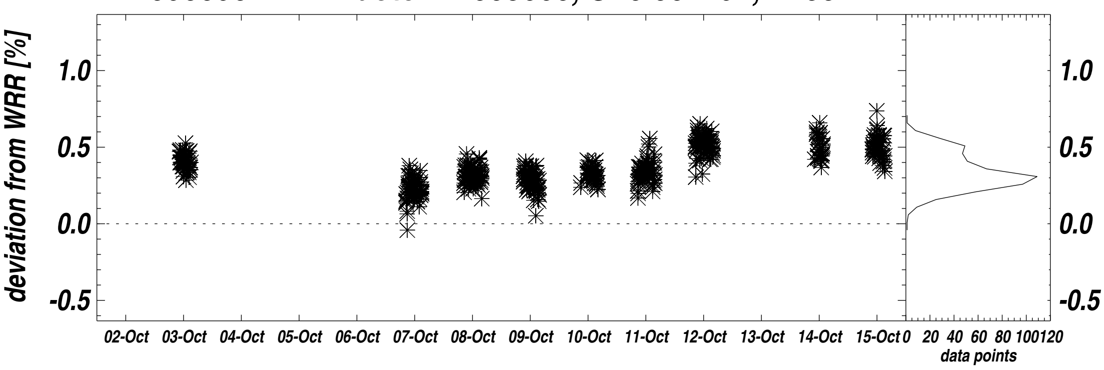

21451E6: WRR factor=0.999193, σ=0.007685, n=453

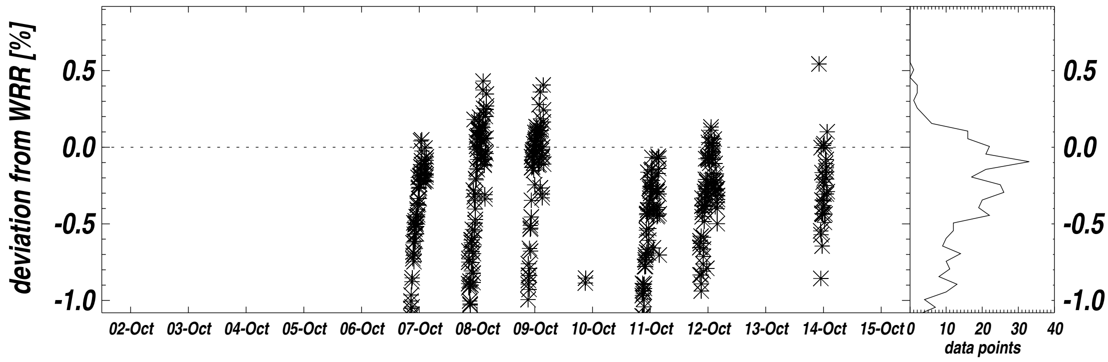

25738E6: WRR factor=0.998843, σ=0.006614, n=453

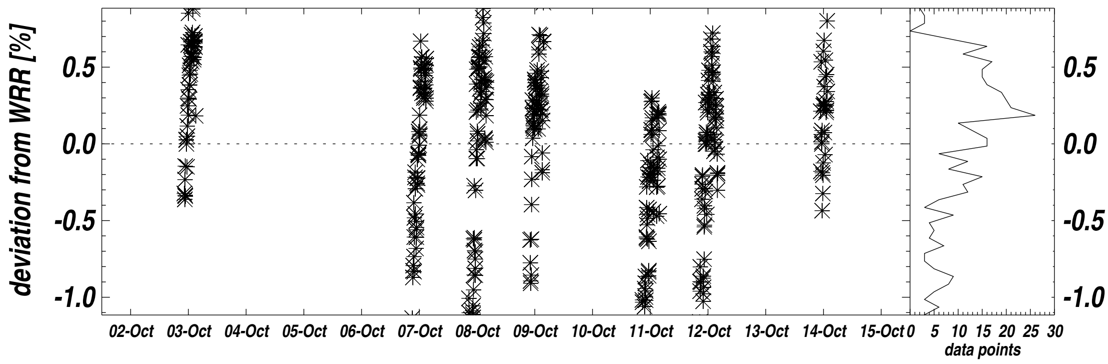

28335: WRR factor=1.009040, σ=0.005413, n=424

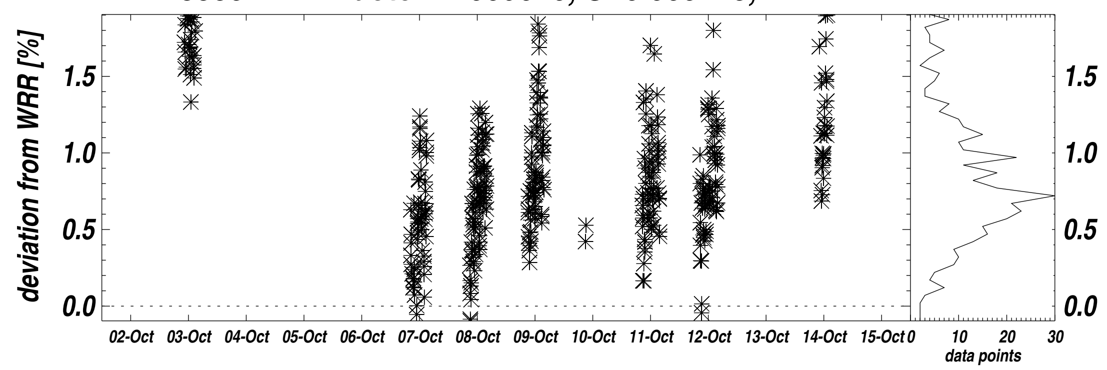

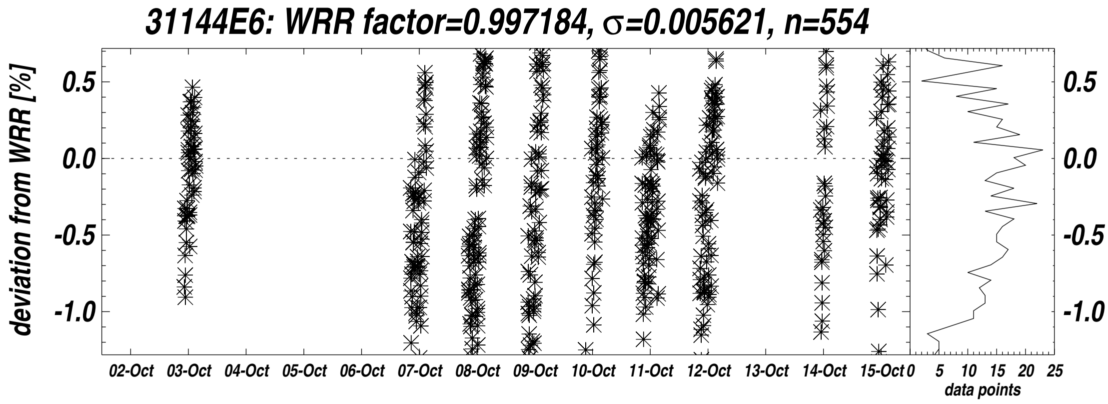
31144E6: WRR factor=0.997184, σ=0.005621, n=554
deviation from WRR [%]
data points

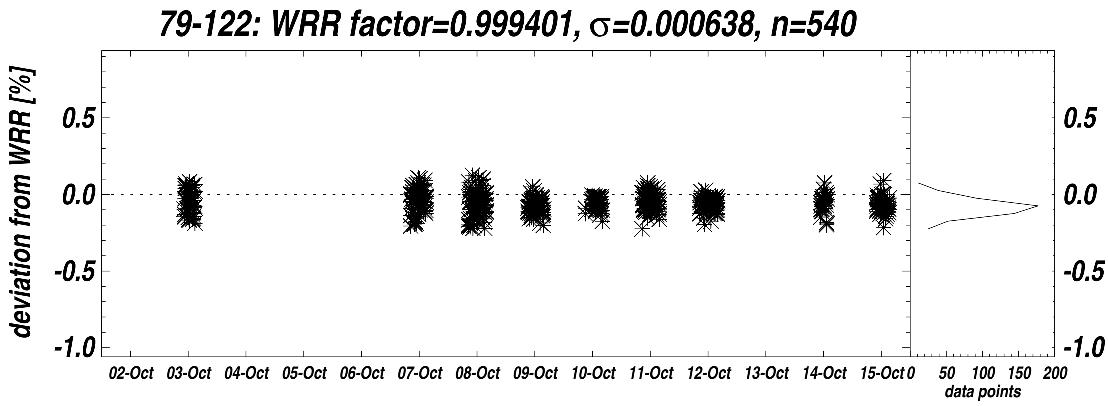
79-122: WRR factor=0.999401, σ=0.000638, n=540
deviation from WRR [%]
data points

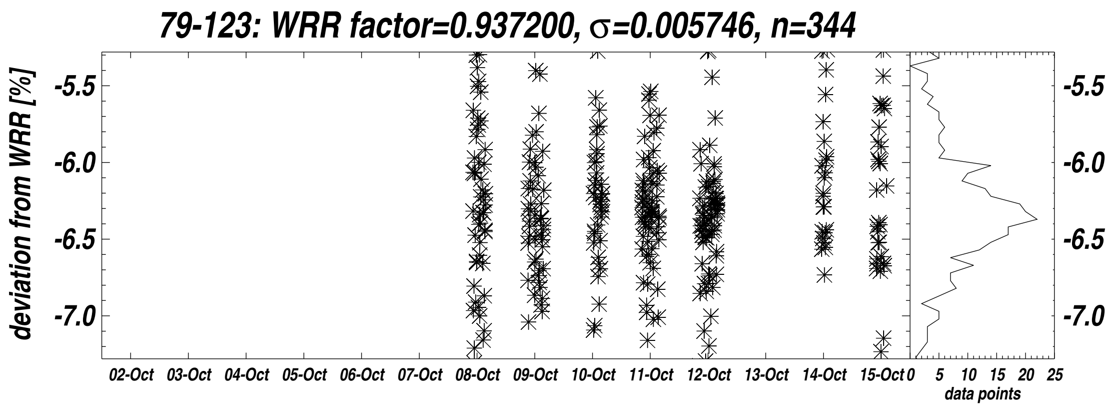
79-123: WRR factor=0.937200, σ=0.005746, n=344
deviation from WRR [%]
data points

80022: WRR factor=1.003080, σ=0.000541, n=493

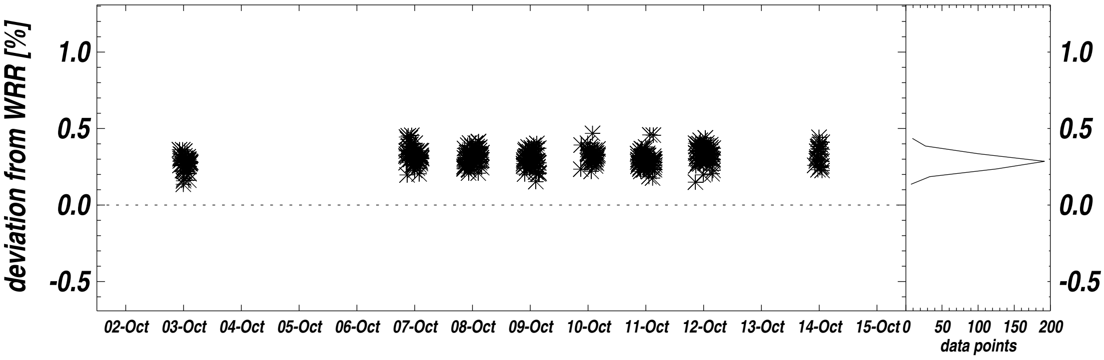

850402: WRR factor=1.003287, σ=0.001234, n=102

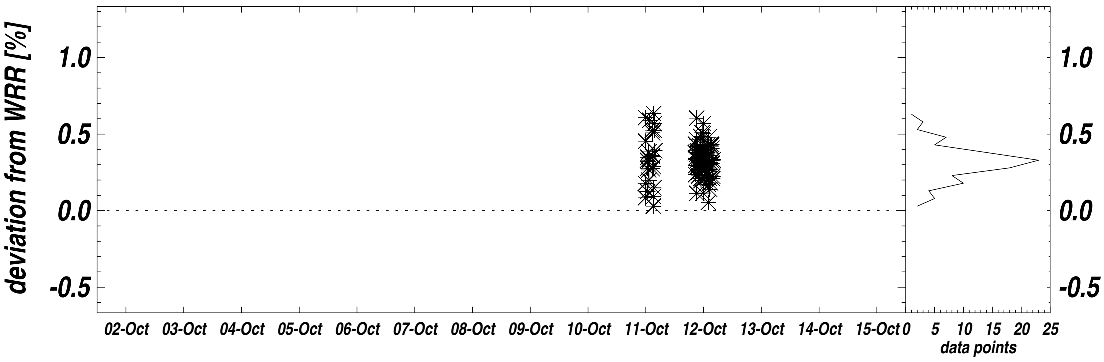

850405: WRR factor=1.000560, σ=0.001610, n=420

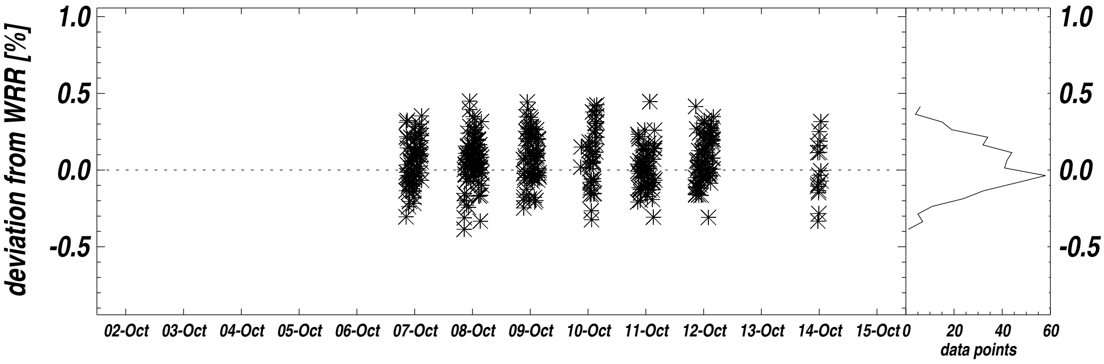

850409: WRR factor=1.004180, σ=0.000576, n=539

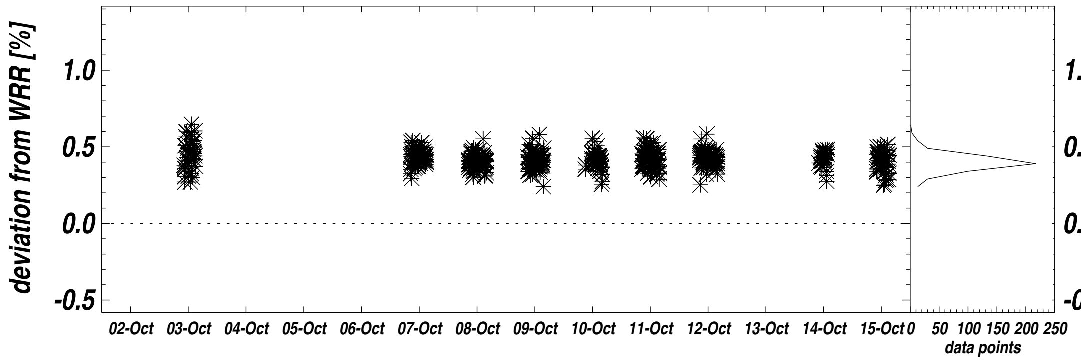

970147: WRR factor=0.996057, σ=0.001739, n=554

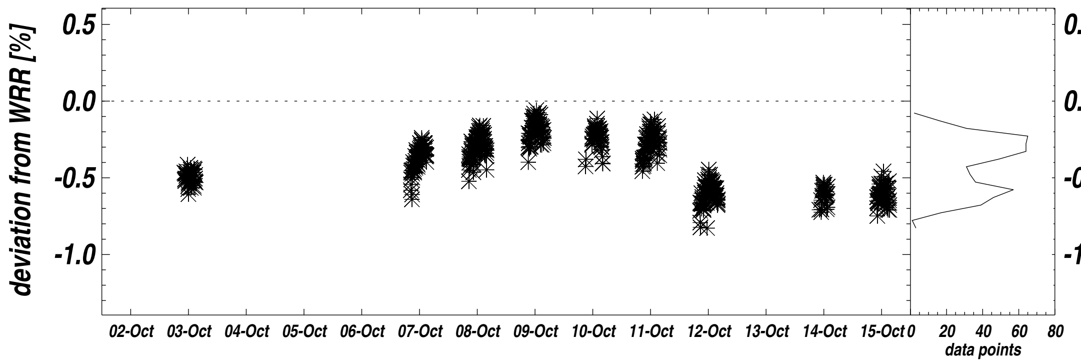

A12578: WRR factor=1.008580, σ=0.004598, n=134

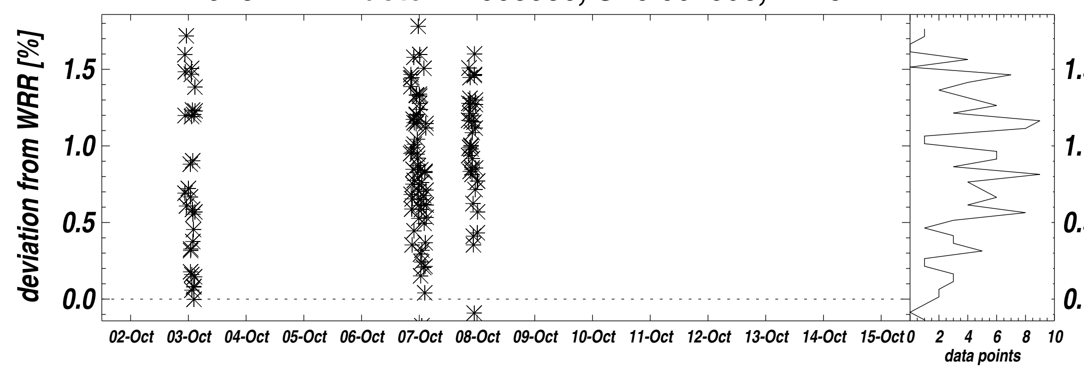

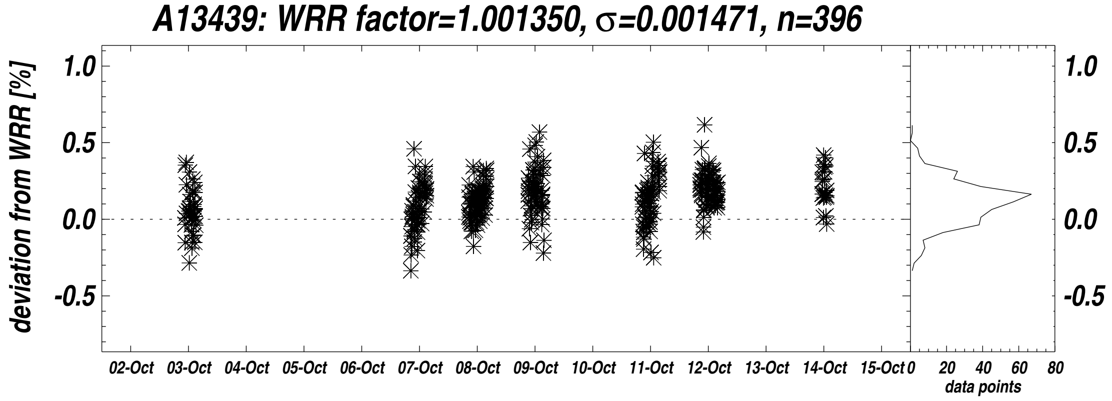
A13439: WRR factor=1.001350, σ=0.001471, n=396
deviation from WRR [%]
data points

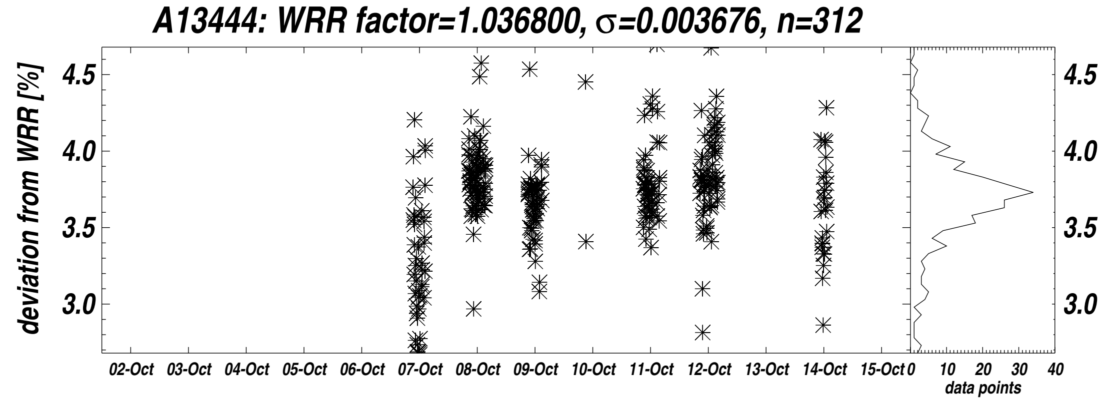
A13444: WRR factor=1.036800, σ=0.003676, n=312
deviation from WRR [%]
data points

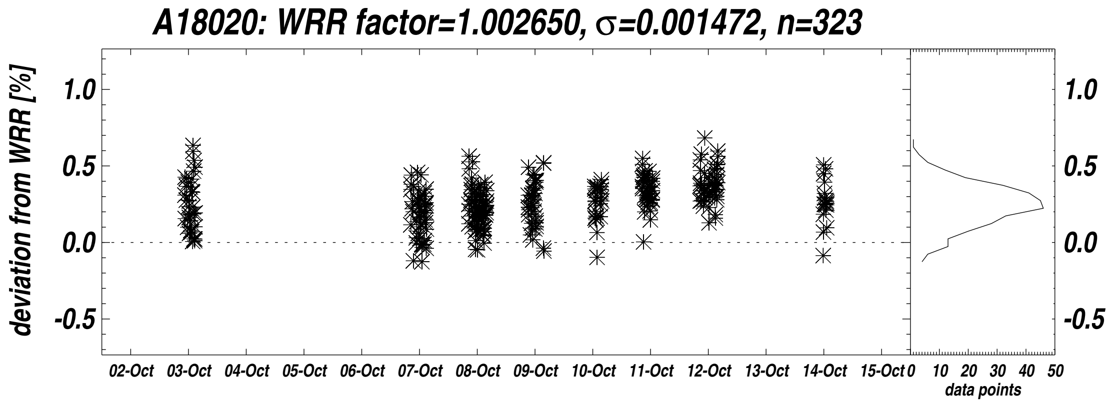
A18020: WRR factor=1.002650, σ=0.001472, n=323
deviation from WRR [%]
data points

A212: WRR factor=0.996482, σ=0.003106, n=258

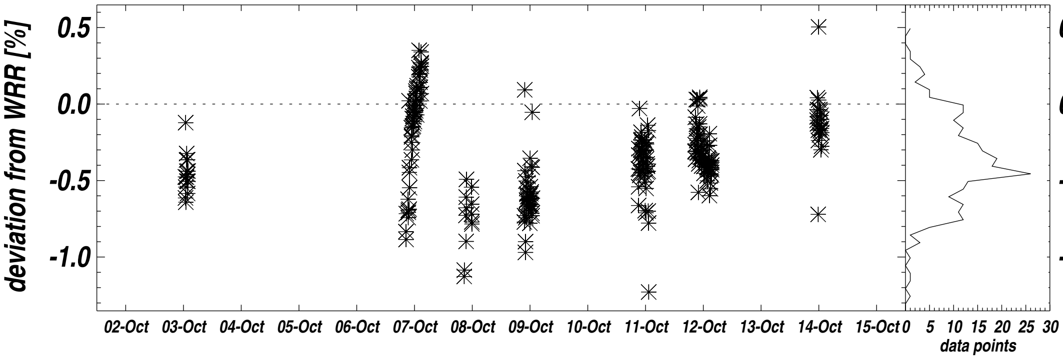

A26839: WRR factor=1.007550, σ=0.002085, n=361

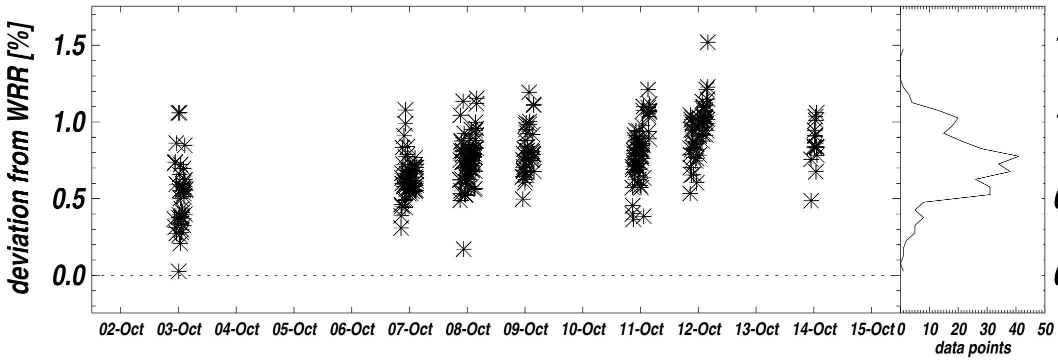

A576: WRR factor=0.990369, σ=0.003963, n=382

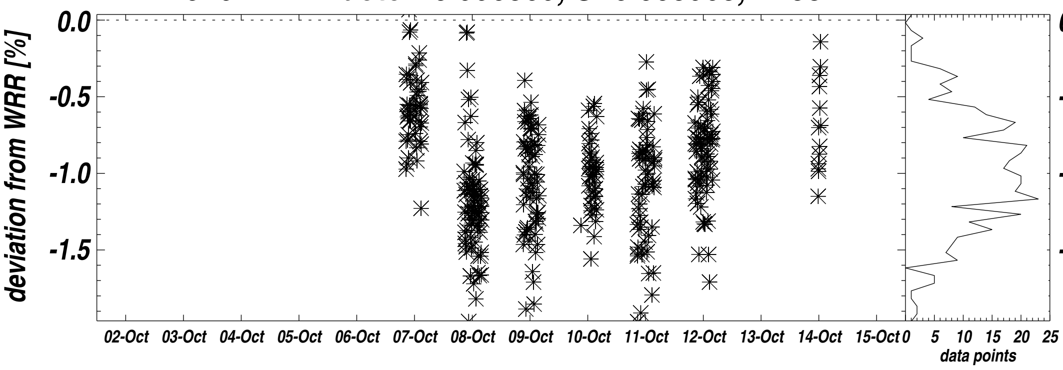

A702: WRR factor=0.998769, σ=0.004789, n=373

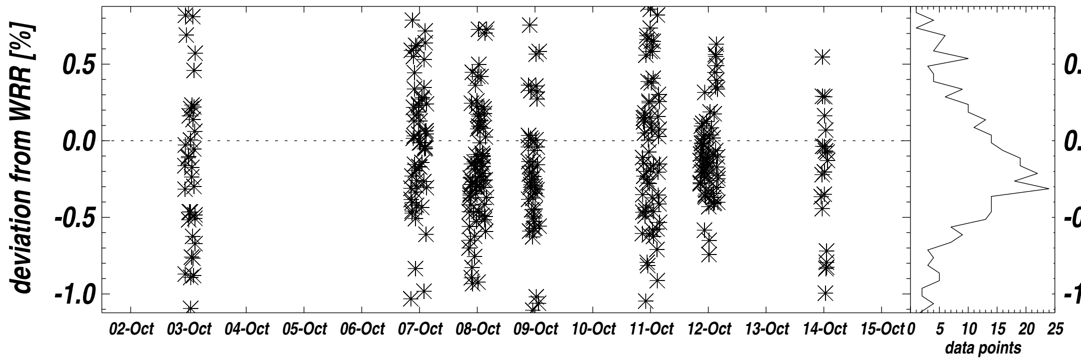

AHF-AWX34320: WRR factor=0.992830, σ=0.000839, n=442

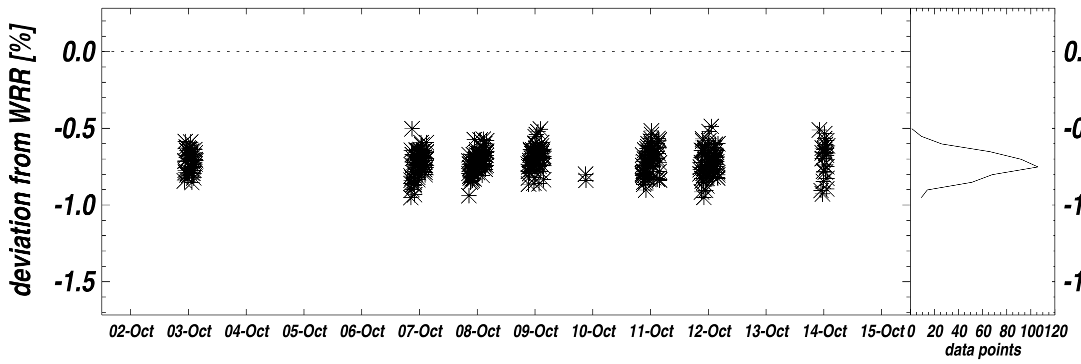

AHF-AWX34321: WRR factor=0.994550, σ=0.000843, n=442

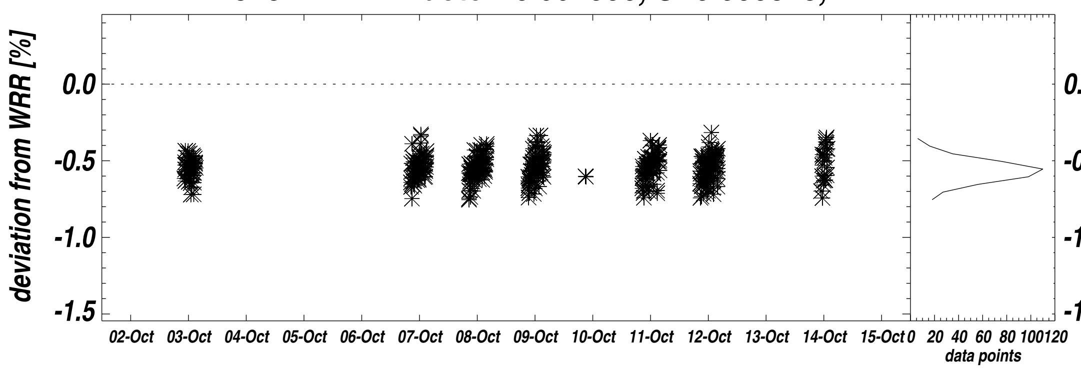

AHF14915: WRR factor=0.999682, σ=0.000920, n=392

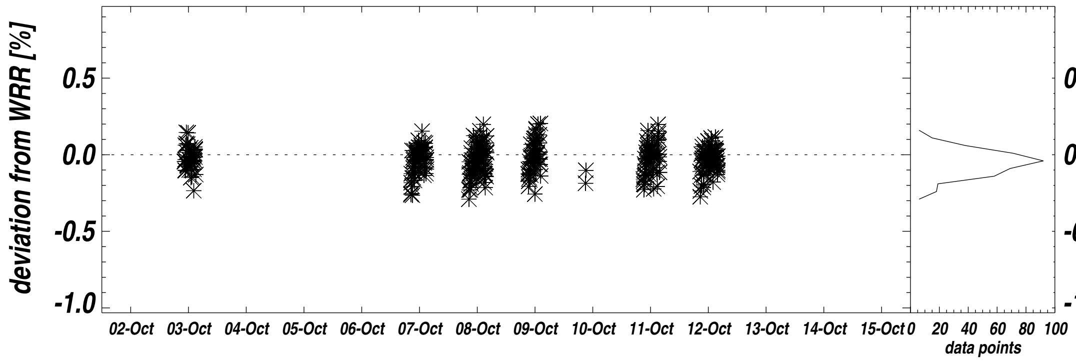

AHF17142: WRR factor=0.998358, σ=0.000908, n=397

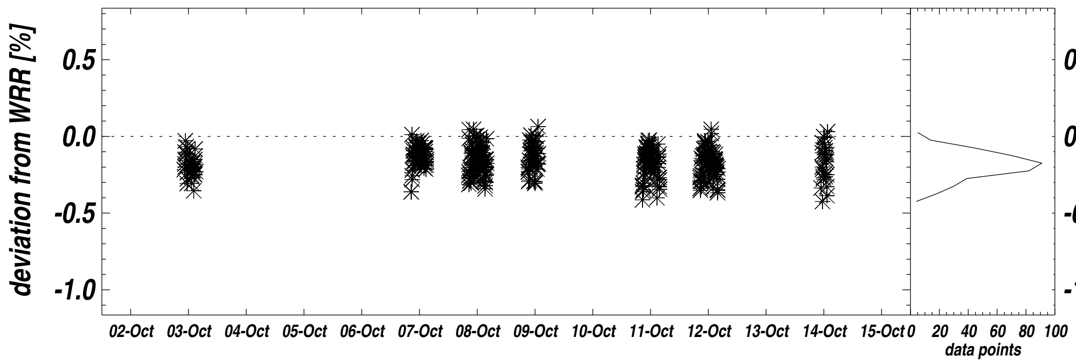

AHF18742: WRR factor=1.002280, σ=0.002283, n=361

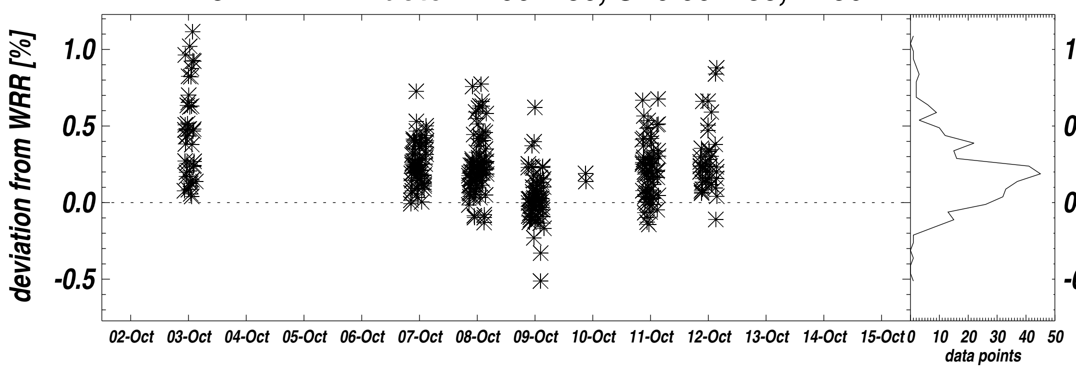

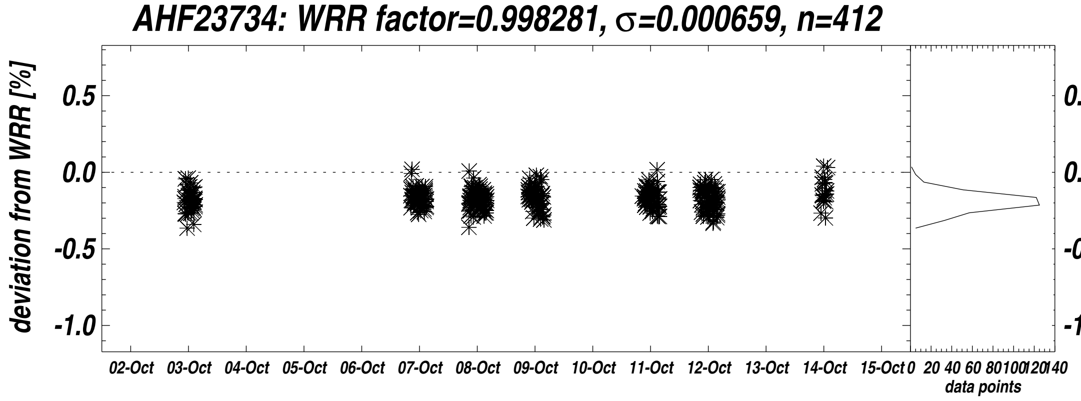
AHF23734: WRR factor=0.998281, σ=0.000659, n=412
deviation from WRR [%]
0.5
0.0
-0.5
-1.0
02-Oct 03-Oct 04-Oct 05-Oct 06-Oct 07-Oct 08-Oct 09-Oct 10-Oct 11-Oct 12-Oct 13-Oct 14-Oct 15-Oct
0 20 40 60 80 100 120 140
data points

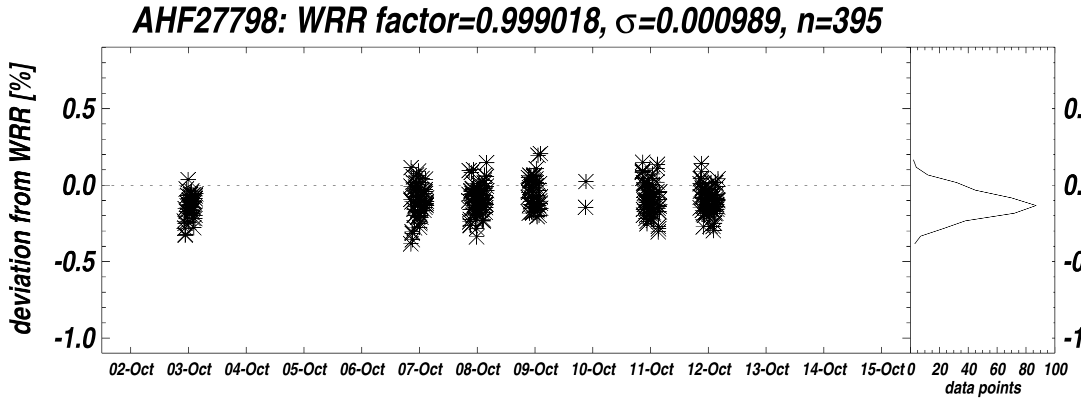
AHF27798: WRR factor=0.999018, σ=0.000989, n=395
deviation from WRR [%]
0.5
0.0
-0.5
-1.0
02-Oct 03-Oct 04-Oct 05-Oct 06-Oct 07-Oct 08-Oct 09-Oct 10-Oct 11-Oct 12-Oct 13-Oct 14-Oct 15-Oct
0 20 40 60 80 100
data points

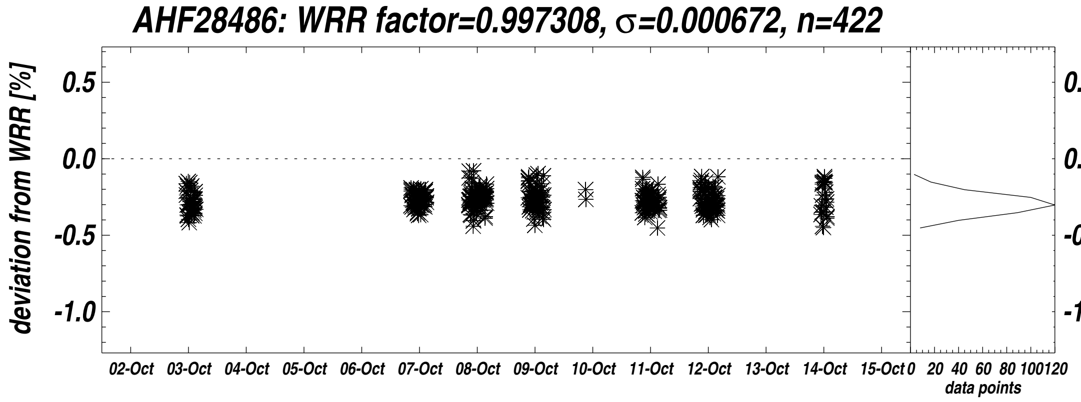
AHF28486: WRR factor=0.997308, σ=0.000672, n=422
deviation from WRR [%]
0.5
0.0
-0.5
-1.0
02-Oct 03-Oct 04-Oct 05-Oct 06-Oct 07-Oct 08-Oct 09-Oct 10-Oct 11-Oct 12-Oct 13-Oct 14-Oct 15-Oct
0 20 40 60 80 100 120
data points

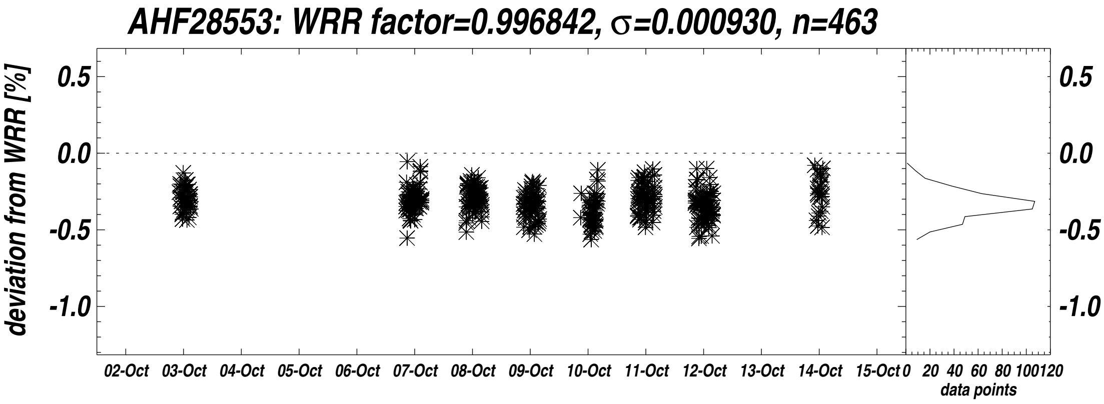
AHF28553: WRR factor=0.996842, σ=0.000930, n=463
deviation from WRR [%]
data points

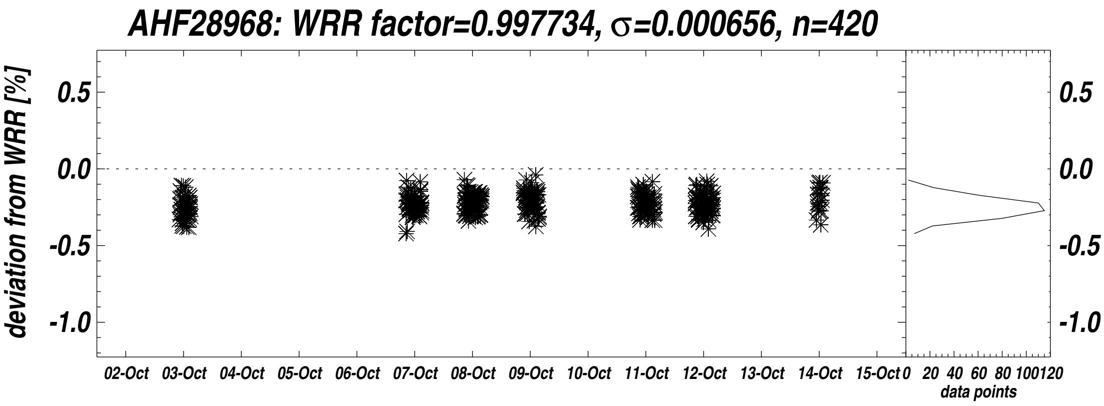
AHF28968: WRR factor=0.997734, σ=0.000656, n=420
deviation from WRR [%]
data points

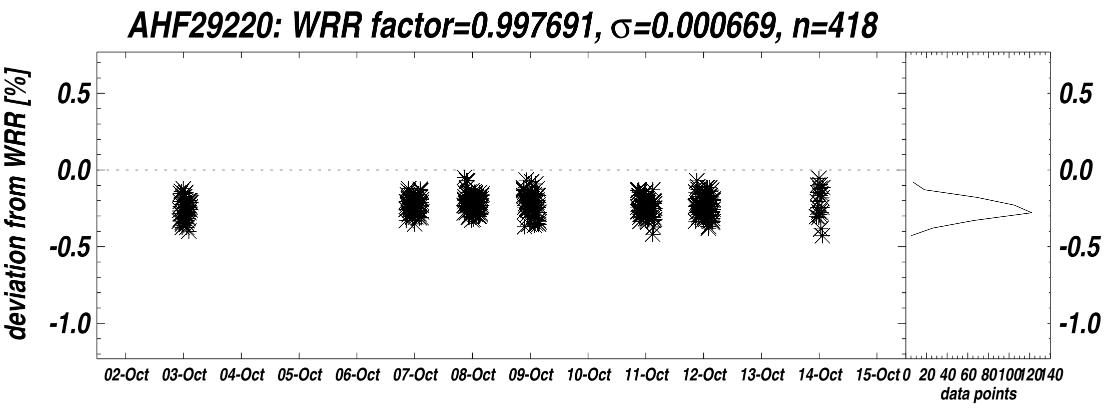
AHF29220: WRR factor=0.997691, σ=0.000669, n=418
deviation from WRR [%]
data points

AHF29223: WRR factor=0.997352, σ=0.000739, n=384

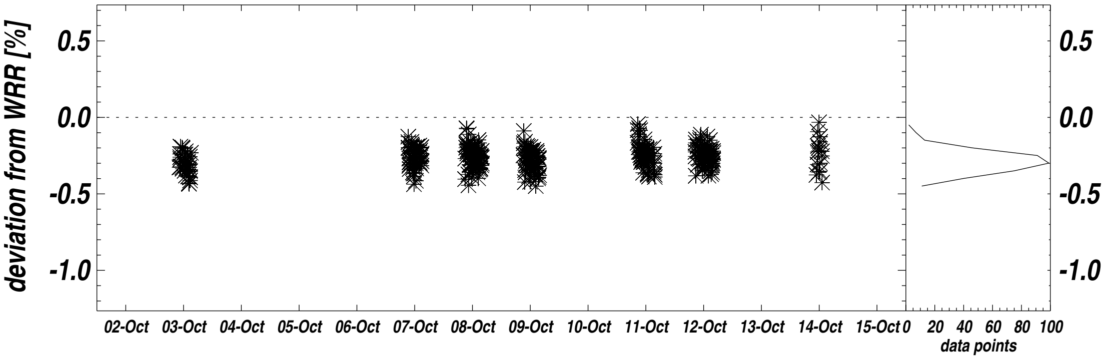

AHF29225: WRR factor=0.996896, σ=0.001026, n=336

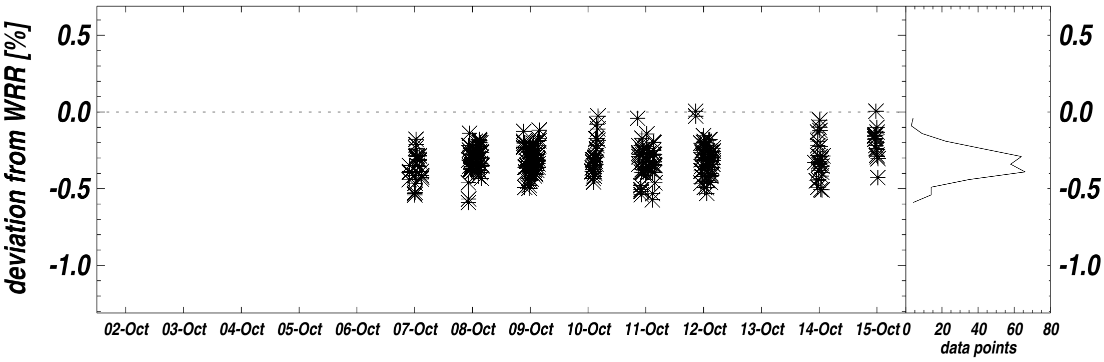

AHF30112: WRR factor=1.011730, σ=0.001995, n= 74

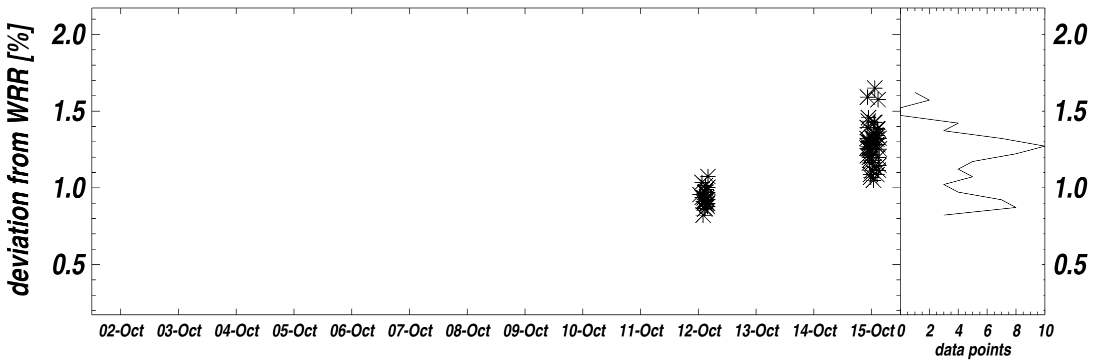

AHF30713: WRR factor=0.997548, σ=0.000679, n=421

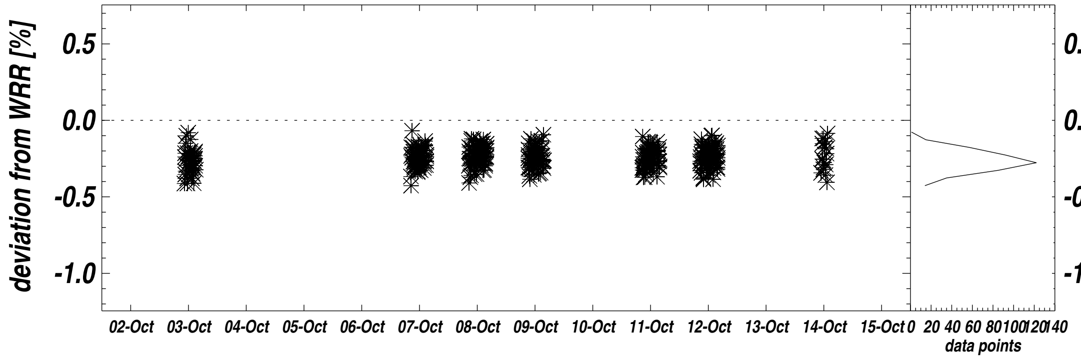

AHF30716: WRR factor=0.997136, σ=0.000656, n=360

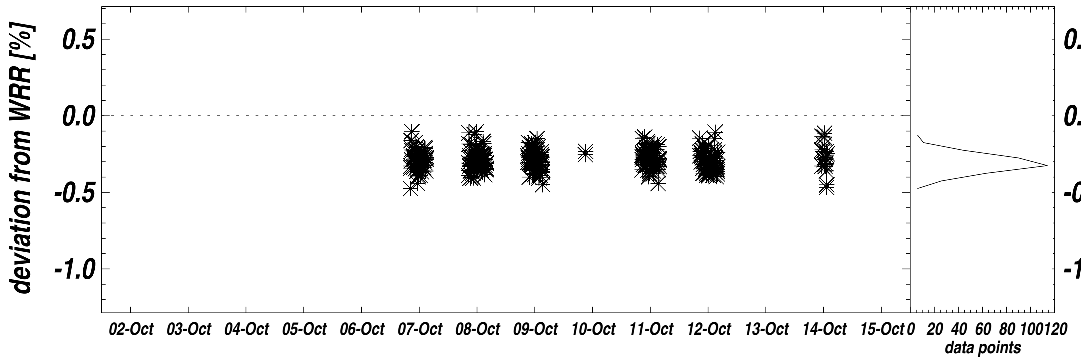

AHF31041: WRR factor=0.996286, σ=0.000699, n=441

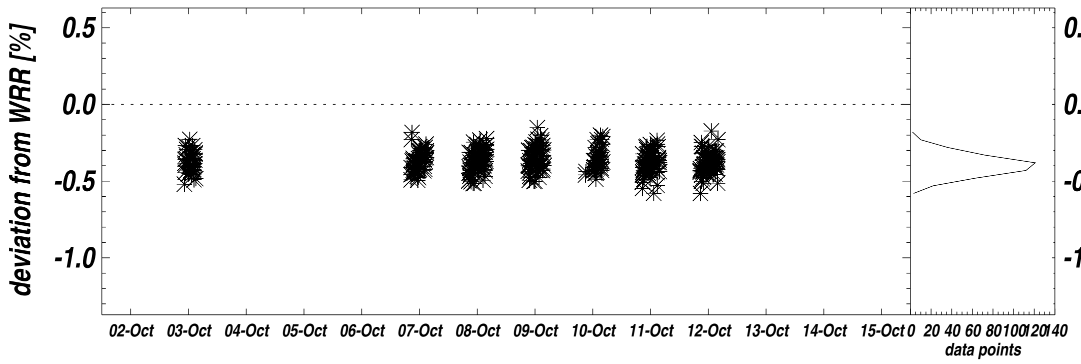

AHF31105: WRR factor=0.999964, σ=0.000708, n=431

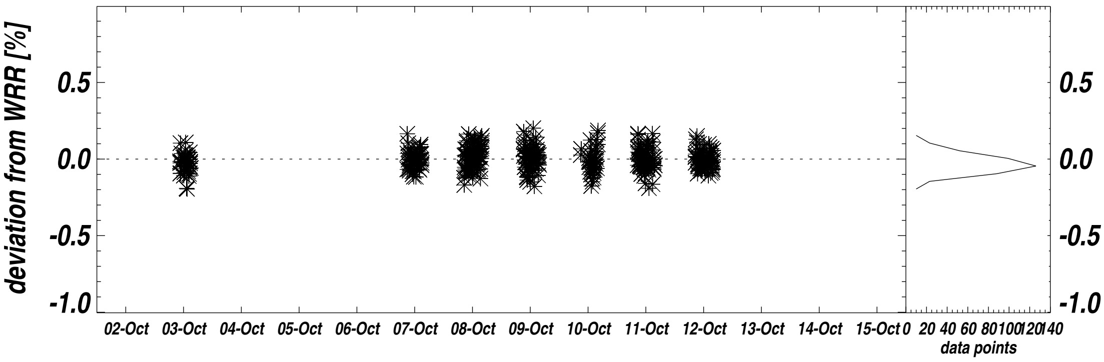

AHF31110: WRR factor=0.996431, σ=0.000627, n=399

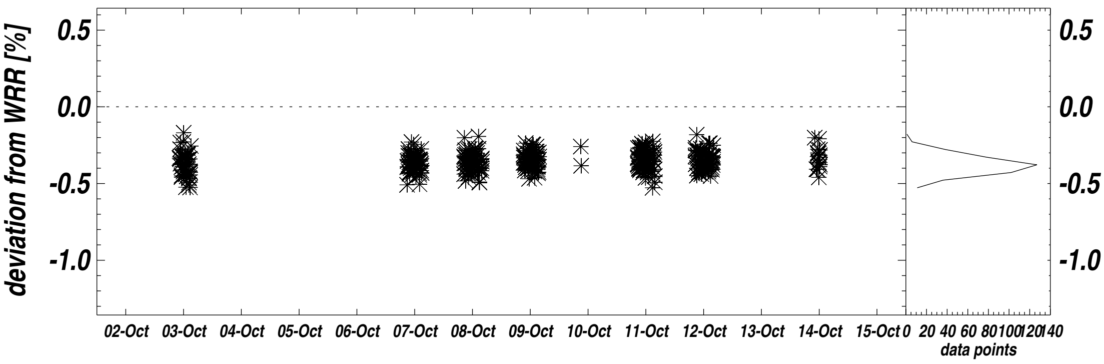

AHF31117: WRR factor=0.998861, σ=0.000641, n=401

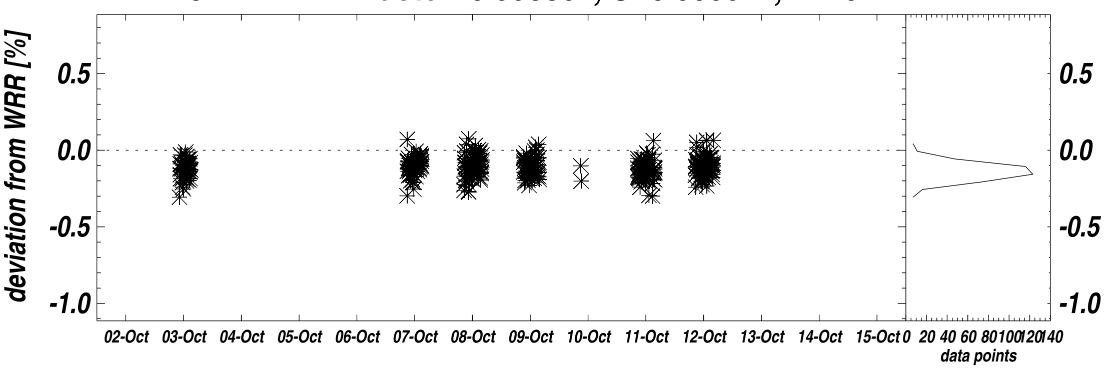

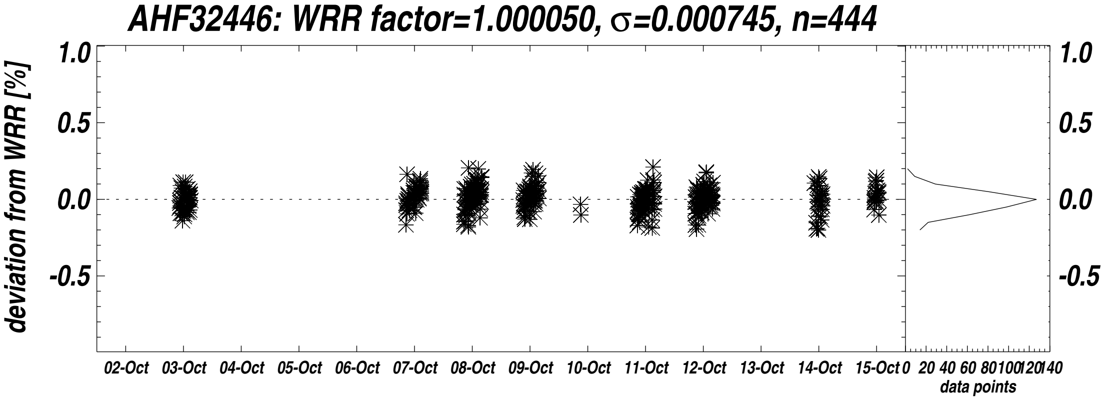
AHF32446: WRR factor=1.000050, σ=0.000745, n=444
deviation from WRR [%]
1.0
0.5
0.0
-0.5
02-Oct 03-Oct 04-Oct 05-Oct 06-Oct 07-Oct 08-Oct 09-Oct 10-Oct 11-Oct 12-Oct 13-Oct 14-Oct 15-Oct
0 20 40 60 80 100 120 140
data points

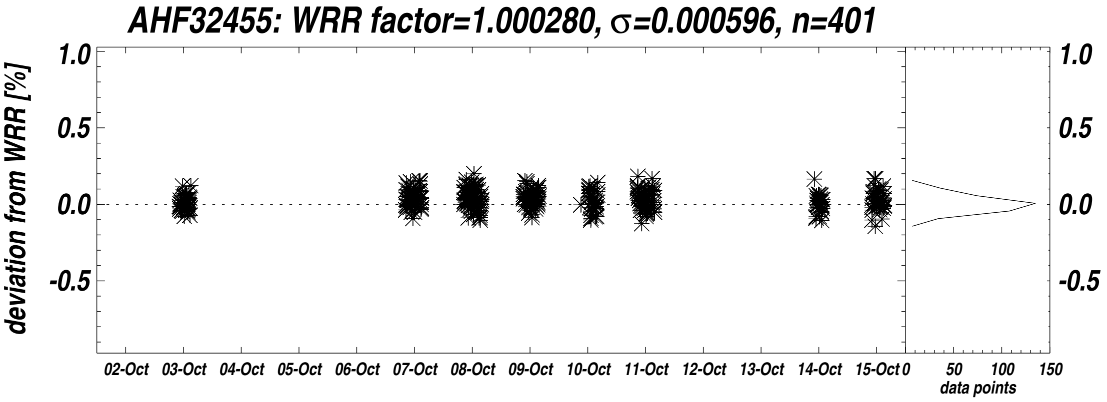
AHF32455: WRR factor=1.000280, σ=0.000596, n=401
deviation from WRR [%]
1.0
0.5
0.0
-0.5
02-Oct 03-Oct 04-Oct 05-Oct 06-Oct 07-Oct 08-Oct 09-Oct 10-Oct 11-Oct 12-Oct 13-Oct 14-Oct 15-Oct
0 50 100 150
data points

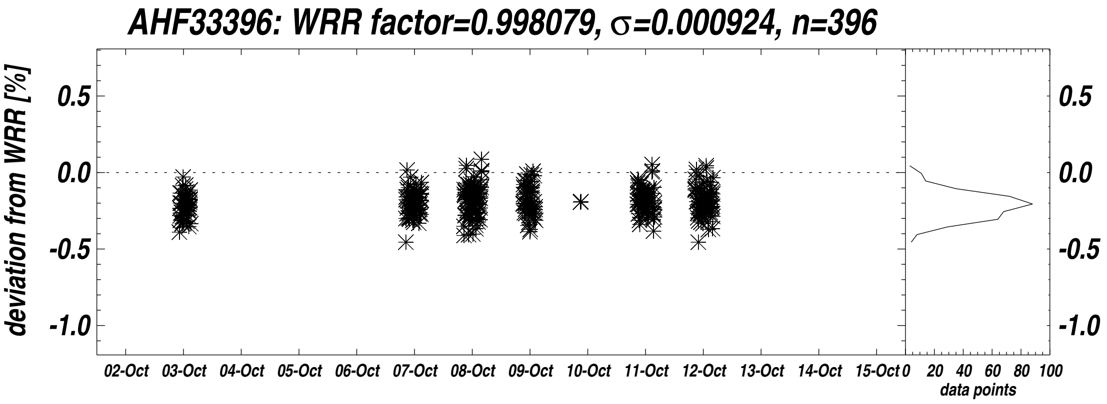
AHF33396: WRR factor=0.998079, σ=0.000924, n=396
deviation from WRR [%]
0.5
0.0
-0.5
-1.0
02-Oct 03-Oct 04-Oct 05-Oct 06-Oct 07-Oct 08-Oct 09-Oct 10-Oct 11-Oct 12-Oct 13-Oct 14-Oct 15-Oct
0 20 40 60 80 100
data points

AHF36011: WRR factor=0.996933, σ=0.002191, n=367

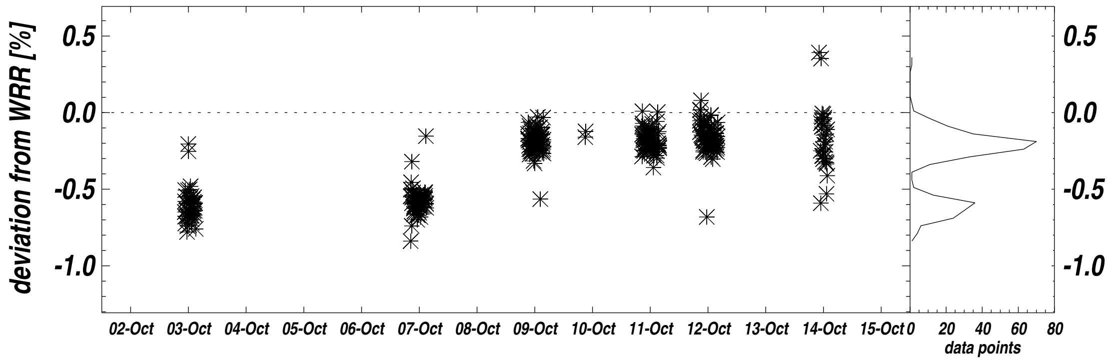

AHF36013: WRR factor=1.058110, σ=0.002462, n=384

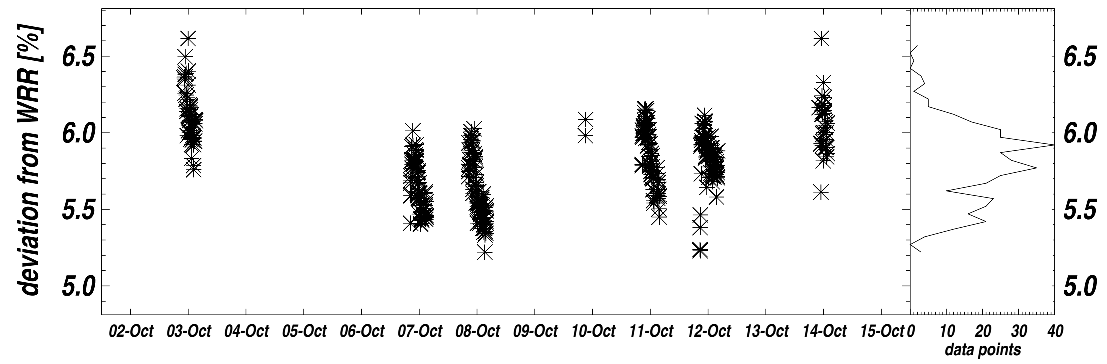

AWX31114: WRR factor=1.001240, σ=0.000893, n=462

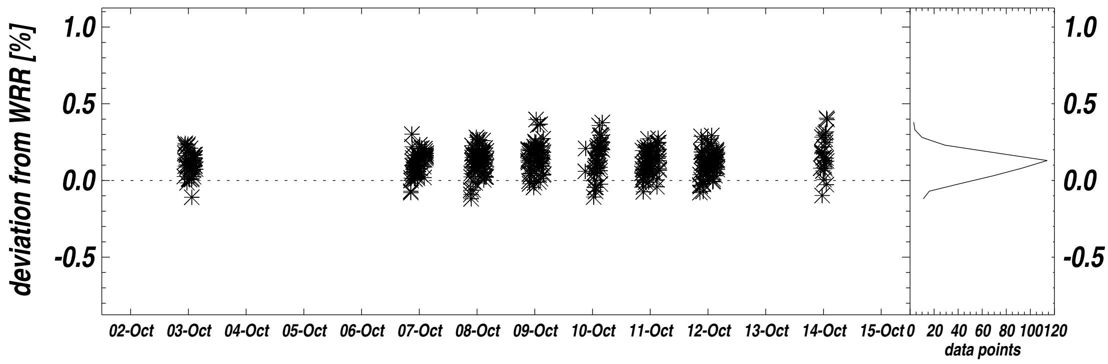

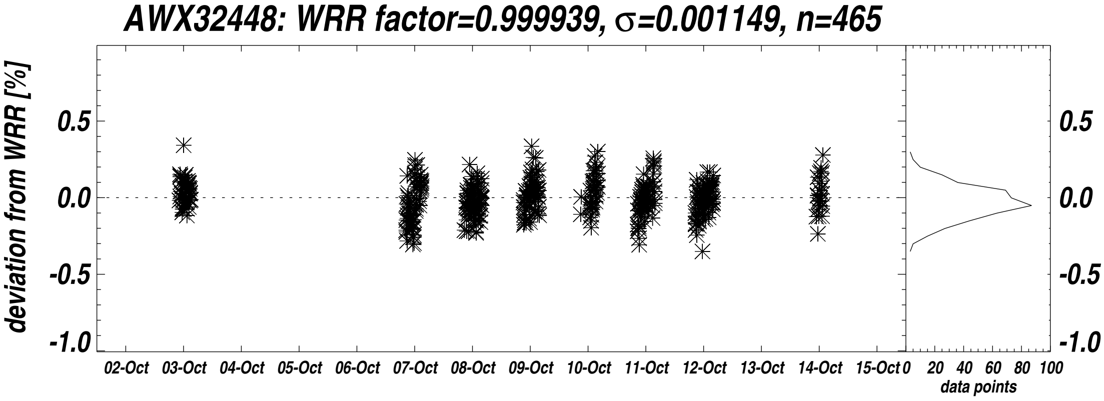
AWX32448: WRR factor=0.999939, σ=0.001149, n=465
deviation from WRR [%]
0.5
0.0
-0.5
-1.0
02-Oct 03-Oct 04-Oct 05-Oct 06-Oct 07-Oct 08-Oct 09-Oct 10-Oct 11-Oct 12-Oct 13-Oct 14-Oct 15-Oct
0 20 40 60 80 100
data points

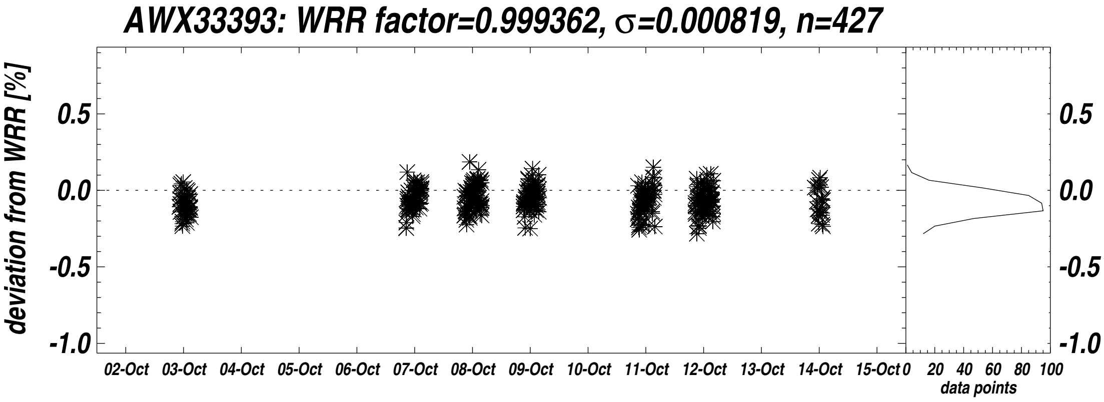
AWX33393: WRR factor=0.999362, σ=0.000819, n=427
deviation from WRR [%]
0.5
0.0
-0.5
-1.0
02-Oct 03-Oct 04-Oct 05-Oct 06-Oct 07-Oct 08-Oct 09-Oct 10-Oct 11-Oct 12-Oct 13-Oct 14-Oct 15-Oct
0 20 40 60 80 100
data points

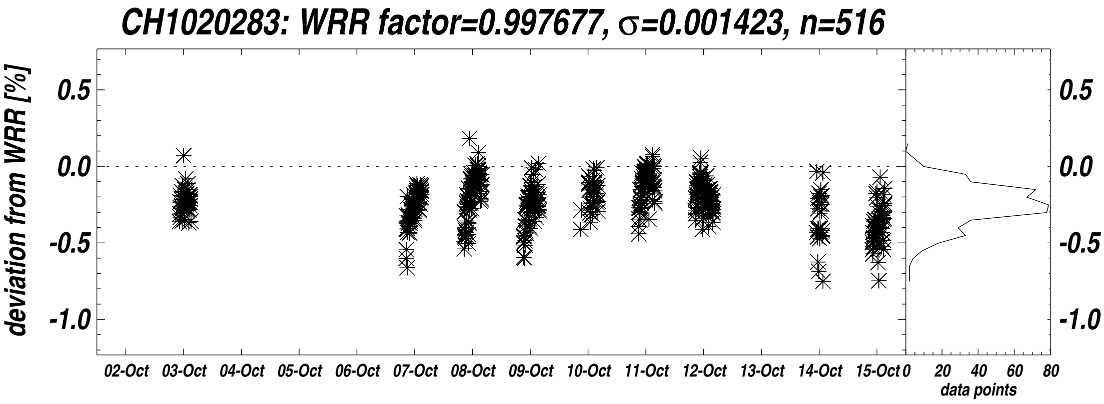
CH1020283: WRR factor=0.997677, σ=0.001423, n=516
deviation from WRR [%]
0.5
0.0
-0.5
-1.0
02-Oct 03-Oct 04-Oct 05-Oct 06-Oct 07-Oct 08-Oct 09-Oct 10-Oct 11-Oct 12-Oct 13-Oct 14-Oct 15-Oct
0 20 40 60 80
data points

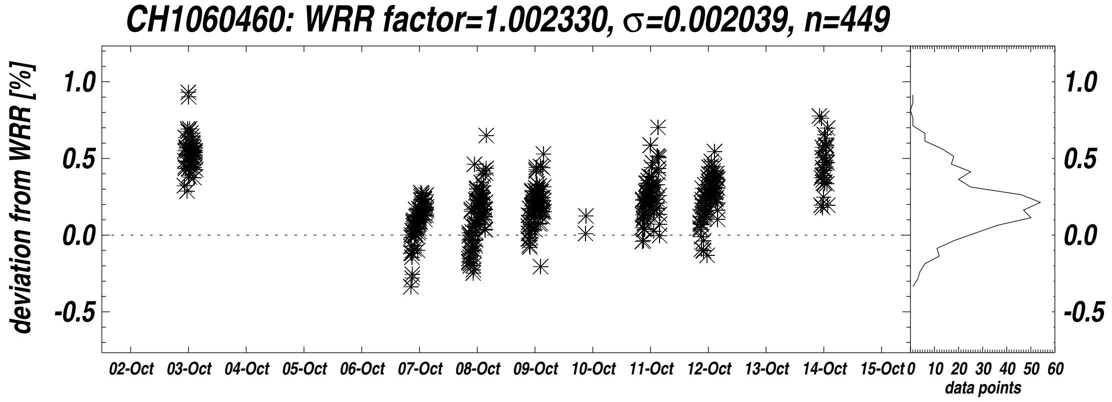
CH1060460: WRR factor=1.002330, σ=0.002039, n=449
deviation from WRR [%]
1.0
0.5
0.0
-0.5
02-Oct 03-Oct 04-Oct 05-Oct 06-Oct 07-Oct 08-Oct 09-Oct 10-Oct 11-Oct 12-Oct 13-Oct 14-Oct 15-Oct
0 10 20 30 40 50 60
data points

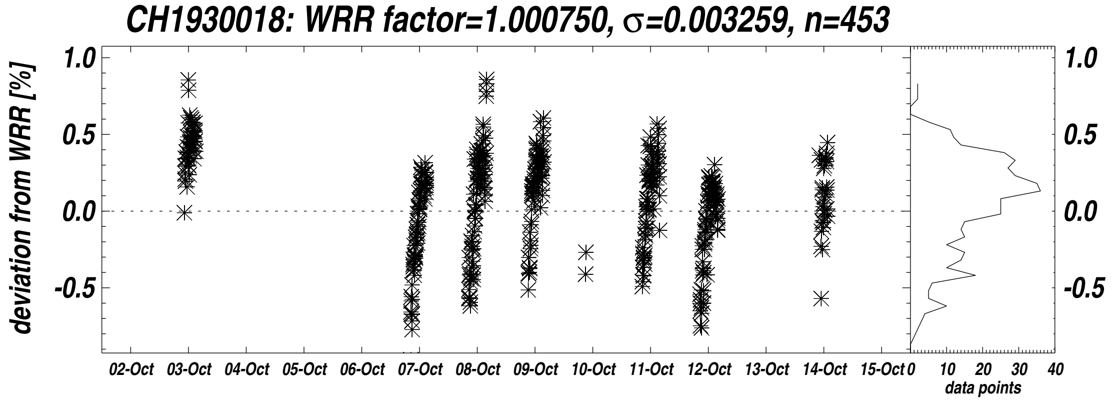
CH1930018: WRR factor=1.000750, σ=0.003259, n=453
deviation from WRR [%]
1.0
0.5
0.0
-0.5
02-Oct 03-Oct 04-Oct 05-Oct 06-Oct 07-Oct 08-Oct 09-Oct 10-Oct 11-Oct 12-Oct 13-Oct 14-Oct 15-Oct
0 10 20 30 40
data points

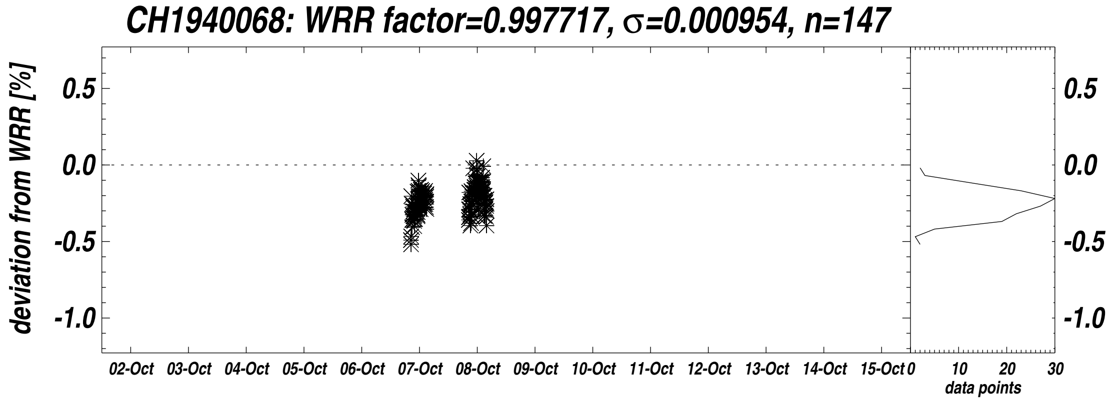
CH1940068: WRR factor=0.997717, σ=0.000954, n=147
deviation from WRR [%]
0.5
0.0
-0.5
-1.0
02-Oct 03-Oct 04-Oct 05-Oct 06-Oct 07-Oct 08-Oct 09-Oct 10-Oct 11-Oct 12-Oct 13-Oct 14-Oct 15-Oct
0 10 20 30
data points

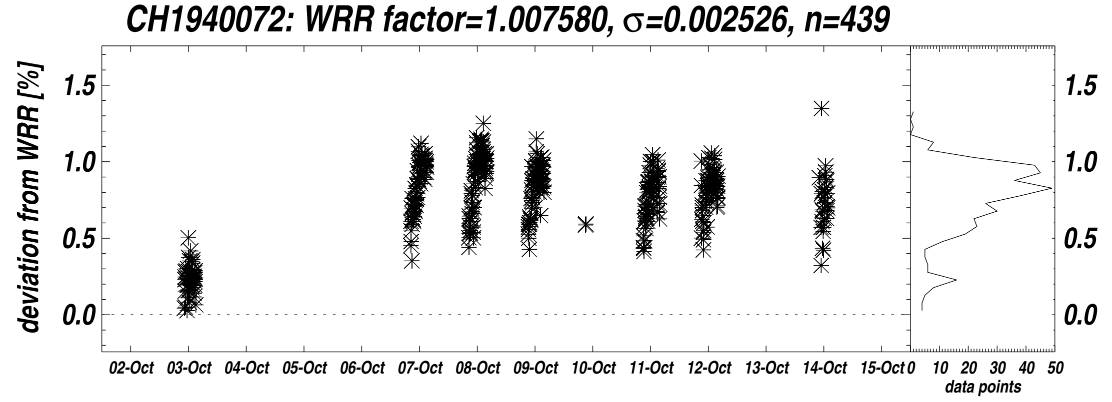
CH1940072: WRR factor=1.007580, σ=0.002526, n=439
deviation from WRR [%]
1.5
1.0
0.5
0.0
02-Oct 03-Oct 04-Oct 05-Oct 06-Oct 07-Oct 08-Oct 09-Oct 10-Oct 11-Oct 12-Oct 13-Oct 14-Oct 15-Oct
0 10 20 30 40 50
data points

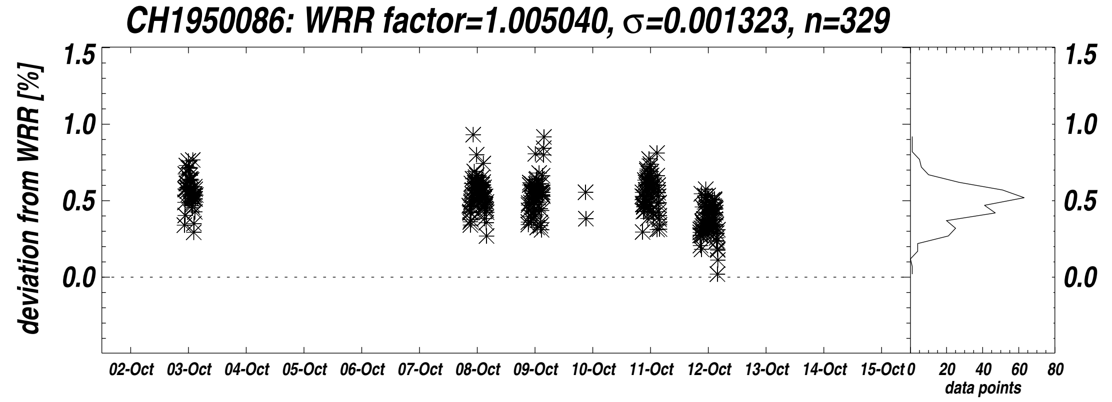
CH1950086: WRR factor=1.005040, σ=0.001323, n=329
deviation from WRR [%]
1.5
1.0
0.5
0.0
02-Oct 03-Oct 04-Oct 05-Oct 06-Oct 07-Oct 08-Oct 09-Oct 10-Oct 11-Oct 12-Oct 13-Oct 14-Oct 15-Oct
0 20 40 60 80
data points

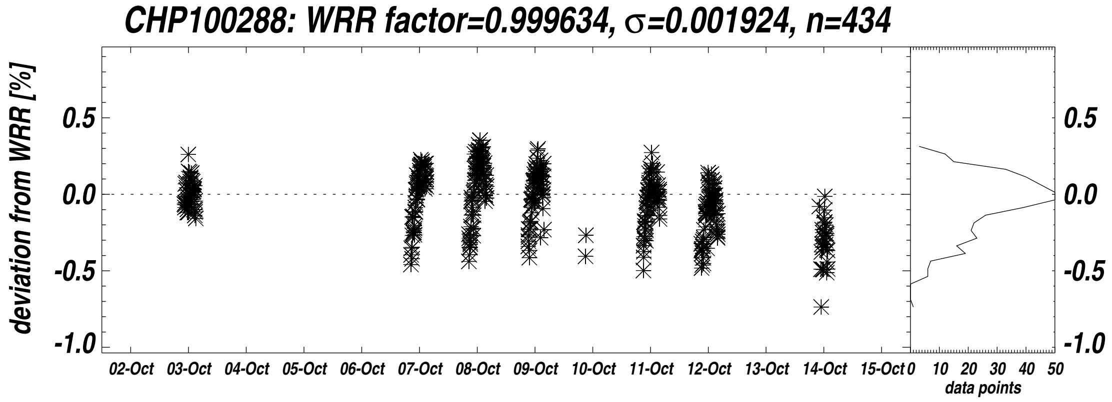
CHP100288: WRR factor=0.999634, σ=0.001924, n=434
deviation from WRR [%]
0.5
0.0
-0.5
-1.0
02-Oct 03-Oct 04-Oct 05-Oct 06-Oct 07-Oct 08-Oct 09-Oct 10-Oct 11-Oct 12-Oct 13-Oct 14-Oct 15-Oct
0 10 20 30 40 50
data points

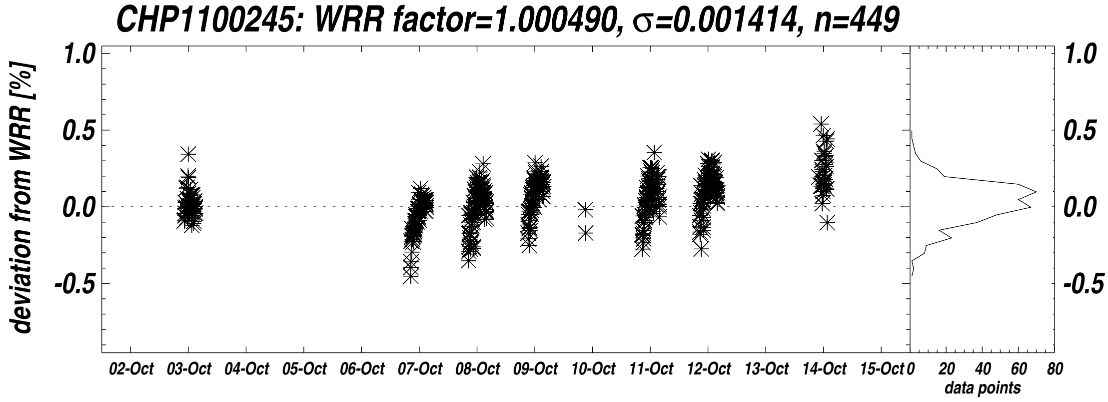
CHP1100245: WRR factor=1.000490, σ=0.001414, n=449
deviation from WRR [%]
1.0
0.5
0.0
-0.5
02-Oct 03-Oct 04-Oct 05-Oct 06-Oct 07-Oct 08-Oct 09-Oct 10-Oct 11-Oct 12-Oct 13-Oct 14-Oct 15-Oct
0 20 40 60 80
data points

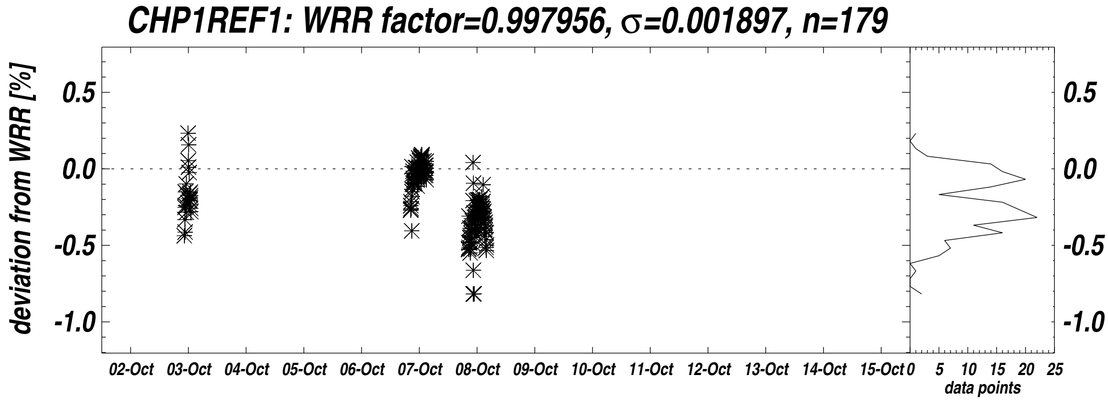
CHP1REF1: WRR factor=0.997956, σ=0.001897, n=179
deviation from WRR [%]
0.5
0.0
-0.5
-1.0
02-Oct 03-Oct 04-Oct 05-Oct 06-Oct 07-Oct 08-Oct 09-Oct 10-Oct 11-Oct 12-Oct 13-Oct 14-Oct 15-Oct
0 5 10 15 20 25
data points

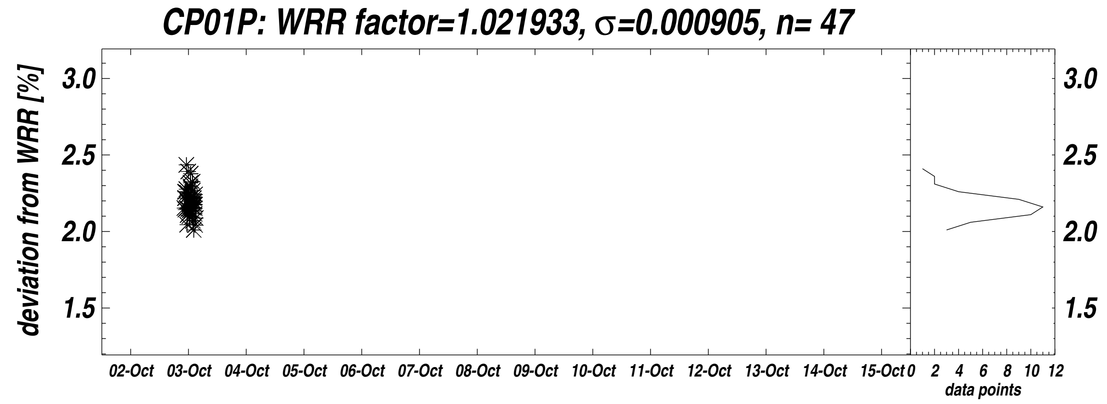
CP01P: WRR factor=1.021933, σ=0.000905, n= 47
deviation from WRR [%]
3.0
2.5
2.0
1.5
02-Oct 03-Oct 04-Oct 05-Oct 06-Oct 07-Oct 08-Oct 09-Oct 10-Oct 11-Oct 12-Oct 13-Oct 14-Oct 15-Oct
0 2 4 6 8 10 12
data points

CP01T: WRR factor=1.008928, σ=0.000635, n= 47

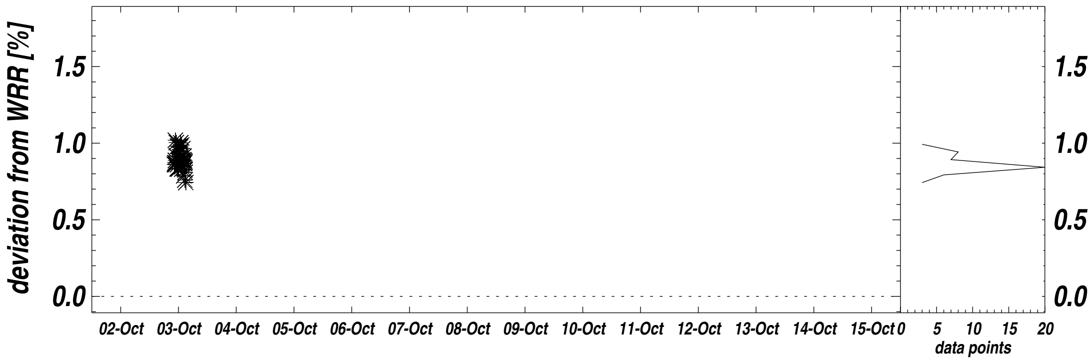

CP01U: WRR factor=1.018302, σ=0.001805, n= 49

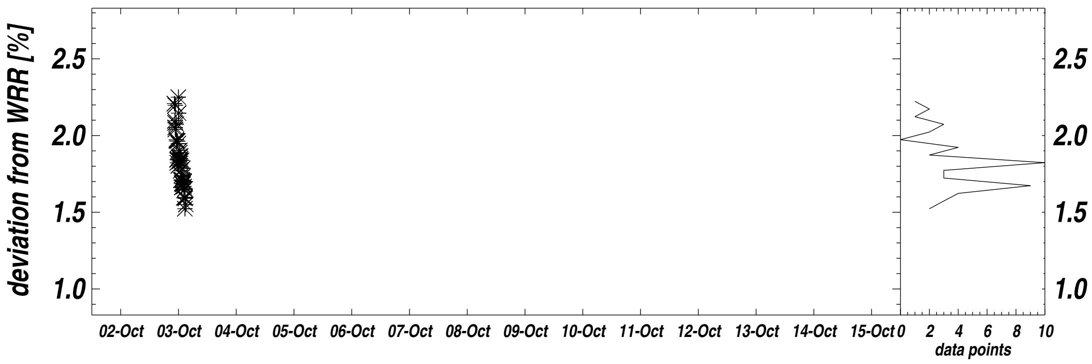

CR09L: WRR factor=0.998363, σ=0.000881, n=220

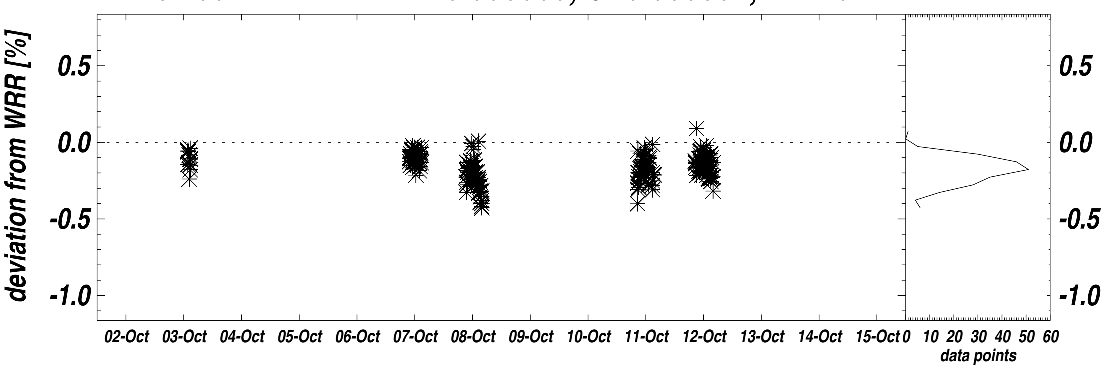

CROM2L: WRR factor=1.003166, σ=0.000451, n=544

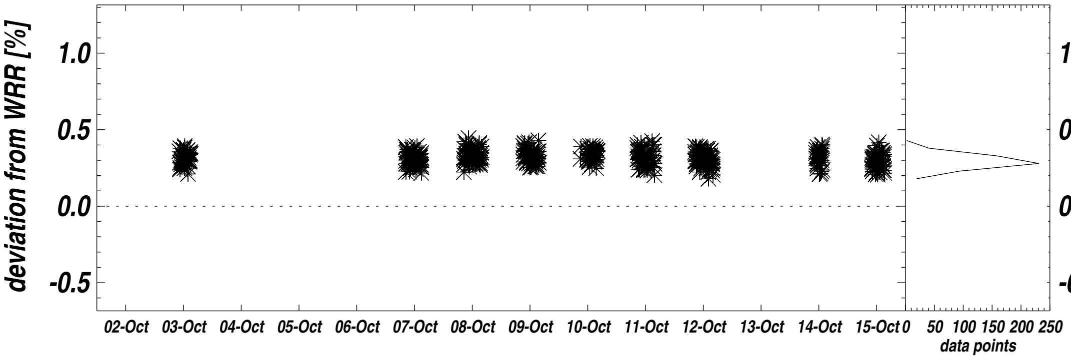

CSAR: WRR factor=0.992123, σ=0.000515, n= 28

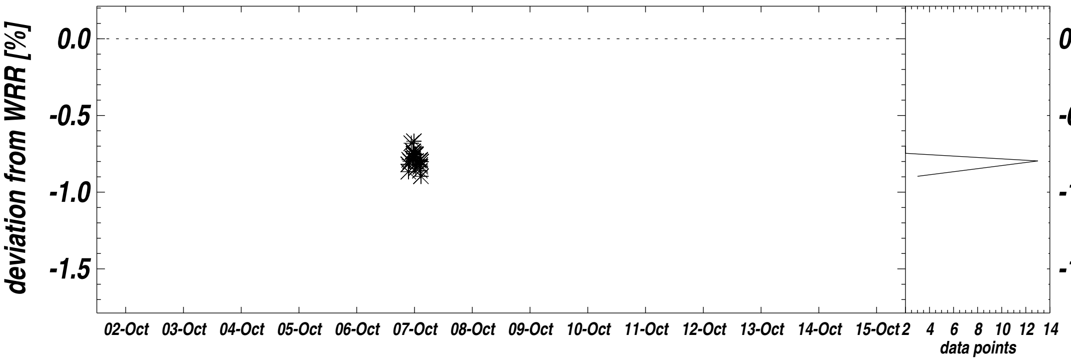

DARAAREFB: WRR factor=1.004210, σ=0.000847, n=143

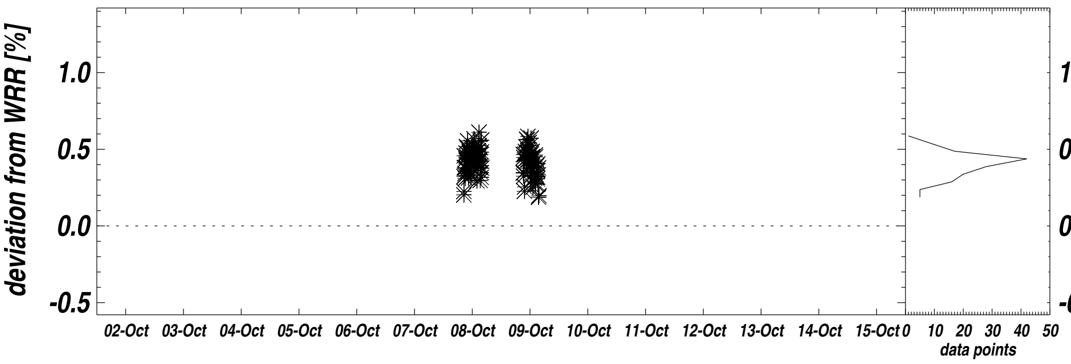

DARAAREFC: WRR factor=1.004358, σ=0.001266, n=141

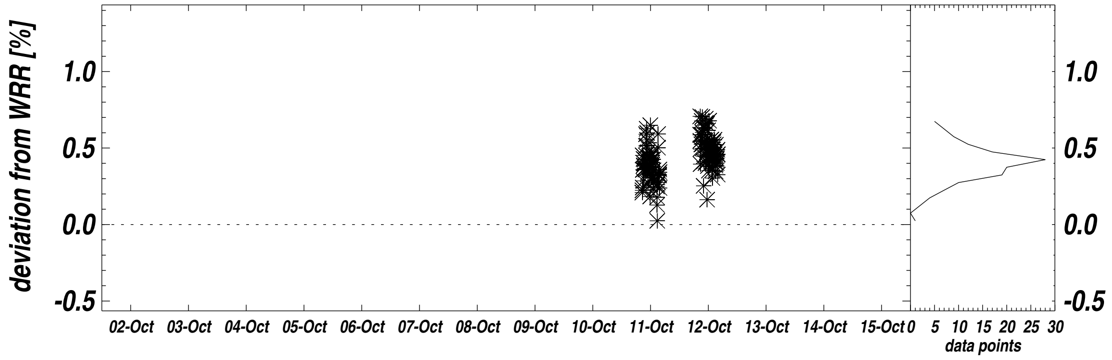

DARABREFC: WRR factor=1.006060, σ=0.001339, n=214

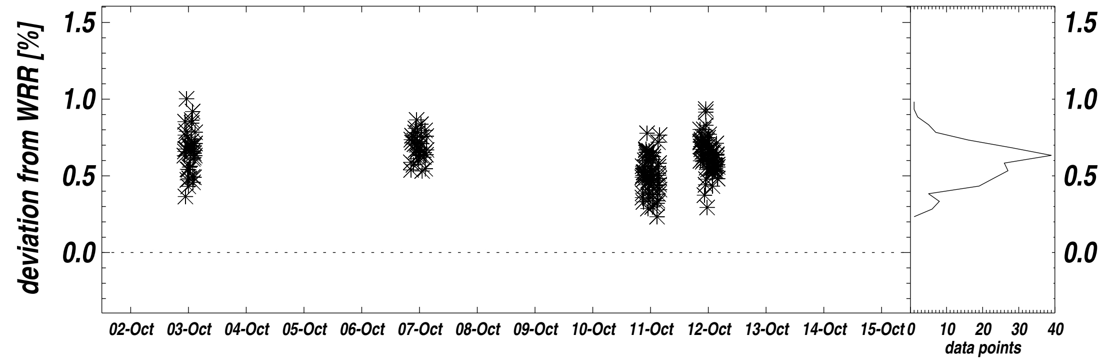

DARACREFB: WRR factor=1.004984, σ=0.001168, n=143

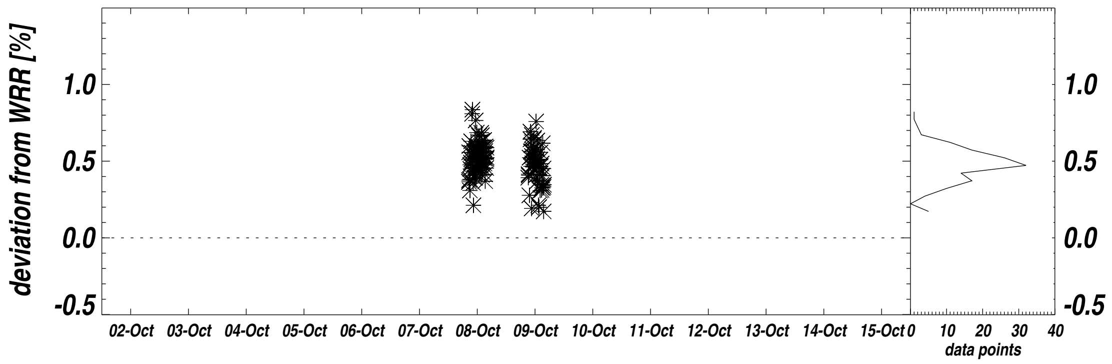

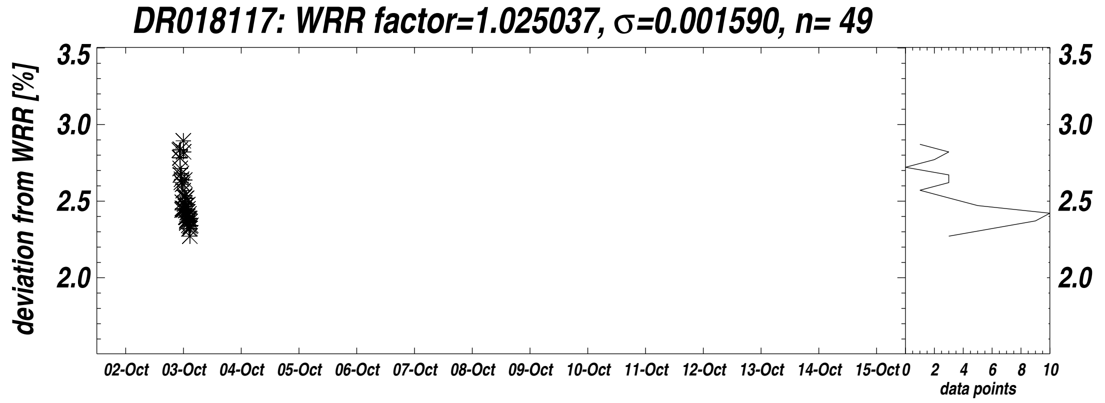
DR018117: WRR factor=1.025037, σ=0.001590, n= 49
deviation from WRR [%]
3.5
3.0
2.5
2.0
02-Oct 03-Oct 04-Oct 05-Oct 06-Oct 07-Oct 08-Oct 09-Oct 10-Oct 11-Oct 12-Oct 13-Oct 14-Oct 15-Oct
0 2 4 6 8 10
data points

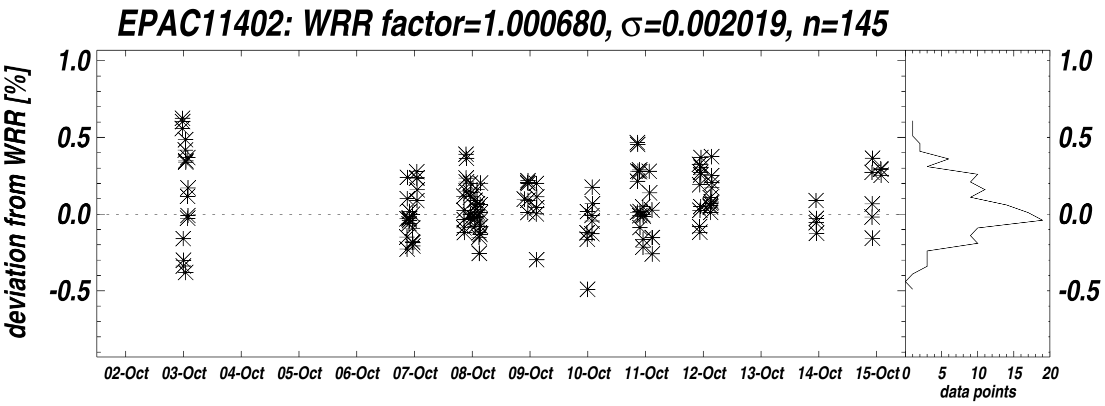
EPAC11402: WRR factor=1.000680, σ=0.002019, n=145
deviation from WRR [%]
1.0
0.5
0.0
-0.5
02-Oct 03-Oct 04-Oct 05-Oct 06-Oct 07-Oct 08-Oct 09-Oct 10-Oct 11-Oct 12-Oct 13-Oct 14-Oct 15-Oct
0 5 10 15 20
data points

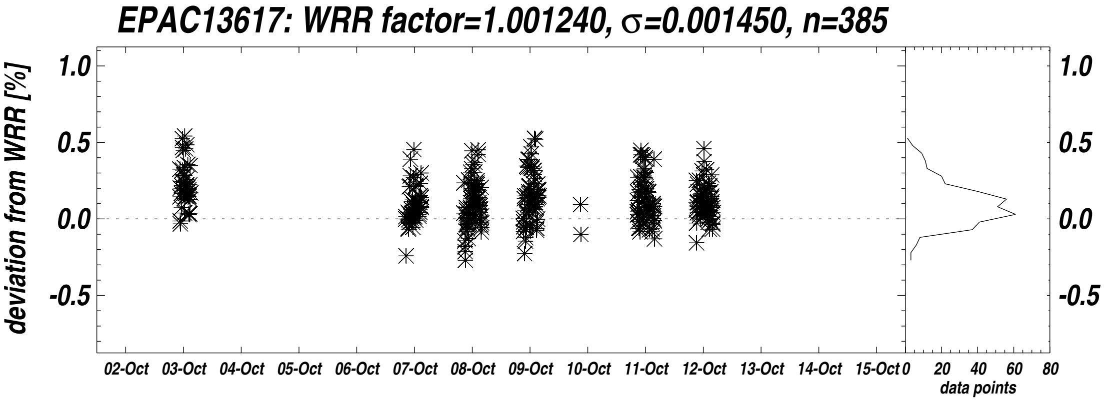
EPAC13617: WRR factor=1.001240, σ=0.001450, n=385
deviation from WRR [%]
1.0
0.5
0.0
-0.5
02-Oct 03-Oct 04-Oct 05-Oct 06-Oct 07-Oct 08-Oct 09-Oct 10-Oct 11-Oct 12-Oct 13-Oct 14-Oct 15-Oct
0 20 40 60 80
data points

HF15744: WRR factor=0.998085, σ=0.000707, n=303

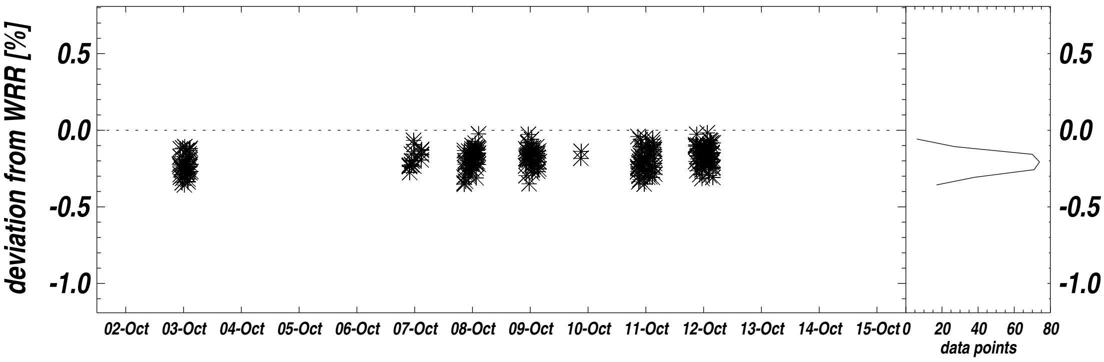

HF18747: WRR factor=1.001870, σ=0.000731, n=483

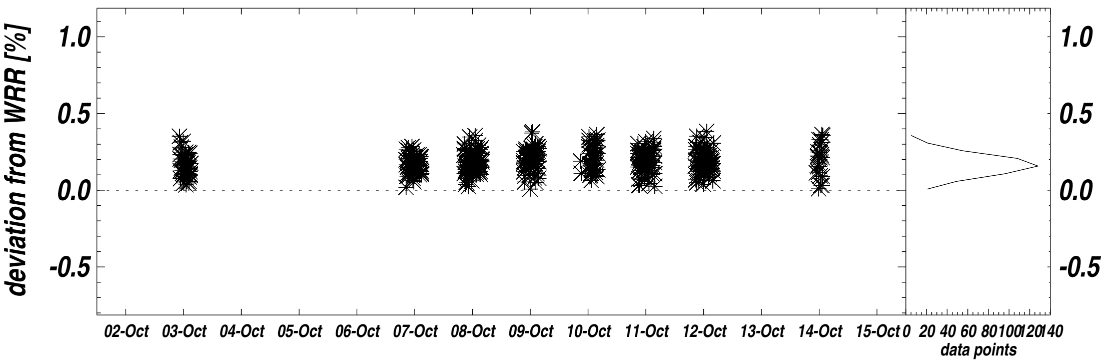

HF18748: WRR factor=0.997230, σ=0.000569, n=493

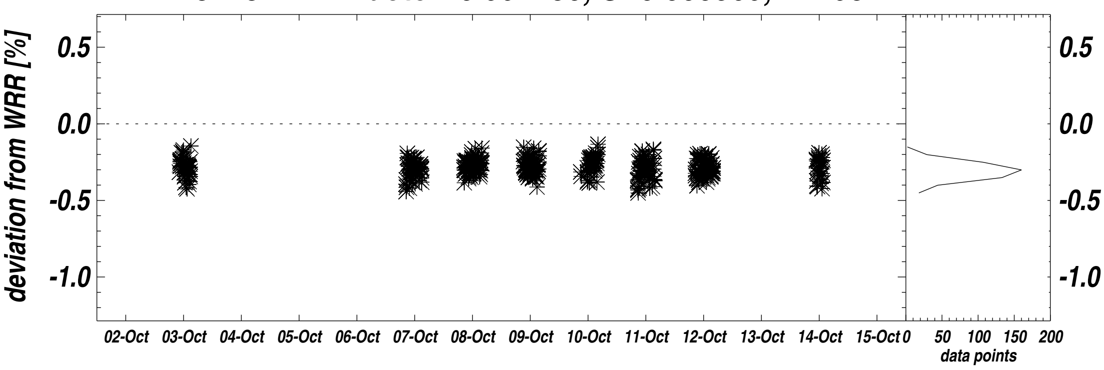

HF19746: WRR factor=0.998886, σ=0.000810, n=262

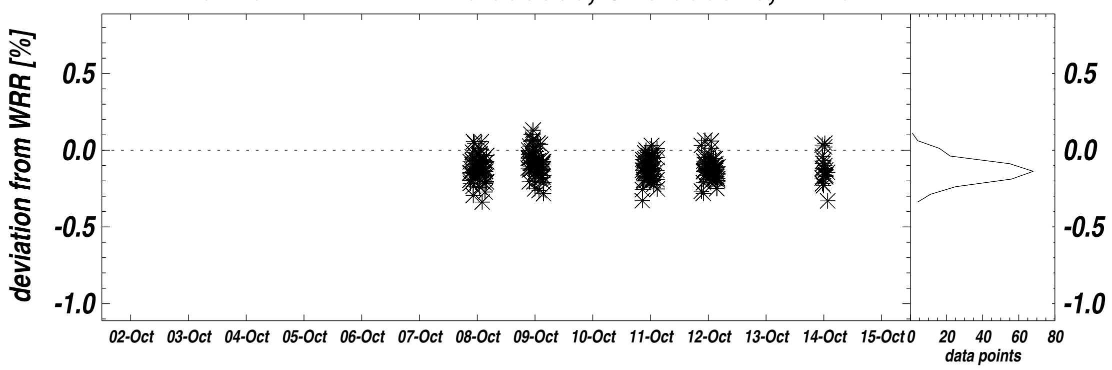

HF20406: WRR factor=1.002430, σ=0.000871, n=477

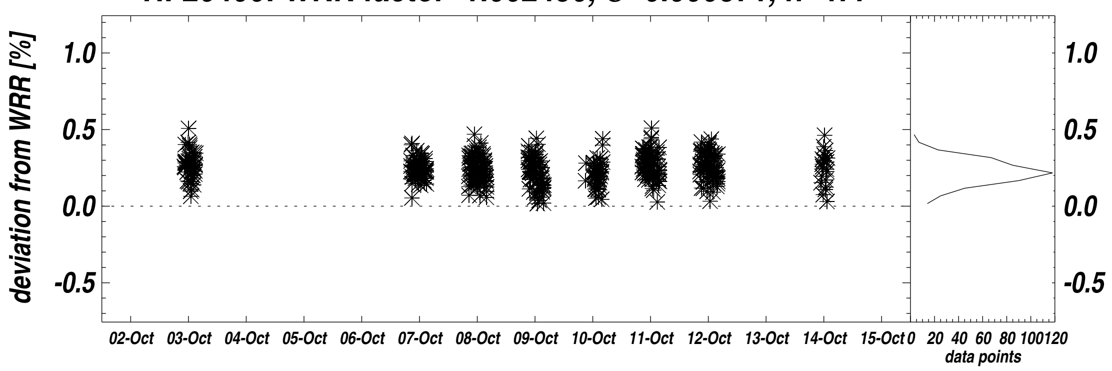

HF27157: WRR factor=0.999647, σ=0.001469, n=394

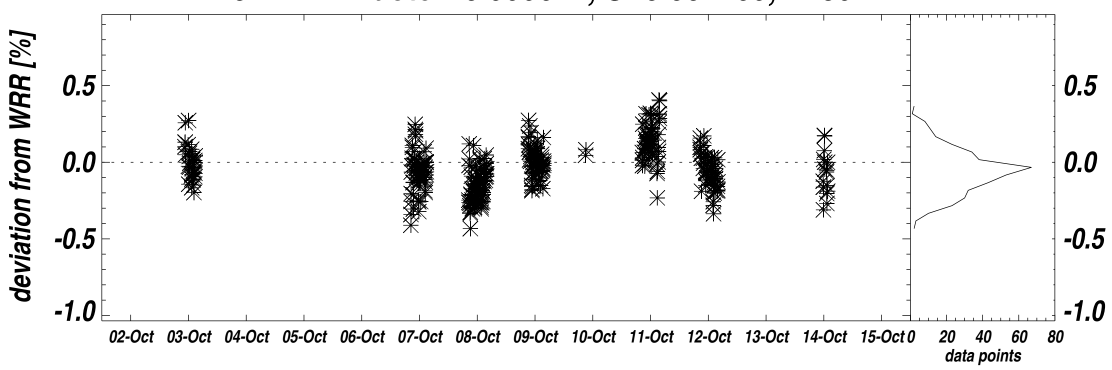

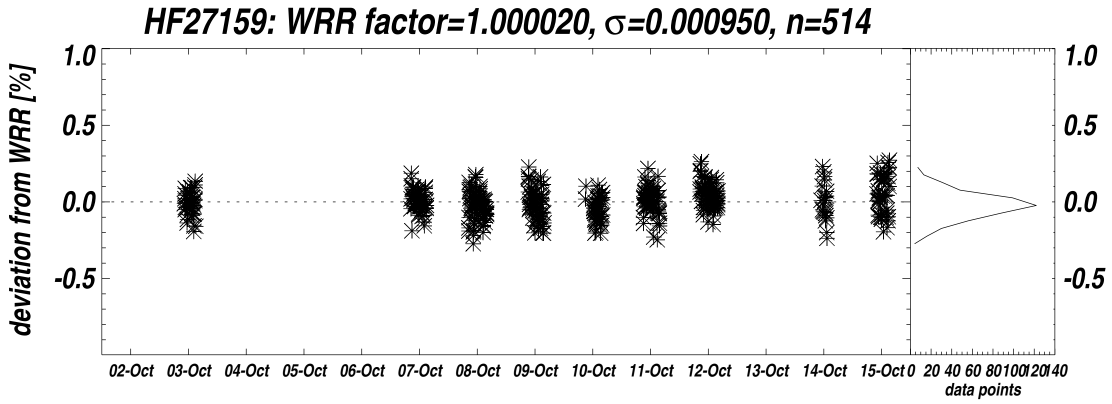
HF27159: WRR factor=1.000020, σ=0.000950, n=514
deviation from WRR [%]
1.0
0.5
0.0
-0.5
02-Oct
03-Oct
04-Oct
05-Oct
06-Oct
07-Oct
08-Oct
09-Oct
10-Oct
11-Oct
12-Oct
13-Oct
14-Oct
15-Oct
0 20 40 60 80 100 120 140
data points

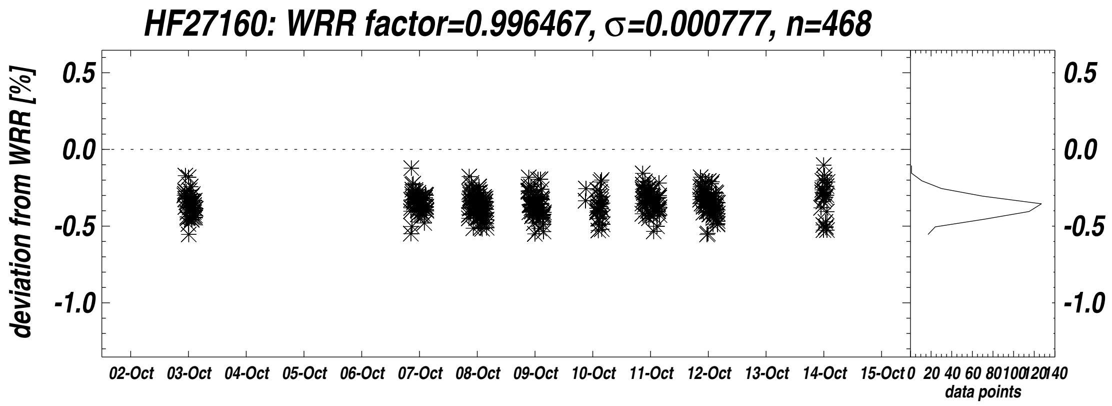
HF27160: WRR factor=0.996467, σ=0.000777, n=468
deviation from WRR [%]
0.5
0.0
-0.5
-1.0
02-Oct
03-Oct
04-Oct
05-Oct
06-Oct
07-Oct
08-Oct
09-Oct
10-Oct
11-Oct
12-Oct
13-Oct
14-Oct
15-Oct
0 20 40 60 80 100 120 140
data points

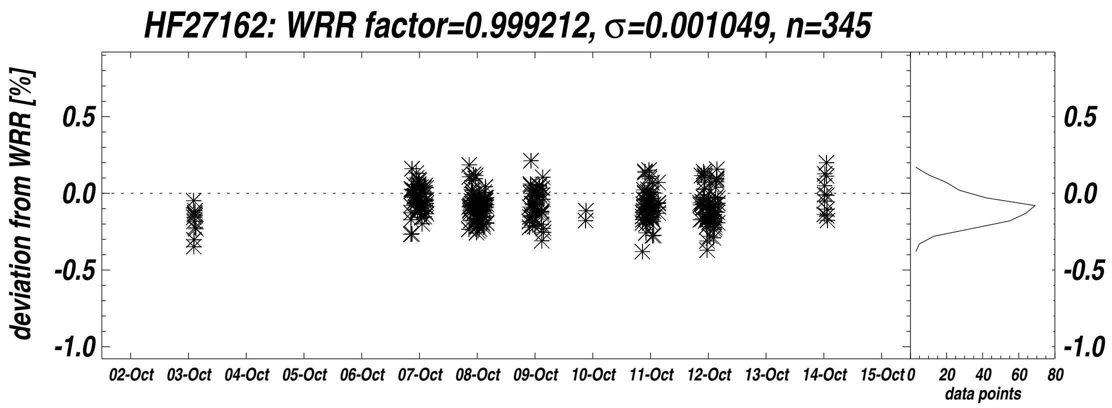
HF27162: WRR factor=0.999212, σ=0.001049, n=345
deviation from WRR [%]
0.5
0.0
-0.5
-1.0
02-Oct
03-Oct
04-Oct
05-Oct
06-Oct
07-Oct
08-Oct
09-Oct
10-Oct
11-Oct
12-Oct
13-Oct
14-Oct
15-Oct
0 20 40 60 80
data points

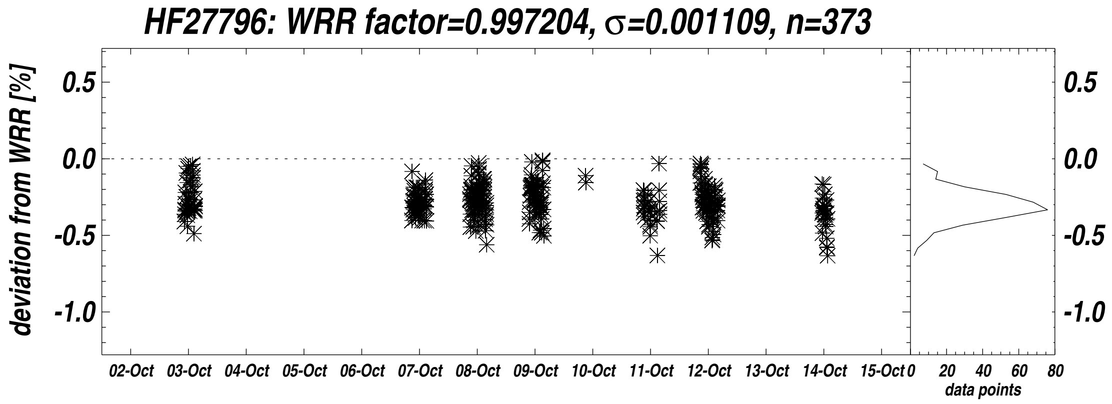
HF27796: WRR factor=0.997204, σ=0.001109, n=373
deviation from WRR [%]
0.5
0.0
-0.5
-1.0
02-Oct 03-Oct 04-Oct 05-Oct 06-Oct 07-Oct 08-Oct 09-Oct 10-Oct 11-Oct 12-Oct 13-Oct 14-Oct 15-Oct
0 20 40 60 80
data points

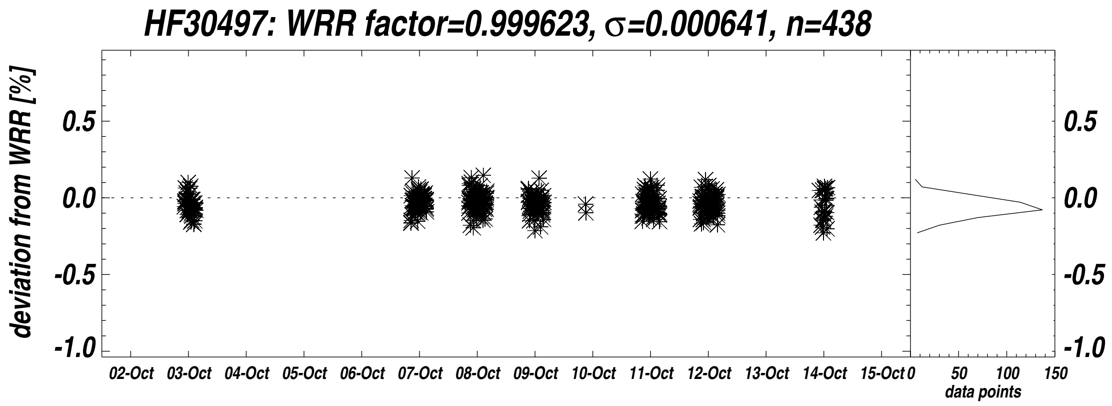
HF30497: WRR factor=0.999623, σ=0.000641, n=438
deviation from WRR [%]
0.5
0.0
-0.5
-1.0
02-Oct 03-Oct 04-Oct 05-Oct 06-Oct 07-Oct 08-Oct 09-Oct 10-Oct 11-Oct 12-Oct 13-Oct 14-Oct 15-Oct
0 50 100 150
data points

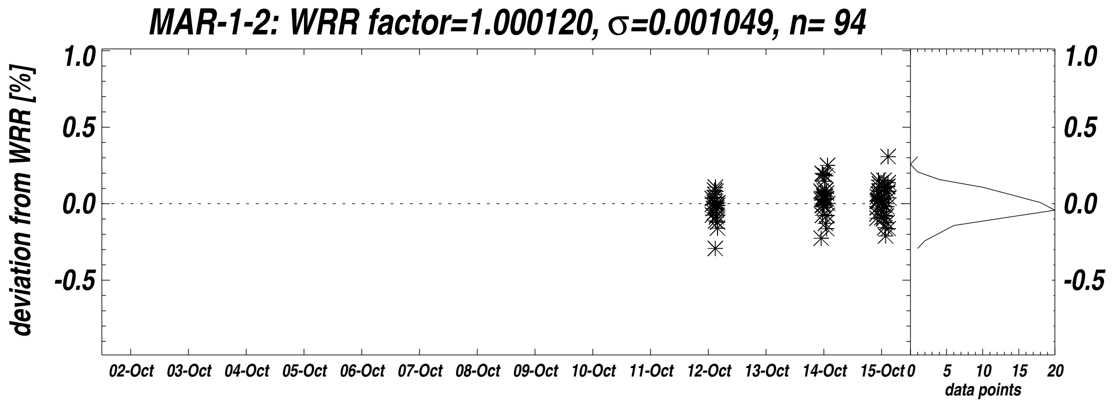
MAR-1-2: WRR factor=1.000120, σ=0.001049, n= 94
deviation from WRR [%]
1.0
0.5
0.0
-0.5
02-Oct 03-Oct 04-Oct 05-Oct 06-Oct 07-Oct 08-Oct 09-Oct 10-Oct 11-Oct 12-Oct 13-Oct 14-Oct 15-Oct
0 5 10 15 20
data points

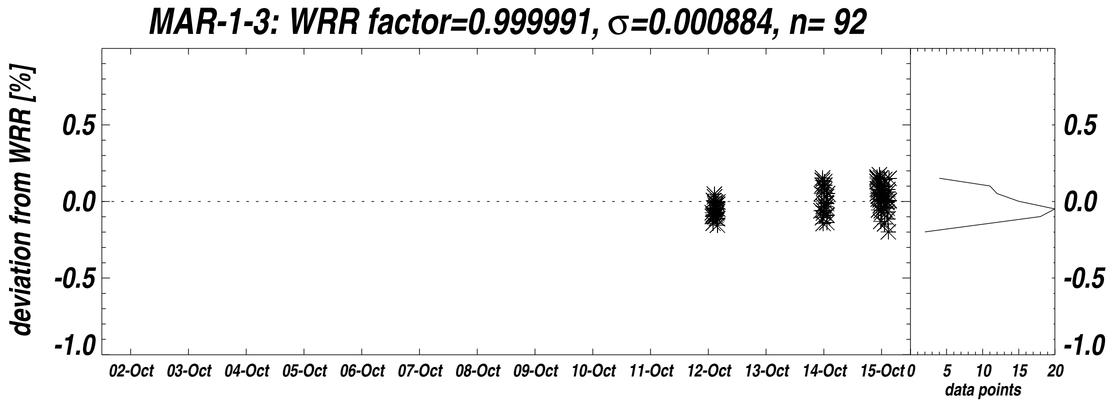
MAR-1-3: WRR factor=0.999991, σ=0.000884, n= 92
deviation from WRR [%]
0.5
0.0
-0.5
-1.0
02-Oct 03-Oct 04-Oct 05-Oct 06-Oct 07-Oct 08-Oct 09-Oct 10-Oct 11-Oct 12-Oct 13-Oct 14-Oct 15-Oct
0 5 10 15 20
data points

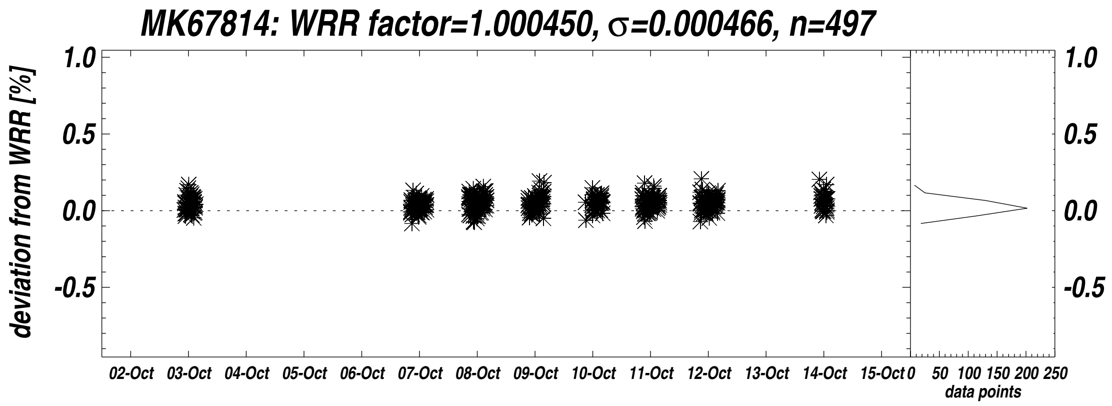
MK67814: WRR factor=1.000450, σ=0.000466, n=497
deviation from WRR [%]
1.0
0.5
0.0
-0.5
02-Oct 03-Oct 04-Oct 05-Oct 06-Oct 07-Oct 08-Oct 09-Oct 10-Oct 11-Oct 12-Oct 13-Oct 14-Oct 15-Oct
0 50 100 150 200 250
data points

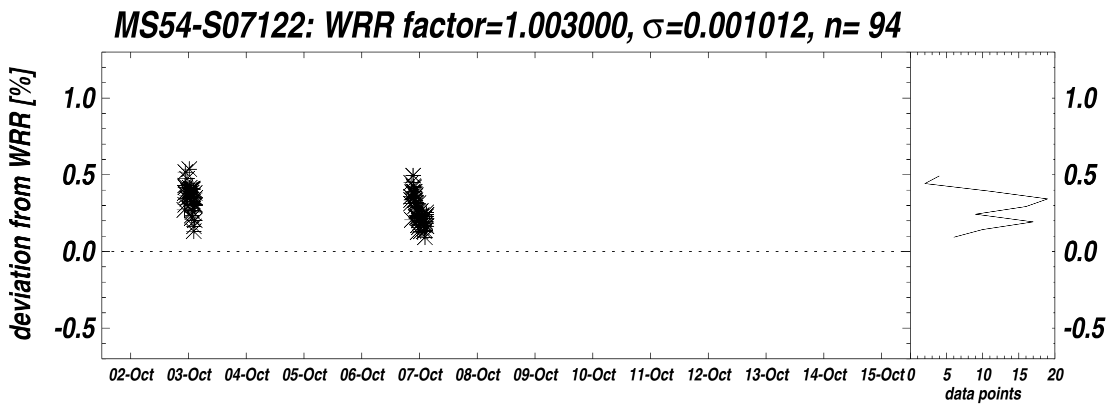
MS54-S07122: WRR factor=1.003000, σ=0.001012, n= 94
deviation from WRR [%]
1.0
0.5
0.0
-0.5
02-Oct 03-Oct 04-Oct 05-Oct 06-Oct 07-Oct 08-Oct 09-Oct 10-Oct 11-Oct 12-Oct 13-Oct 14-Oct 15-Oct
0 5 10 15 20
data points

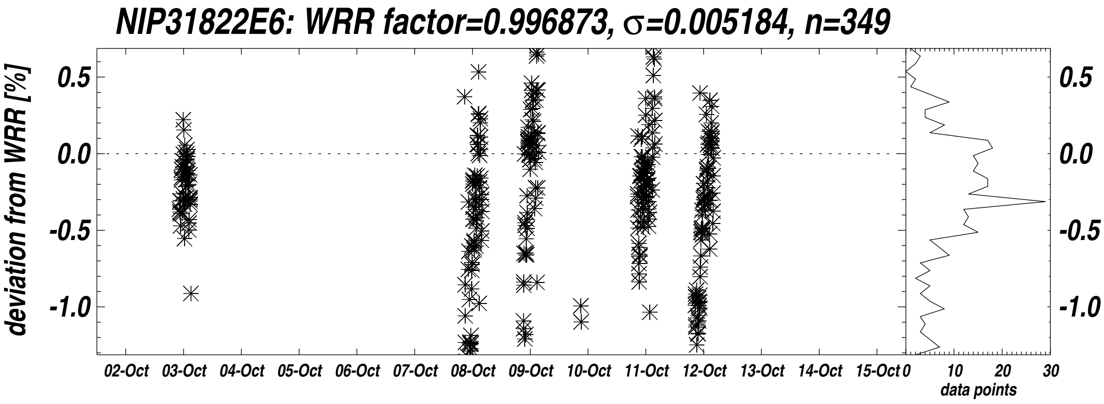
NIP31822E6: WRR factor=0.996873, σ=0.005184, n=349
deviation from WRR [%]
data points

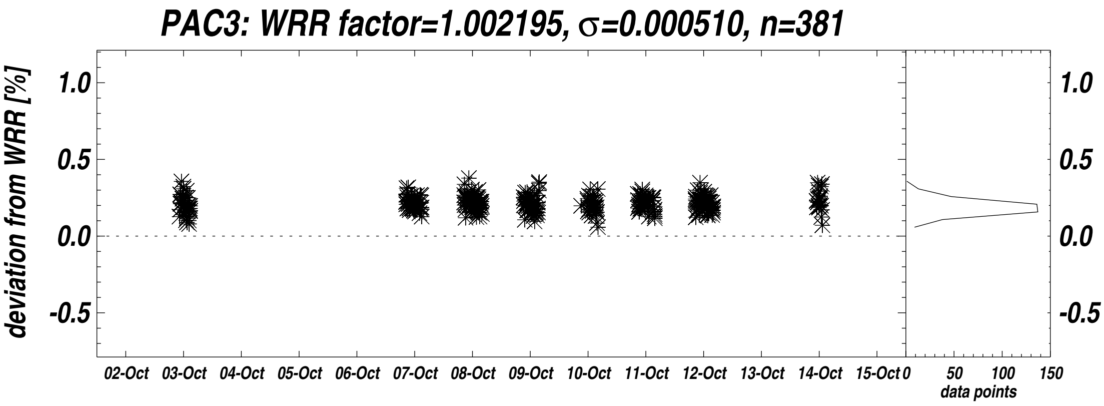
PAC3: WRR factor=1.002195, σ=0.000510, n=381
deviation from WRR [%]
data points

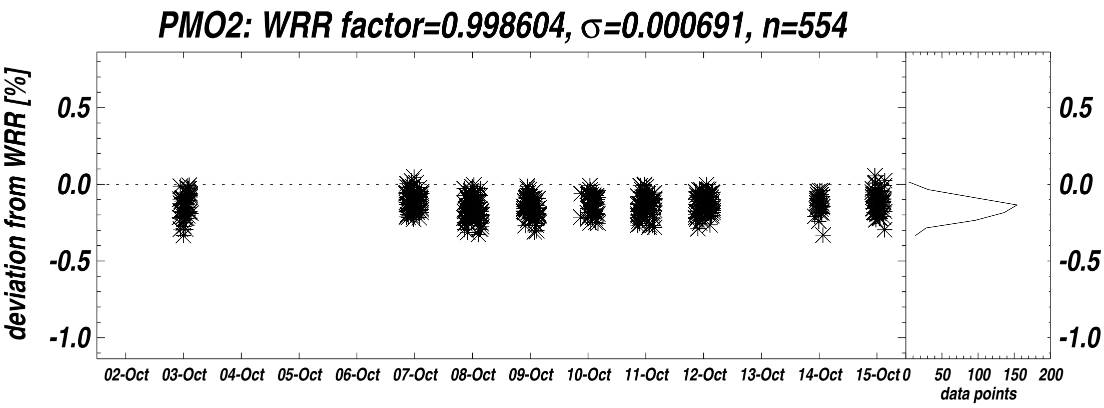
PMO2: WRR factor=0.998604, σ=0.000691, n=554
deviation from WRR [%]
data points

PMO5: WRR factor=0.999044, σ=0.000528, n=554

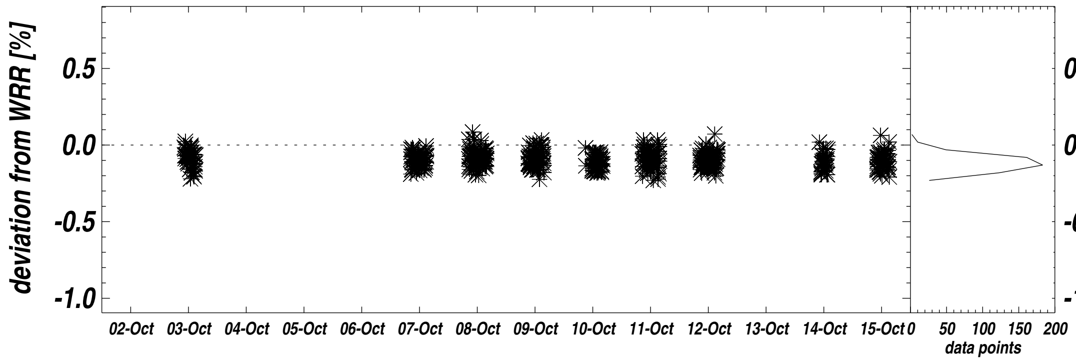

PMO6-0101-CERNY-PS: WRR factor=1.005155, σ=0.000465, n=437

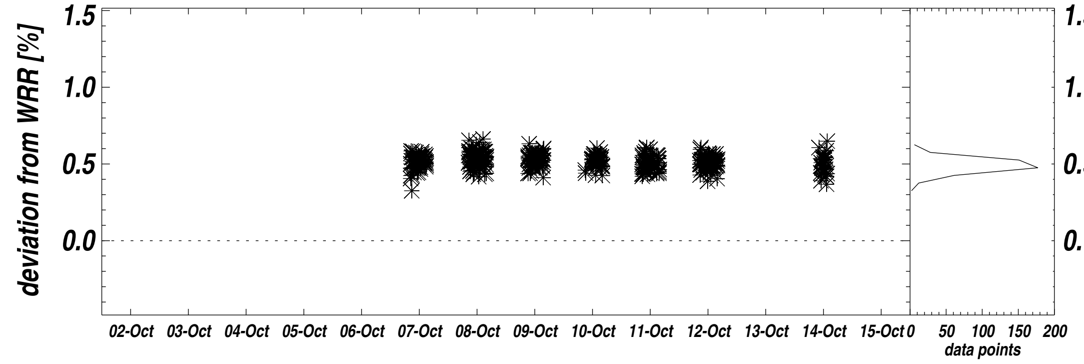

PMO6-0101-CERNY-T: WRR factor=1.004938, σ=0.000505, n=486

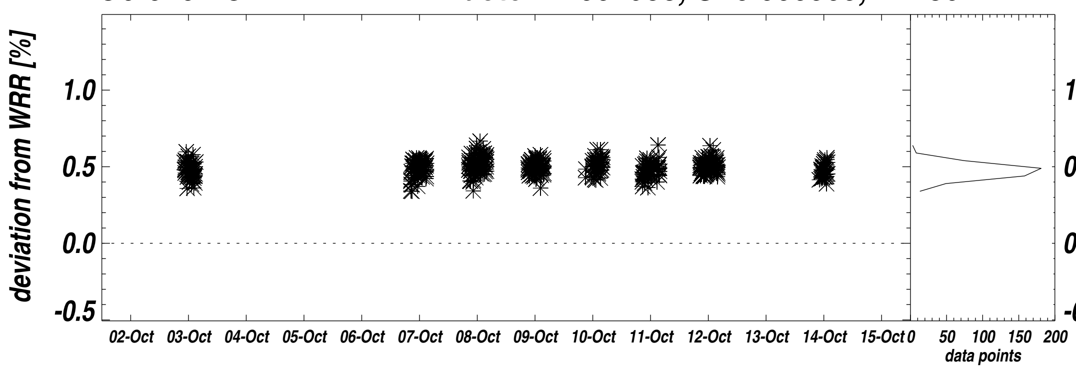

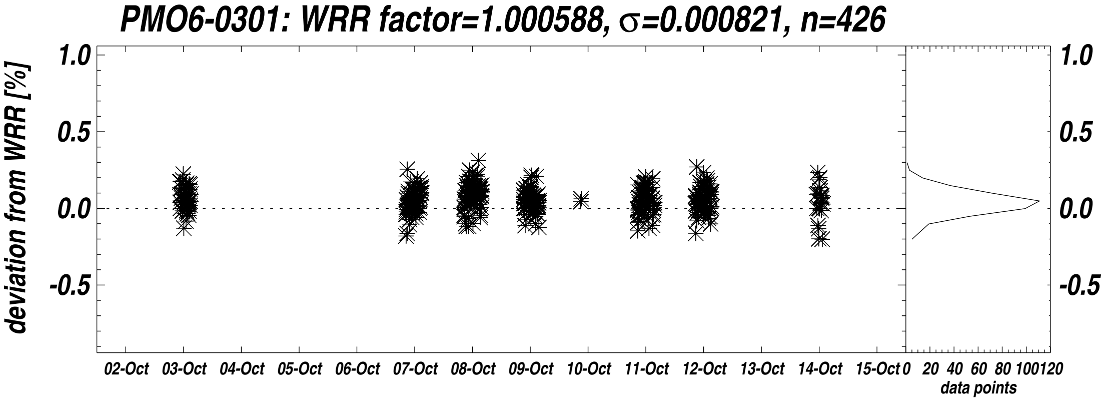
PMO6-0301: WRR factor=1.000588, σ=0.000821, n=426
deviation from WRR [%]
1.0
0.5
0.0
-0.5
02-Oct 03-Oct 04-Oct 05-Oct 06-Oct 07-Oct 08-Oct 09-Oct 10-Oct 11-Oct 12-Oct 13-Oct 14-Oct 15-Oct
0 20 40 60 80 100 120
data points

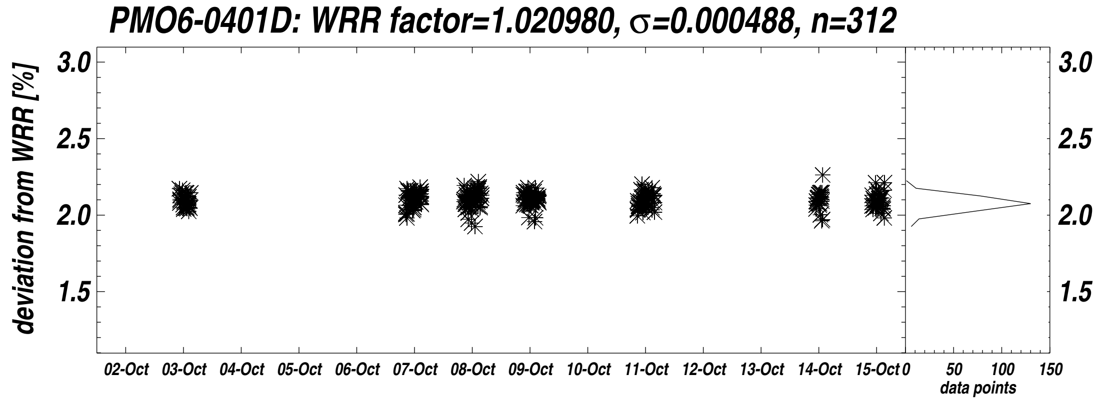
PMO6-0401D: WRR factor=1.020980, σ=0.000488, n=312
deviation from WRR [%]
3.0
2.5
2.0
1.5
02-Oct 03-Oct 04-Oct 05-Oct 06-Oct 07-Oct 08-Oct 09-Oct 10-Oct 11-Oct 12-Oct 13-Oct 14-Oct 15-Oct
0 50 100 150
data points

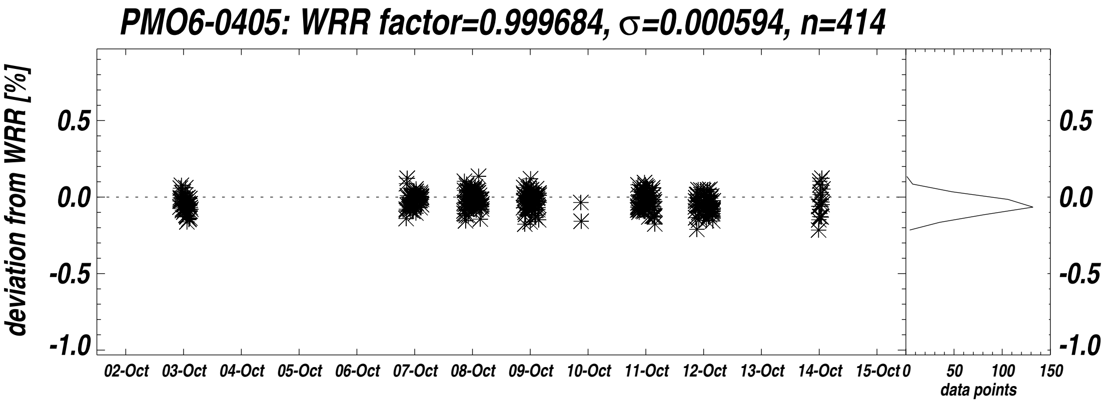
PMO6-0405: WRR factor=0.999684, σ=0.000594, n=414
deviation from WRR [%]
0.5
0.0
-0.5
-1.0
02-Oct 03-Oct 04-Oct 05-Oct 06-Oct 07-Oct 08-Oct 09-Oct 10-Oct 11-Oct 12-Oct 13-Oct 14-Oct 15-Oct
0 50 100 150
data points


PMO6-0801D: WRR factor=1.137201, σ=0.001542, n=484
deviation from WRR [%]
14.5
14.0
13.5
13.0
02-Oct 03-Oct 04-Oct 05-Oct 06-Oct 07-Oct 08-Oct 09-Oct 10-Oct 11-Oct 12-Oct 13-Oct 14-Oct 15-Oct
0 20 40 60 80
data points

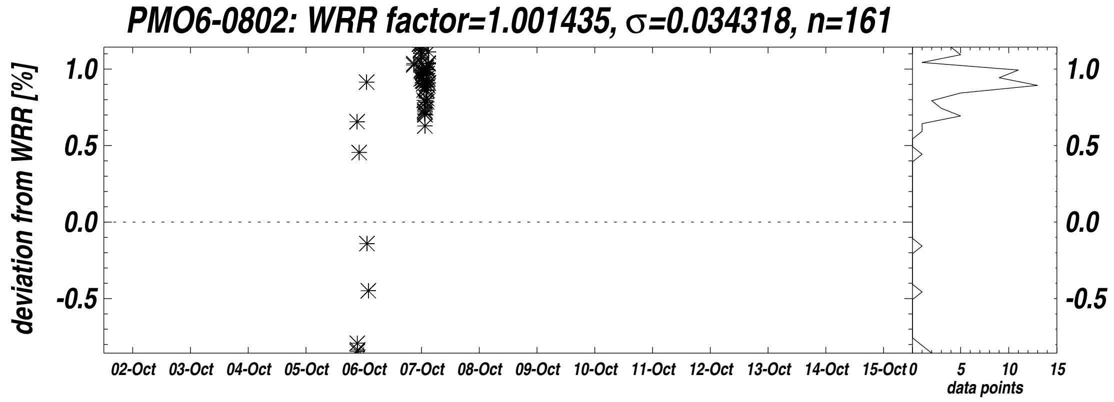
PMO6-0802: WRR factor=1.001435, σ=0.034318, n=161
deviation from WRR [%]
1.0
0.5
0.0
-0.5
02-Oct 03-Oct 04-Oct 05-Oct 06-Oct 07-Oct 08-Oct 09-Oct 10-Oct 11-Oct 12-Oct 13-Oct 14-Oct 15-Oct
0 5 10 15
data points

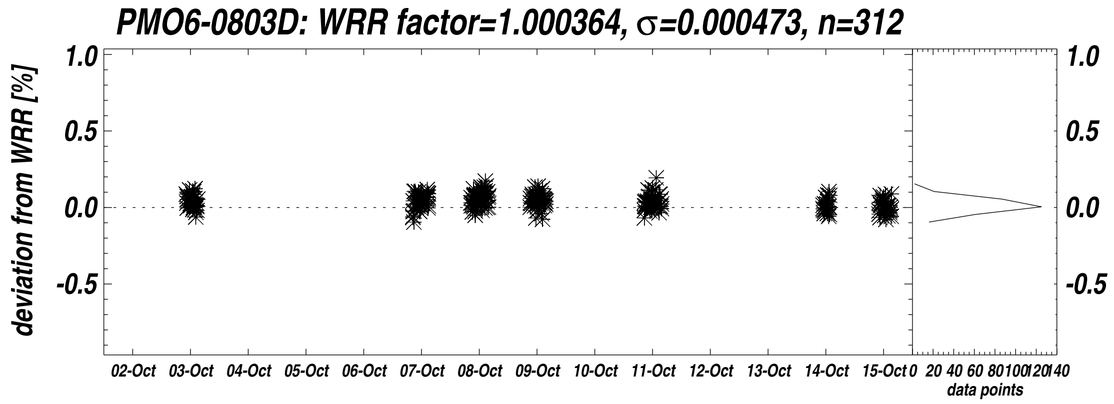
PMO6-0803D: WRR factor=1.000364, σ=0.000473, n=312
deviation from WRR [%]
1.0
0.5
0.0
-0.5
02-Oct 03-Oct 04-Oct 05-Oct 06-Oct 07-Oct 08-Oct 09-Oct 10-Oct 11-Oct 12-Oct 13-Oct 14-Oct 15-Oct
0 20 40 60 80 100 120 140
data points

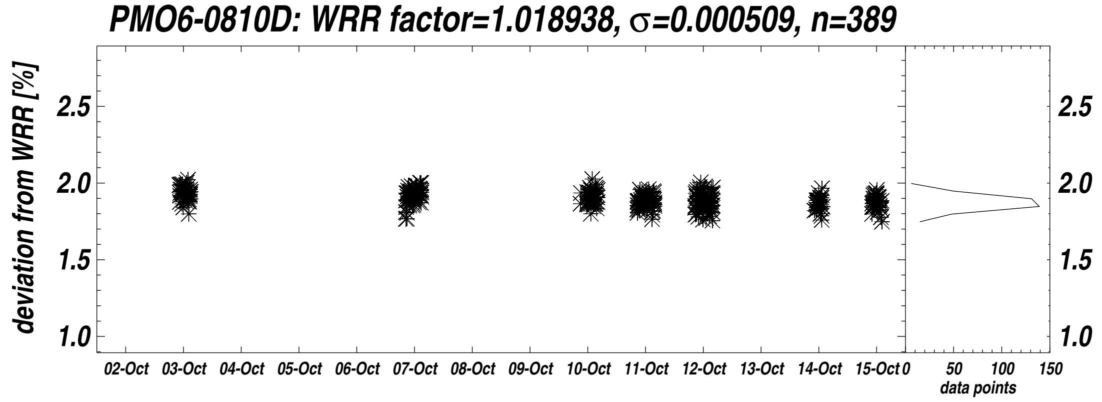
PMO6-0810D: WRR factor=1.018938, σ=0.000509, n=389
deviation from WRR [%]
2.5
2.0
1.5
1.0
02-Oct 03-Oct 04-Oct 05-Oct 06-Oct 07-Oct 08-Oct 09-Oct 10-Oct 11-Oct 12-Oct 13-Oct 14-Oct 15-Oct
0 50 100 150
data points

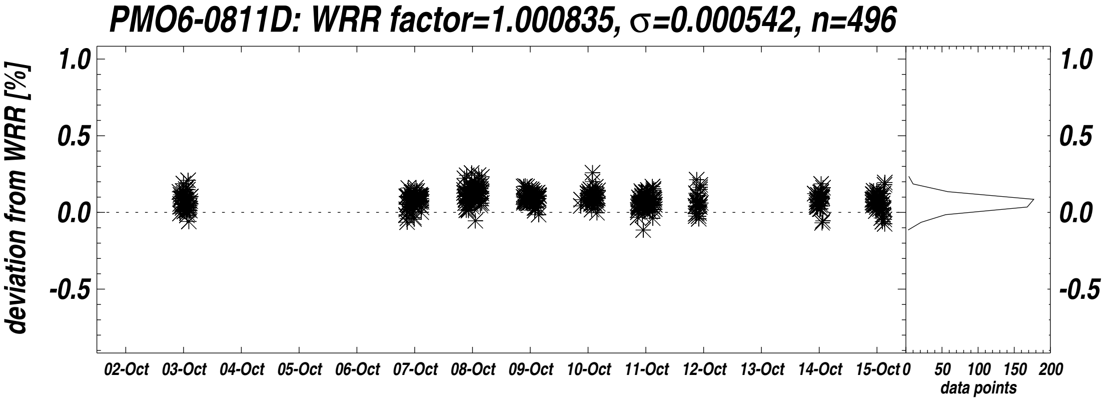
PMO6-0811D: WRR factor=1.000835, σ=0.000542, n=496
deviation from WRR [%]
1.0
0.5
0.0
-0.5
02-Oct 03-Oct 04-Oct 05-Oct 06-Oct 07-Oct 08-Oct 09-Oct 10-Oct 11-Oct 12-Oct 13-Oct 14-Oct 15-Oct
0 50 100 150 200
data points

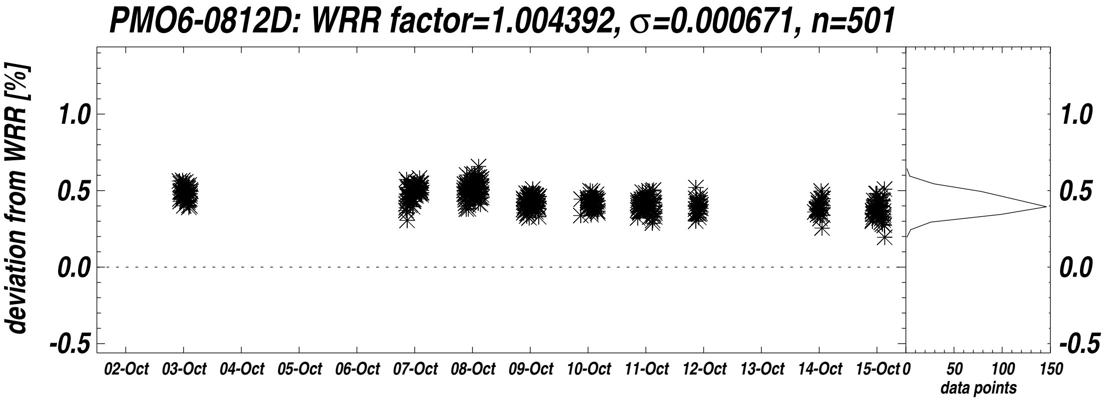
PMO6-0812D: WRR factor=1.004392, σ=0.000671, n=501
deviation from WRR [%]
1.0
0.5
0.0
-0.5
02-Oct 03-Oct 04-Oct 05-Oct 06-Oct 07-Oct 08-Oct 09-Oct 10-Oct 11-Oct 12-Oct 13-Oct 14-Oct 15-Oct
0 50 100 150
data points

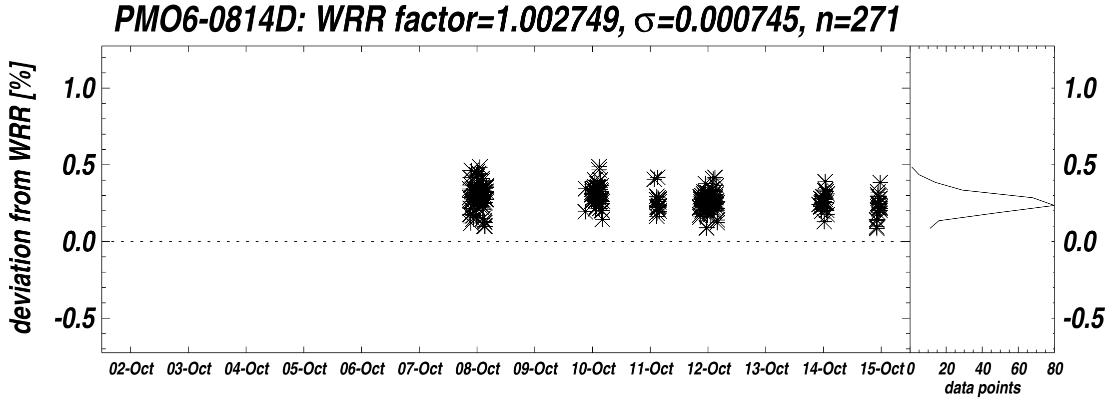
PMO6-0814D: WRR factor=1.002749, σ=0.000745, n=271
deviation from WRR [%]
1.0
0.5
0.0
-0.5
02-Oct
03-Oct
04-Oct
05-Oct
06-Oct
07-Oct
08-Oct
09-Oct
10-Oct
11-Oct
12-Oct
13-Oct
14-Oct
15-Oct
0
20
40
60
80
data points

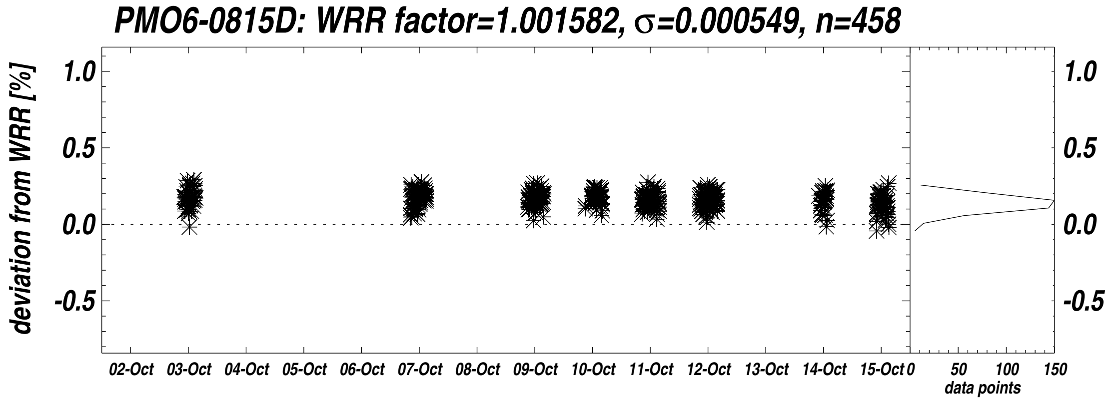
PMO6-0815D: WRR factor=1.001582, σ=0.000549, n=458
deviation from WRR [%]
1.0
0.5
0.0
-0.5
02-Oct
03-Oct
04-Oct
05-Oct
06-Oct
07-Oct
08-Oct
09-Oct
10-Oct
11-Oct
12-Oct
13-Oct
14-Oct
15-Oct
0
50
100
150
data points

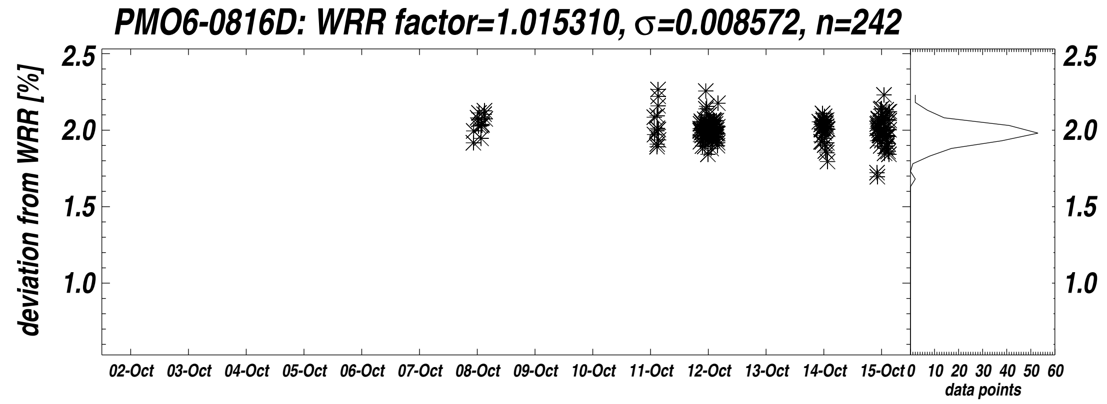
PMO6-0816D: WRR factor=1.015310, σ=0.008572, n=242
deviation from WRR [%]
2.5
2.0
1.5
1.0
02-Oct
03-Oct
04-Oct
05-Oct
06-Oct
07-Oct
08-Oct
09-Oct
10-Oct
11-Oct
12-Oct
13-Oct
14-Oct
15-Oct
0
10
20
30
40
50
60
data points

PMO6-5: WRR factor=0.999116, σ=0.000725, n=419

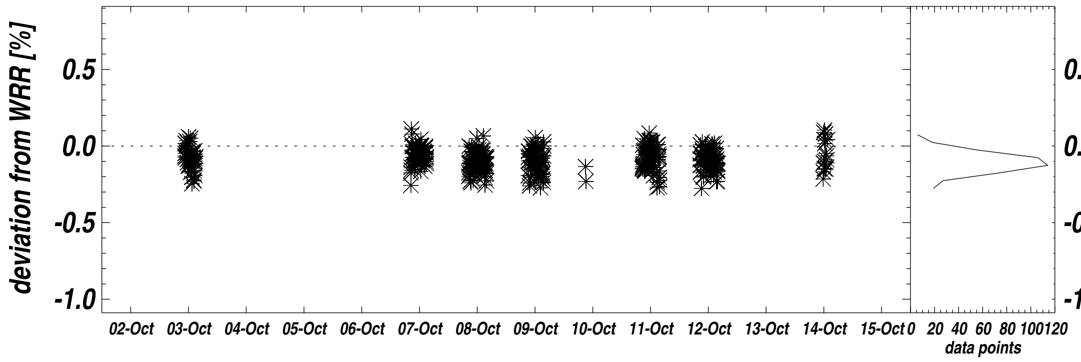

PMO6-81109: WRR factor=0.998577, σ=0.000708, n=426

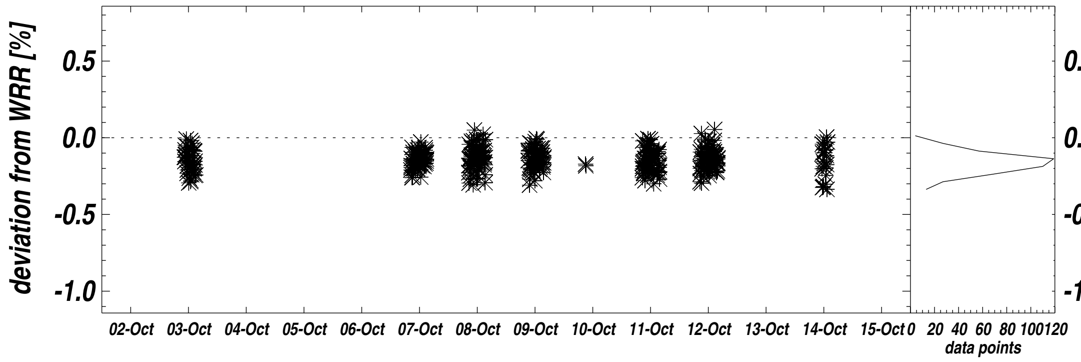

PMO6-850410: WRR factor=0.990890, σ=0.001145, n=434

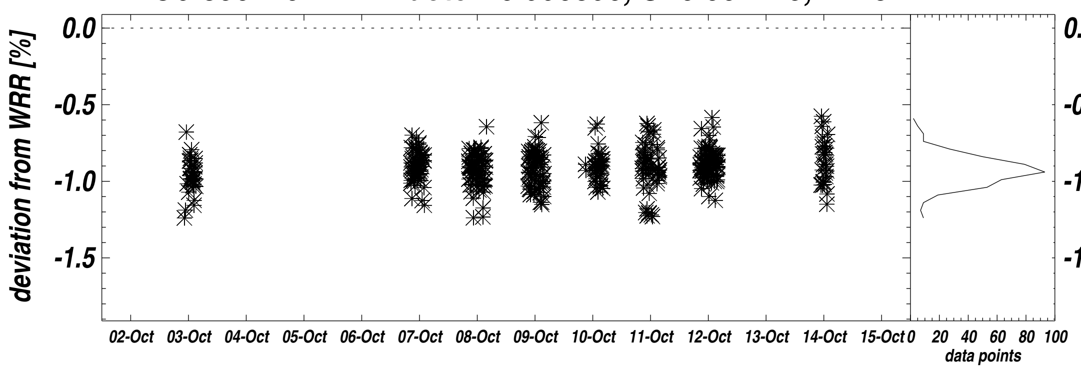

PMO6-911204: WRR factor=0.999711, σ=0.001049, n=437

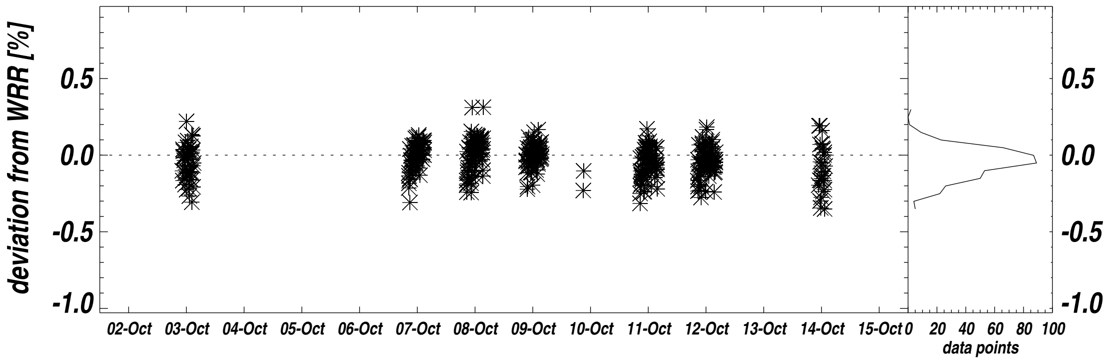

PMO6-CC0403: WRR factor=1.000160, σ=0.000732, n=425

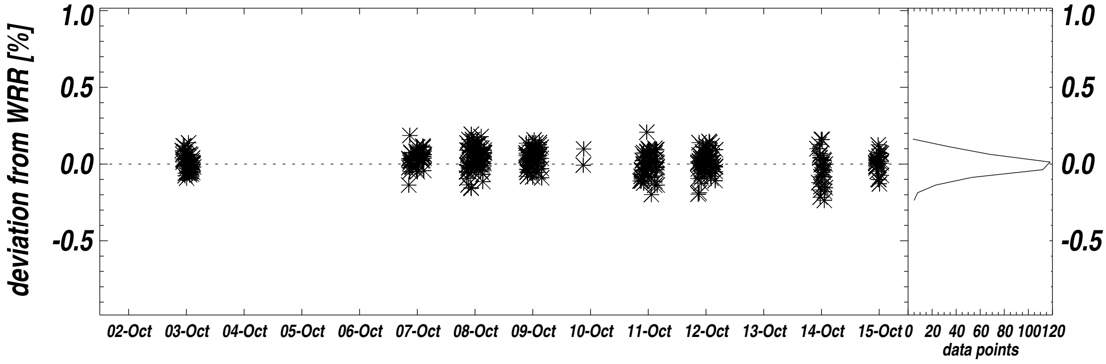

PMO6850406: WRR factor=1.000200, σ=0.000877, n=323

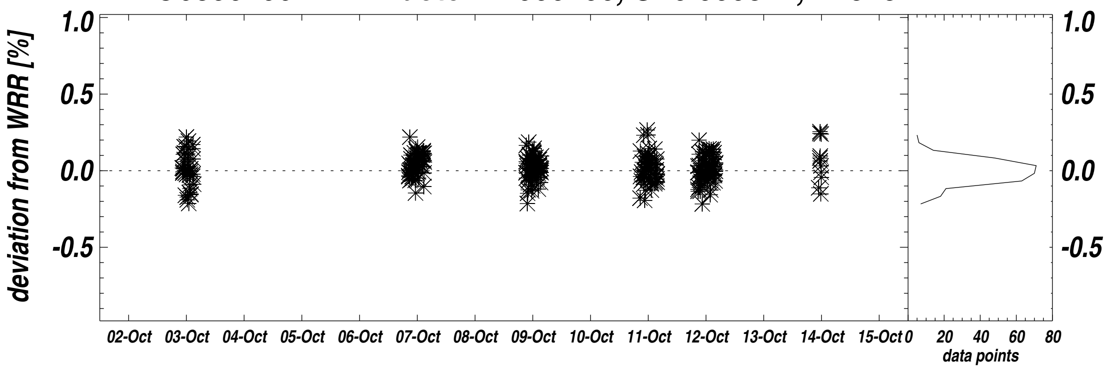

PMO8-P01: WRR factor=0.994812, σ=0.006959, n=497

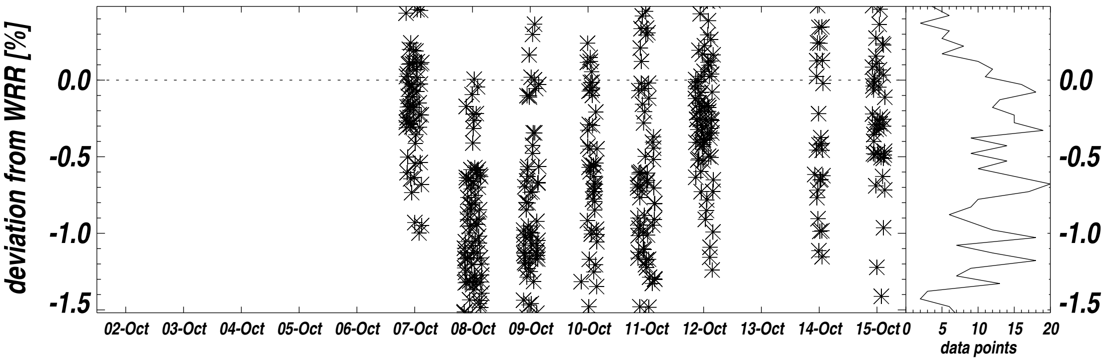

PMO811108: WRR factor=1.000660, σ=0.000727, n=417

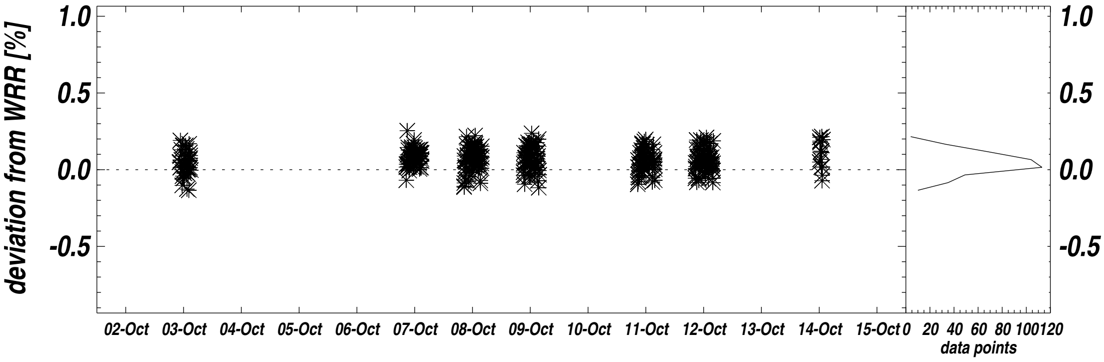

SIAR-1A: WRR factor=1.002400, σ=0.000997, n=440

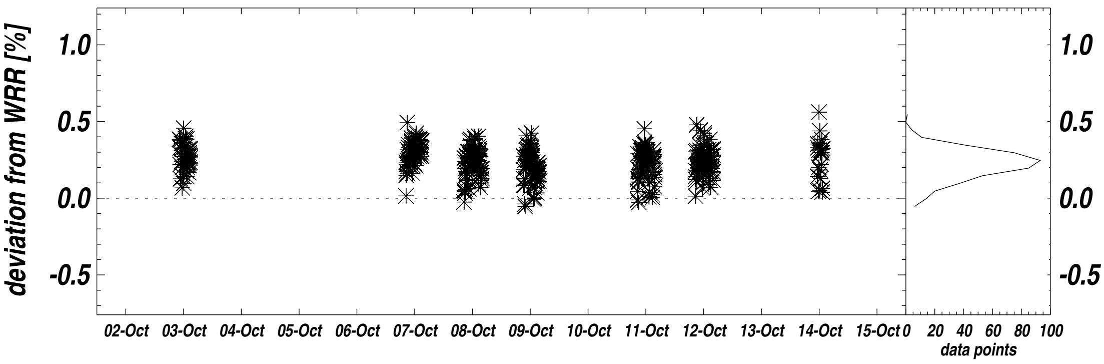

SIAR-2A: WRR factor=0.991696, σ=0.000732, n=495

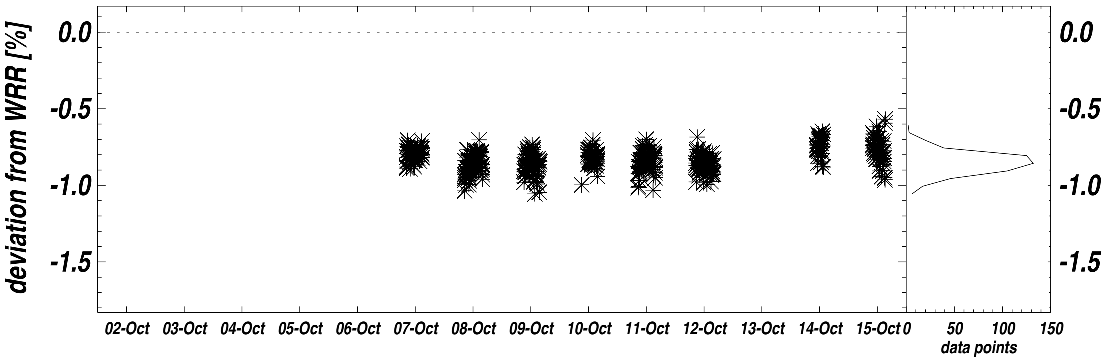

SIAR-2B: WRR factor=1.000290, σ=0.000668, n=427

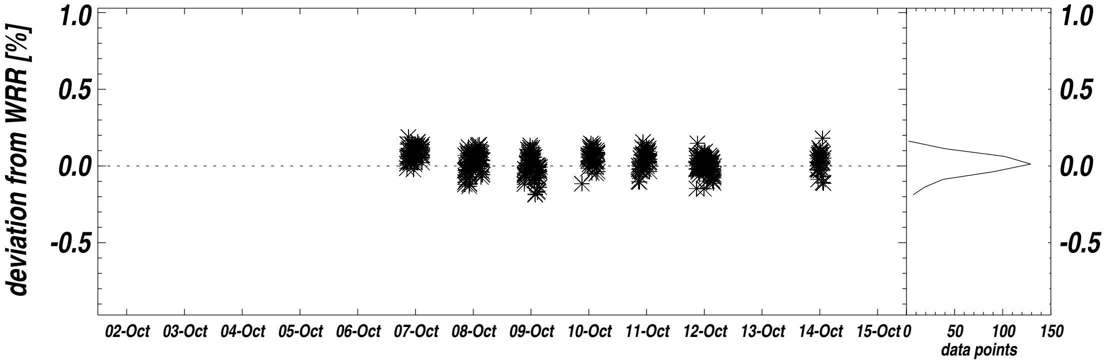

SIAR-2C: WRR factor=0.999839, σ=0.001125, n=441

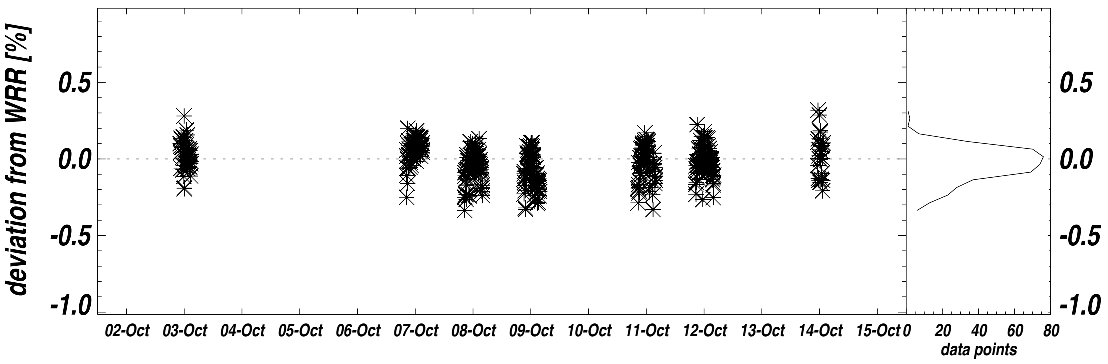

TIM-WITNESS: WRR factor=0.997303, σ=0.001417, n=278

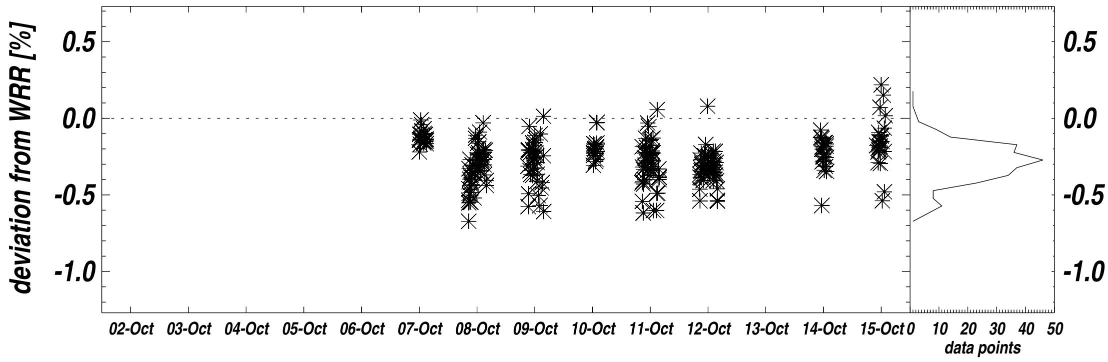

TMI67502: WRR factor=0.999294, σ=0.001024, n=454

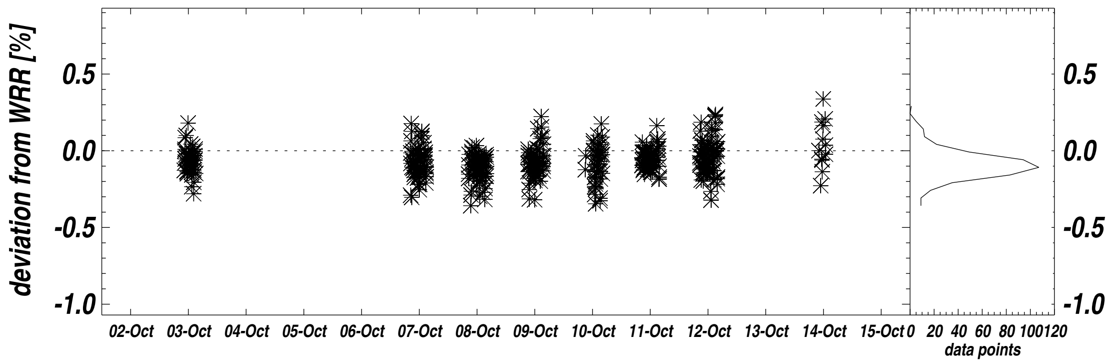

TMI67604: WRR factor=0.998226, σ=0.001341, n=440

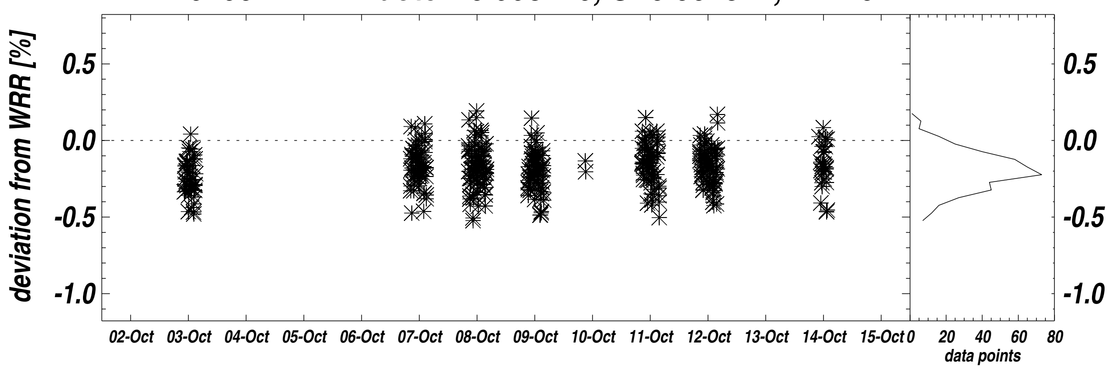

TMI68016: WRR factor=0.999858, σ=0.000758, n=462

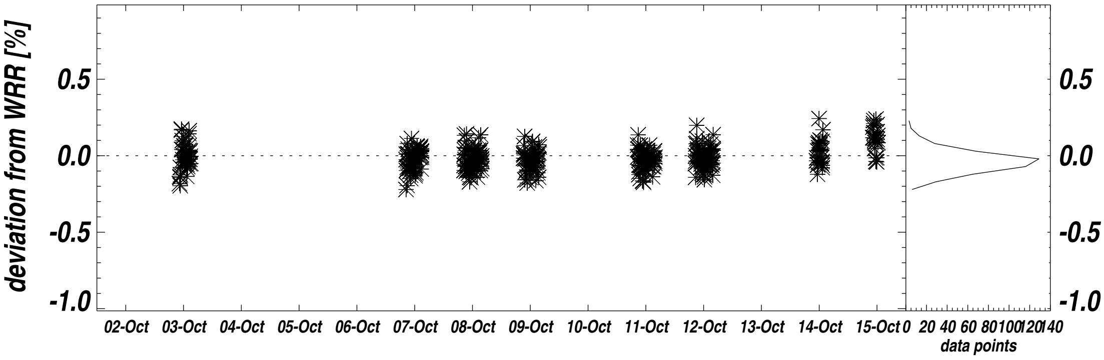

TMI68018: WRR factor=0.996804, σ=0.000642, n=415

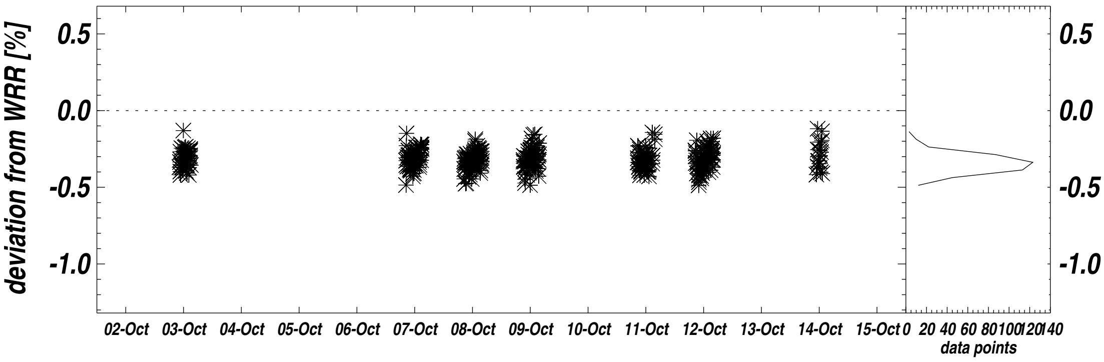

TMI68025: WRR factor=0.998613, σ=0.000920, n=436

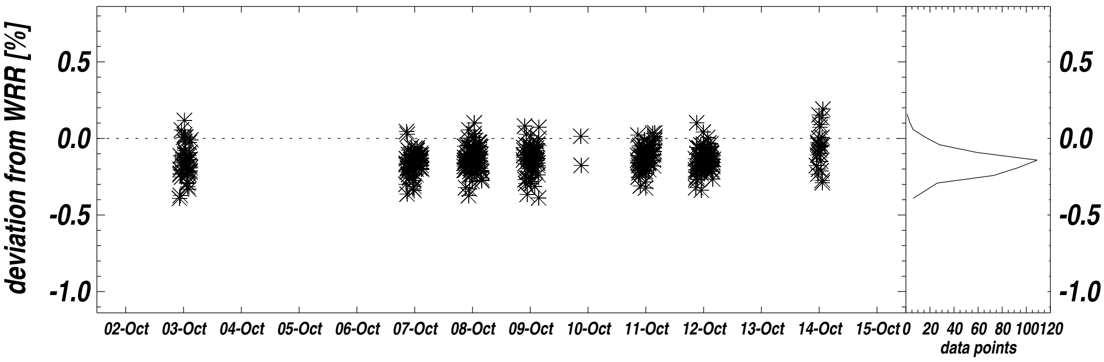

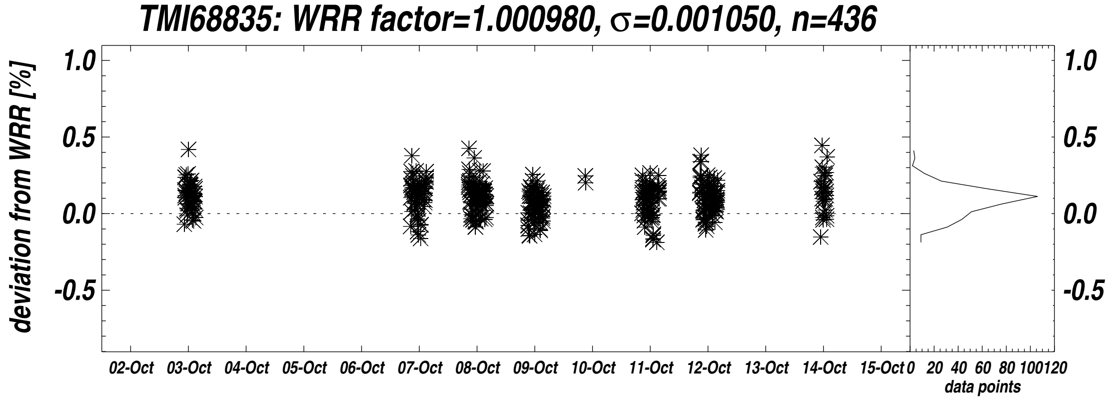
TMI68835: WRR factor=1.000980, σ=0.001050, n=436
deviation from WRR [%]
1.0
0.5
0.0
-0.5
02-Oct 03-Oct 04-Oct 05-Oct 06-Oct 07-Oct 08-Oct 09-Oct 10-Oct 11-Oct 12-Oct 13-Oct 14-Oct 15-Oct
0 20 40 60 80 100 120
data points

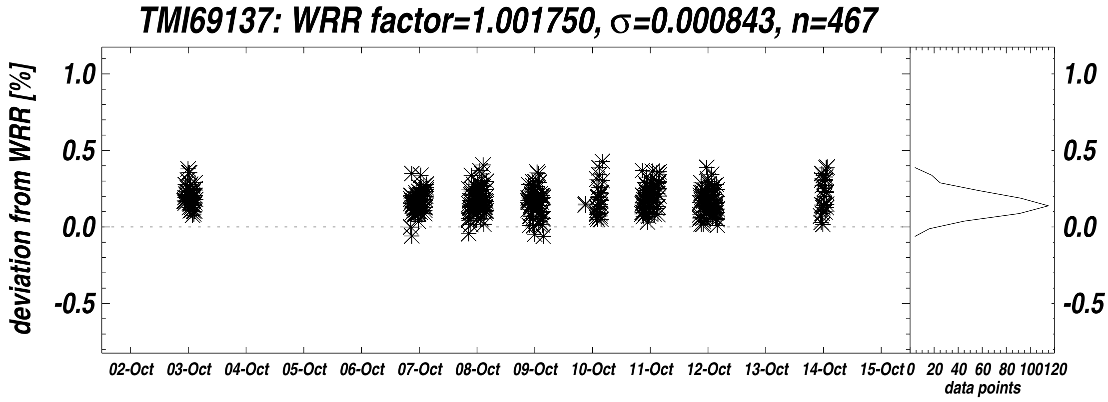
TMI69137: WRR factor=1.001750, σ=0.000843, n=467
deviation from WRR [%]
1.0
0.5
0.0
-0.5
02-Oct 03-Oct 04-Oct 05-Oct 06-Oct 07-Oct 08-Oct 09-Oct 10-Oct 11-Oct 12-Oct 13-Oct 14-Oct 15-Oct
0 20 40 60 80 100 120
data points

Chapter 4 Auxiliary Data

4.1 Direct and Diffuse Irradiance

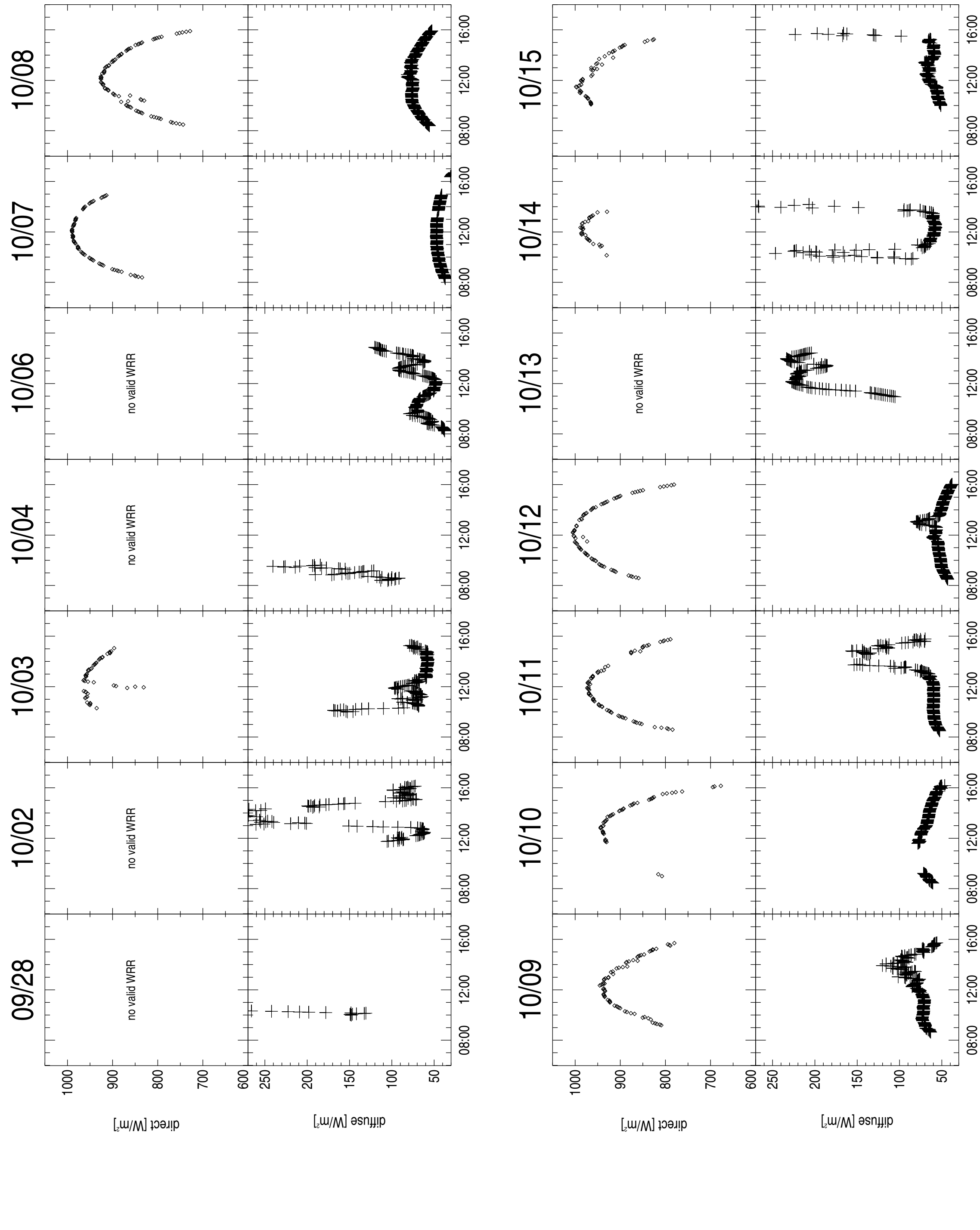

Direct (WRR) and diffuse irradiance (shaded K&Z CM22 S/N 020059).

4.2 Meteorological Data

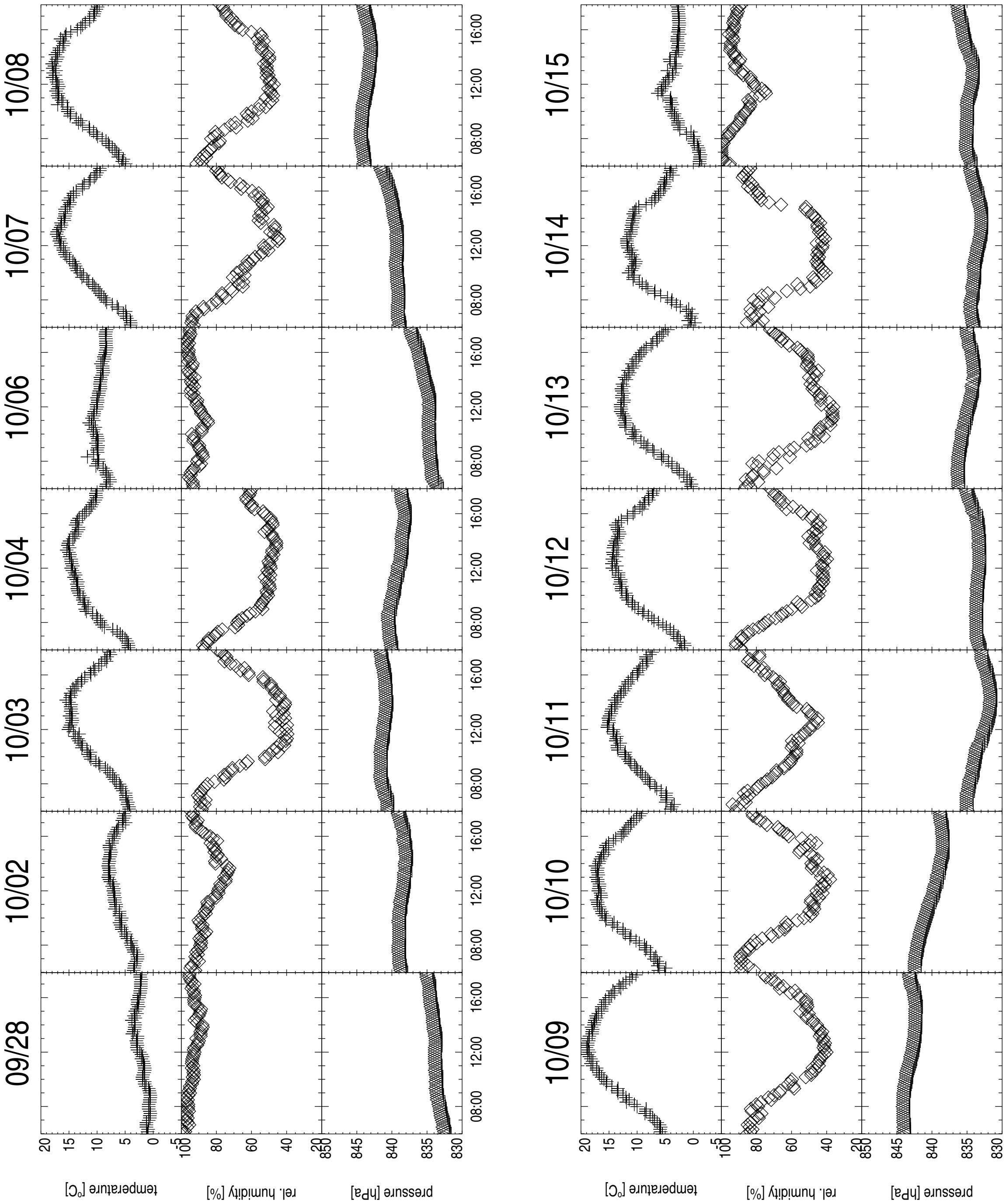

Meteorological parameters measured by the SwissMetNet Davos station of MeteoSwiss (adjacent to IPC-XI measuring field).

4.3 Airmass and Aerosol Optical Depth (AOD)

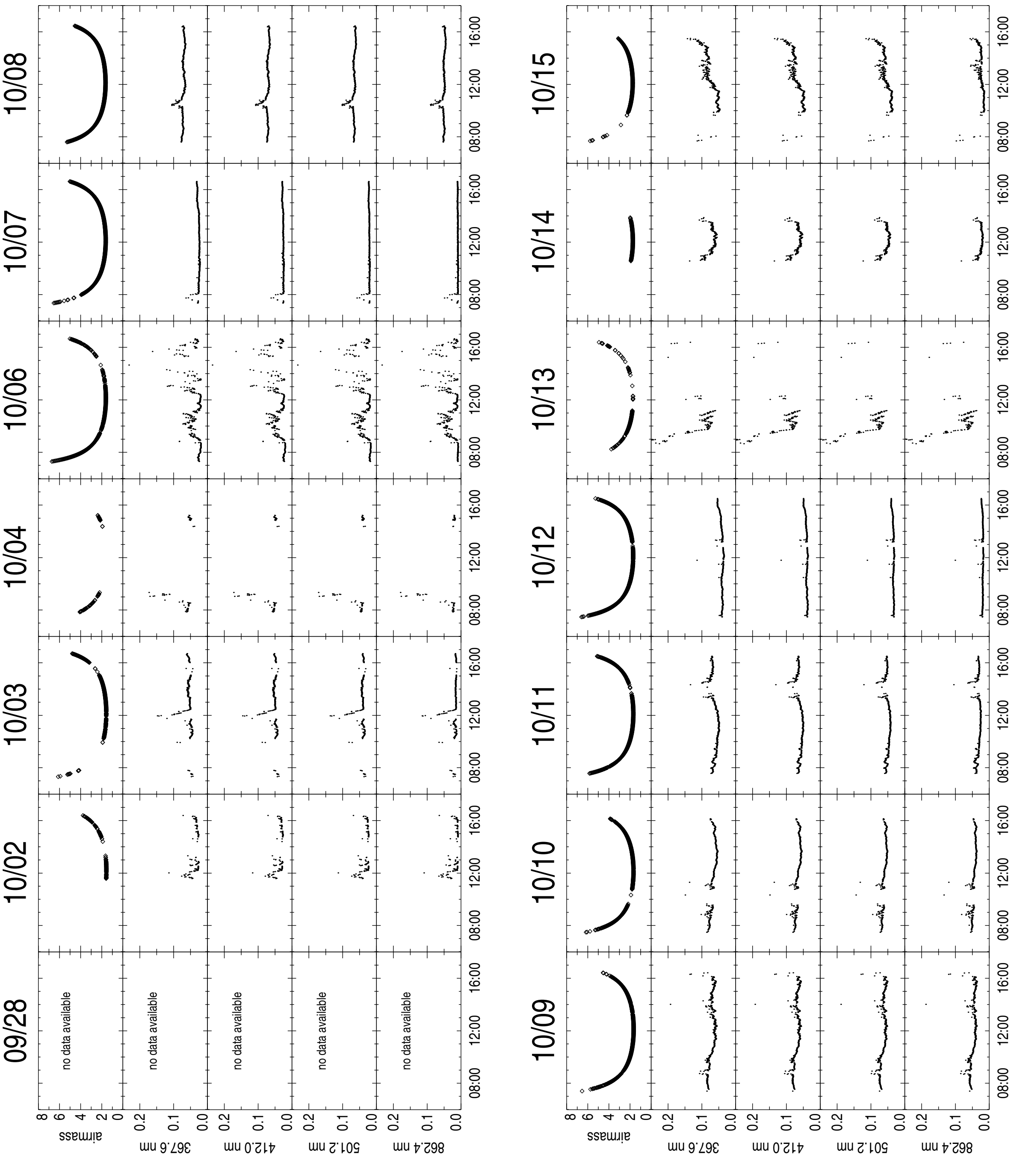

A four-channel Precision Filter Radiometer (PFR) was used to determine AOD.

4.4 Scattering parameters

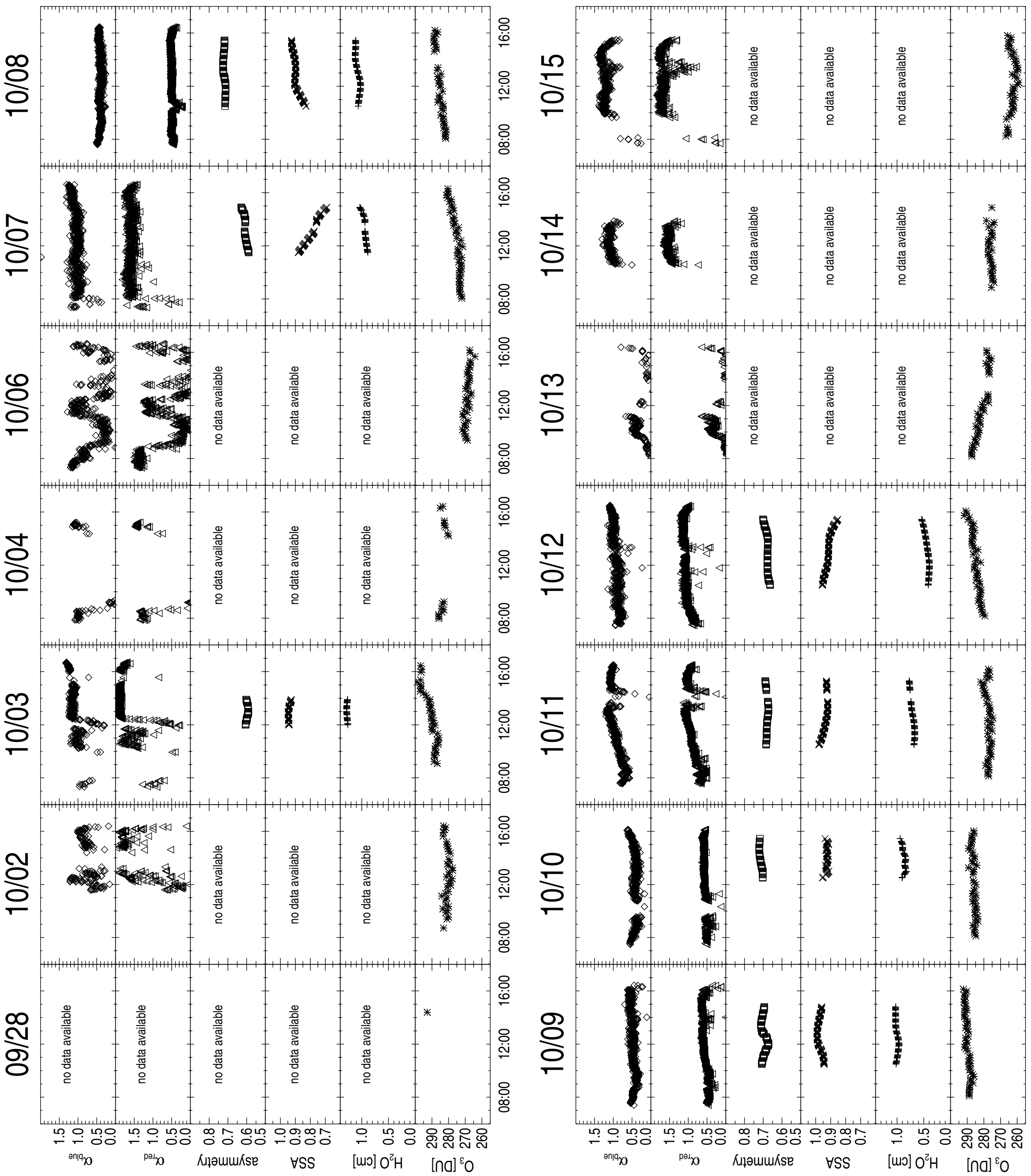

Ångström exponents (α) from PFR AOD data. Scattering asymmetry, single scattering albedo (SSA), and water column (H_2O) based on data from the AERONET Davos station. Ozon (O_3) measured by the WRC Brewer #163.

4.5 Scattering phase functions

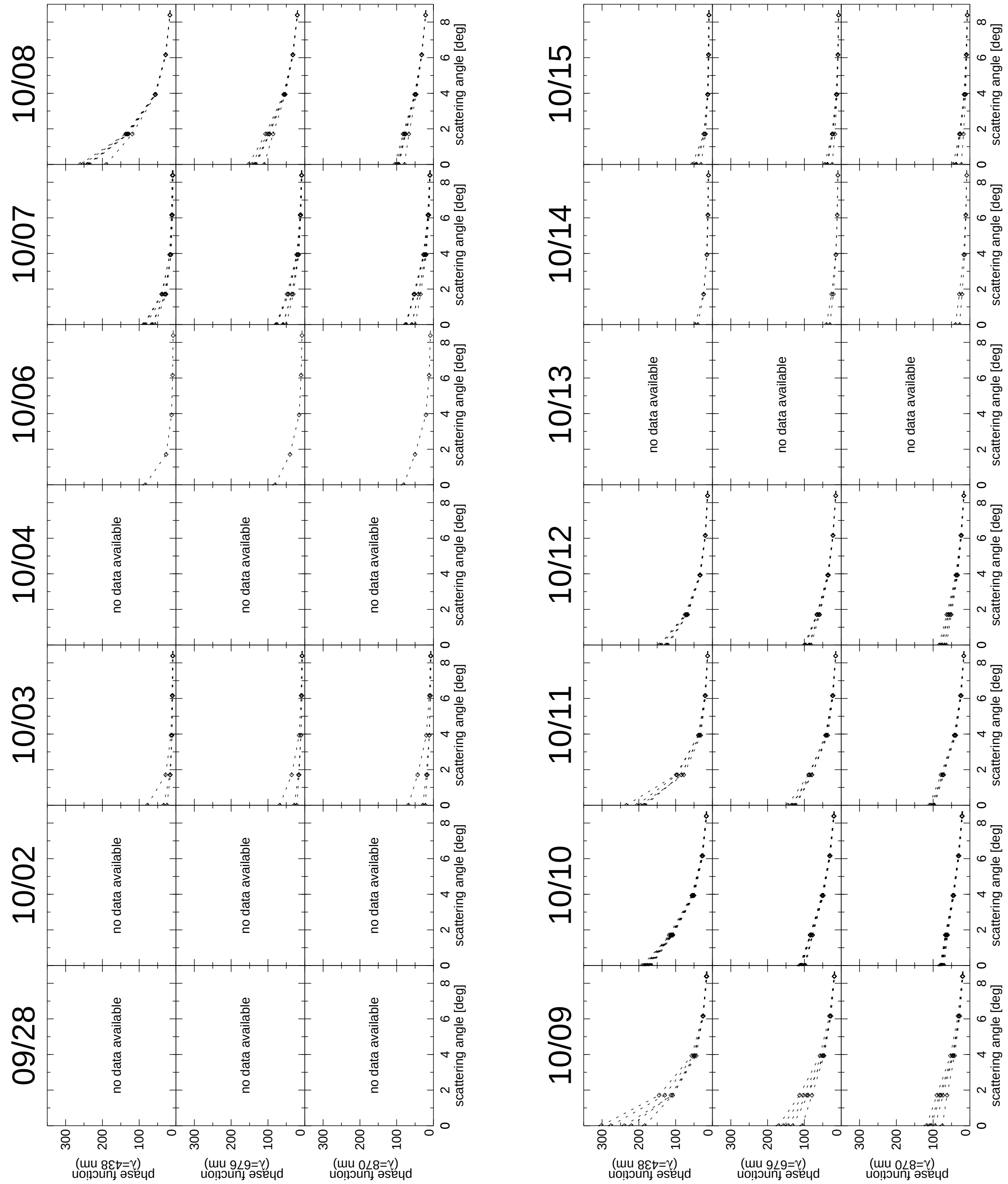

Scattering phase functions derived from AERONET inversions. These data were used to correct for the aureole effect in pyrheliometers with non-standard viewing geometries.

Chapter 5 Symposium

5.1 To Build and Share Knowledge

On cloudy, overcast, or rainy days when no measurements were possible the IPC-XI symposium and course on radiation measurement were held. Radiation experts from PMOD/WRC as well as may IPC-XI participants presented their work and/or national radiation infrastructure in order to share and build knowledge.

Over the three weeks, more than 30 talks and presentations were given, most of which are available for download on the IPC-XI ftp site ftp://ftp.pmodwrc.ch/stealth/ipc-xi.

5.2 Artistic Representation

During IPC-XI an art photographer was collecting photographic and video material for an art project in Bergen, Norway. Many of the photographs as well as a short movie are available on the IPC-XI ftp site ftp://ftp.pmodwrc.ch/stealth/ipc-xi/presentations/from ellen/.

Chapter 6 Supplementary Information

6.1 Addresses of Participants

Ihab Abboud
Environment Canada
Meteorological Service of Canada
P.O. Box 160
S0G 5E0 Wilcox, SK
Canada
phone: 001 306 546 6444
fax: 001 306 546 6400
e-mail: Ihab.Abboud@ec.gc.ca

Akihito Akiyama
EKO Instruments Europe B.V.
Middelstegracht 87H
2312 TT Leiden
The Netherlands
phone: 0031 71 5141 300

Anne Andersson
SP Technical Research Institut
Box 857
50115 Boras
Sweden
phone: 0046 33 165 403
fax: 0046 33 165 620
e-mail: anne.andersson@sp.se

Mohamed Badrane
Meteo Maroc
51 Residence Aouzal 3
Avenue Ain Tawajtate
Bourgone Casablanca
Maroc
phone: 0021 266 362 94 98
e-mail: mohamed.badrane@hotmail.com

Sami Bali
R.M.I.
Ringlaan 3 Avenue Circulaire
1180 Uccle-Brussels
Belgium
phone: 0032 2 373 06 26
fax: 0032 2 374 67 88
e-mail: Sami.Bali@oma.be

Alexander Baskis
Israel Meteorological Service
P.O. Box 25
50250 Bet-Dagan
Israel
phone: 00972 3 9682144
fax: 00972 3 9604854
e-mail: balex@ims.gov.il

Klaus Behrens
Deutscher Wetterdienst
Met. Obs. Lindenberg
Am Observatorium 12
15848 Tauche-OT Lindenberg
Germany
phone: 0049 33 677 601 51
fax: 0049 33 677 602 80
e-mail: klaus.behrens@dwd.de

Francesco J. Bernal Garcia
IDEAM
Carrera 10 20-30
Bogata D.C.
Colombia
phone: 0057 3002 130286
e-mail: frabernal@ideam.gov.co

Barbara Bogdanska
Institute of Meteorology
and Water Management
61, Podlesna Str.
448147 Warsaw
Poland
phone: 0048 22 569 41 78
fax: 0048 22 569 43 25
e-mail: Barbara.Bogdanska@imgw.pl

Gerardo Carbajal Benítez
Servicio Meteorologico Naciona
25 de Mayo 658
1427 Buenos Aires
Argentina
phone: 0054 115 1676767
e-mail: gcarbajal@smn.gov.ar

Thomas Carlund
Swedish Meteorological and
Hydrological Institut SMHI
Filkborgsvägen 1
60176 Norrköping
Sweden
phone: 0046 11 495 8229
e-mail: thomas.carlund@smhi.se

André Chevalier
RMI
Department of Aerology
Ringlaan 3 Avenue Circulaire
1180 Uccle-Brussels
Belgium
phone: 0032 2 373 0602
fax: 0032 2 374 6788
e-mail: a.chevalier@oma.be

Miroslav Chmelik
Slovak Hydrometeorological Institute
Jeseniova 17
833 15 Bratislava
Slovakia
phone: 00421 5 2773 1097
e-mail: miroslav.chmelik@shmu.sk

Alessandra Colli
Institute for Renewable Energy
EURAC research
Viale Druso 1
39100 Bolzano
Italy
phone: 0039 0471 055 630
fax: 0039 0471 055 699
e-mail: alessandra.colli@eurac.edu

Frederick Denn
NASA Langley
1 Enterprise Parkway
Hampton VA, 23693
USA
phone: 001 757 951 1636
fax: 001 757 951 1900
e-mail: frederick.m.denn@nasa.gov

Steven Dewitte
RMI
Department of Aerology
Ringlaan 3 Avenue Circulaire
1180 Bruxelles
Belgium
phone: 0032 2 373 06 24
fax: 0032 2 3746788
e-mail: Steven.Dewitte@oma.be

Vivien S. Esquivel
Philippine Atmospheric, Geophys.
and Astron. Services
PAGASA
Quezon City
Philippines
phone: 0063 927 5509
fax: 0063 373 3420
e-mail: vivien.esquivel@yahoo.com

Patrick Fishwick
Met Office
Fitzroy Road
Exeter, EX1 3PB
United Kingdom
phone: 0044 139 288 6289
fax: 0044 13 9288 5681
e-mail: patrick.fishwick@metoffice.gov.uk

Bruce Forgan
Bureau of Meteorology
Atmosphere Watch Section, OEB
700 Collins St.
Docklands 3008
Australia
phone: 0061 39669 4111
fax: 0061 39669 4736
e-mail: b.forgan@bom.gov.au

Luis Gonzalez
R.M.I.
Ringlaan 3 Avenue Circulaire
1180 Uccle-Brussels
Belgium

Luke Green
Met Office
Fitzroy Road
Exeter, EX1 3PB
United Kingdom
phone: 0044 139 288 6283
fax: 0044 13 9288 5681
e-mail: luke.green@metoffice.gov.uk

David Halliwell
BSRN Observatory Site Scientist
Environment Canada
100 R-Y Trail, RM of Bratt's Lake
Wilcox, SK, S0G 5E0
Canada
phone: 001 306 352 3818
fax: 001 306 546 6400
e-mail: david.halliwell@ec.gc.ca

Karl Heuermann
LASP
1234 Innovation Drive
Boulder, CO 80303
USA

John R. Hickey
The Eppley Laboratory Inc.
P.O. Box 419
02840-0419 Newport, Rhode Island
USA
phone: 001 401 847 1020
fax: 001 401 847 1031
e-mail: johnh@eppleylab.com

Gary Hodges
University of Colorado
325 Broadway Street
80501 Boulder
United States
e-mail: gary.hodges@noaa.gov

Kees Hoogendijk
EKO Instruments Europe B.V.
Middelstegracht 87H
2312 TT Leiden
The Netherlands
phone: 0031 71 5141 300
e-mail: hoogendijk@eko-eu.com

Osamu Ijima
Japan Meteorological Agency
Radiation Section
1-3-4 Otemachi, Chiyoda-ku
Tokyo 100-8122
Japan
phone: 0081 3 3212 8341
fax: 0081 3 3211 4640
e-mail: ijima@met.kishou.go.jp

Somchit Janjai
Solar Energy Research Lab.
Silpakorn University
Muang - Nakhon Pathom 73000
Thailand

Ain Kallis
Estonian Meteor. & Hydrological Institute
Toompuiestee 24
10149 Tallinn
Estonia
phone: 00372 7 410 136
fax: 00372 7 410205
e-mail: ain.kallis@gmail.com

Jan-Erik Karlsson
Swedish Meteorological and
Hydrological Institut SMHI
Filkborgsvägen 1
60176 Norrköping
Sweden
phone: 0046 11 158 381
fax: 0046 11 151 707

Thomas Kirk
The Eppley Laboratory Inc.
P.O. Box 419
02840-0419 Newport, Rhode Island
United States
phone: 001 401 847 1020
e-mail: info@eppleylab.com

Wouter Knap
KNMI
P.O. Box 201
3730 AE De Bilt
The Netherlands
phone: 0031 30 2206 469
fax: 0031 30 221 04 07
e-mail: knap@knmi.nl

Jorgen Konings
Hukseflux Thermal Sensors
Electronikaweg 25
2628 XG Delft
The Netherlands

Greg Kopp
LASP
1234 Innovation Drive
Boulder, CO 80303
USA
phone: 001 303 735 0934
e-mail: Greg.Kopp@LASP.Colorado.edu

Stefan Källberg
SP Technical Research Institut of Sweden
Box 857
50115 Borås
Sweden
phone: 0046 33 165 626
fax: 0046 33 165 620
e-mail: stefan.kallberg@sp.se

Alexander Los
ECO INSTRUMENTS Europe B.V.
Direktor
Middelstegracht 87H
2312 TT Leiden
The Netherlands
phone: 0031 71 5141 300
fax: 0031 71 5126 222
e-mail: alexander.los@eko-eu.com

Chang Lou
China Meteorological Administration
National Center for Meteo. Met.
No.46, Zhongguancun Nandajie
100081 Beijing
China
phone: 0086 0571 86783487
fax: 0086 0571 86783487
e-mail: luochang@hzcnc.com

Meena Lysko
CSIR
PO Box 395
Pretoria 1, Gauteng
South Africa
e-mail: mlysko@csir.co.za

Martin Mair
ZAMG
Hohe Warte 38
1190 Wien
Österreich
phone: 0043 1360 262 706
fax: 0043 3602 627 20
e-mail: martin.mair@zamg.ac.at

Pierre Malcorps
IRMB
3 Avenue Circulaire
1180 Brussels
Belgium
phone: 0032 2 373 0601
fax: 0032 2 374 6788

Artur Maria Mandlate
National Inst. of Meteo Mozambique
Rua Mukumbura 164 maputo
Maputo 256
Mozambique
phone: 00258 824 277493
fax: 00258 214 91150
e-mail: artur_m@inam.gov.mz

Itsara Masiri
Solar Energy Research Lab.
Silpakorn University
Muang - Nakhon Pathom 73000
Thailand
phone: 0066 848 841 765
fax: 0066 34 271189
e-mail: itsara@su.ac.th

Joop Mes
Kipp & Zonen
Delftechpark 36
2628 XH Delft
The Netherlands
phone: 0031 15 2755 210
fax: 0031 15 2620 351
e-mail: joop.mes@kippzonen.com

Joseph Michalsky
NOAA/OAR
325 Broadway R/GMD
Boulder, CO 80305-3337
USA
phone: 001 303 497 6360
fax: 001 303 497 6546
e-mail: joseph.michalsky@noaa.gov

Darius Mikalajunas
Lithuanian Hydromet. Service
Rudnios Str. 6
2600 Vilnius
Lithuania
phone: 00370 6 030 9478
fax: 00370 5 272 8874
e-mail: d.mikalajunas@meteo.lt

Michael Milner
Bureau Of Meteorology
700 Collins Street
Docklands 3008
Australia
phone: 0061 39669 4122
fax: 0061 39669 4122
e-mail: m.milner@bom.gov.au

Jean-Philippe Morel
Météo-France
Chef du Centre Radiomètrique
785 Chemin de l'Hermitage
84200 Carpentras - Serres
France
phone: 0033 490 636 967
fax: 0033 490 636 959
e-mail: jean-philippe.morel@meteo.fr

Svetlana Morozova
FGUP VNIIOFI
Ozernaya Str., 46
119361 Moscow
Russia
phone: 007 095 437 3700
fax: 007 095 437 3700
e-mail: morozova-m4@vniiofi.ru

Pedro Mostraj
Dirección Meteorológica de Chile
Av. Diego Portales 3450
Estacion Central
Santiago
Chile
phone: 0056 2 4364549
fax: 0056 2 4364549
e-mail: pmostraj@meteochile.cl

Sophie Mulaudzi
CSIR
P.O. Box 395
Pretoria 1, Gauteng
South Africa
e-mail: Sophie.Mulaudzi@univen.ac.za

Kolawole Salimon Muyiolu
Nigerian Meteorological Agency
33 Pope John Paul Street
Maitama District
PMB 0615 Abuja
Nigeria
phone: 00234 805 3059787
fax: 00234 941 30710
e-mail: muyiolu_kolawole@yahoo.com

Zoltán Nagy
Hungarian Meteorological Service
Measurement Techniques and
Methodology Division
1181 Budapest
Hungary
phone: 0036 1 3464 855
fax: 0036 1 3464 849
e-mail: nagy.z@met.hu

Erik Naranen
Atlas Weathering/DSET Labs
45601 North 47th Ave.
85087 Phoenix, Arizona
USA
phone: 001 623 201 1032
fax: 001 623 465 9409
e-mail: enaranen@atlas-mts.com

Donald W. Nelson
NOAA/CMDL
R/CMDL1
325 Broadway St.
Boulder, CO 80305
USA
phone: 001 303 497 6662
fax: 001 303 497 5590
e-mail: donald.w.nelson@noaa.gov

Ormanda Niebergall
Environment Canada
P.O Box 160
S0G 5E0 Wilcox, Saskatchewan
Canada
phone: 001 306 352 3818
fax: 001 306 546 6400
e-mail: Ormanda.Niebergall@ec.gc.ca

Ifeanyi Daniel Nnodu
Nigerian Meteorological Agency
33 Pope John Paul Street
Maitama District
PMB 0615 Abuja
Nigeria
phone: 00234 803 3339282
fax: 00234 941 30710
e-mail: idnnodu@yahoo.com

Yaseen Odan
Sudan Meteorological Authority
P.O.Box 574 Khartoum Sudan
1111 Khartoum
Sudan
phone: 00249 0 9122 20246
fax: 00249 1 8377 1693
e-mail: yaseen@ersad.gov.sd

Jan Alse Olseth
University of Bergen
Geophysical Institute
5007 Bergen
Norway
phone: 0047 55 582 892
fax: 0047 97 577 829
e-mail: jan.asle.olseth@gfi.uib.no

Cristian Oprea
National Institute of Meteorology
and Hydrology
Sos. Bucuresti-Ploiesti 97
13686 Bucharest
Romania
phone: 0040 21 316 31 16
fax: 0040 21 316 88 62
e-mail: relatii@meteo.inmh.ro

Bouziane Ouchene
Météorologie Algérie
Boite postale 31
11000 El hofra, Tamanrasset
Algeria
phone: 00213 2934 4673
fax: 00213 2934 4226
e-mail: b_ouchene@yahoo.fr

Alexander Pavlov
Voeikov MGO
7, Karbyshev st.
194021 St. Petersburg
Russia
phone: 007 812 297 4390
fax: 007 812 247 8661
e-mail: etalon@main.mgo.rssi.ru

Maria Pavlovich
VNIIOFI
46, Ozernaya Str.
Moscow 119361
Russia
phone: 007 495 437 2992
fax: 007 495 437 3700
e-mail: pavlovitch-m4@vniiofi.ru

Vladimir Pavlovich
VNIIOFI
46, Ozernaya Str.
Moscow 119361
Russia
phone: 007 495 437 2992
fax: 007 495 437 2992
e-mail: VLP.47@mail.ru

Jiri Pokorny
Czech Hydromet.I Institute
Husova 456
50008 Hradec Kralove
Czech Republic
phone: 00420 495 260 352
e-mail: jiri.pokorny@ehmi.cz

Krunoslav Premec
Meteorological Service
Gric 3
10000 Zagreb
Croatia
phone: 00385 1 4565 607
fax: 00385 1 4852 036
e-mail: krunoslav.premec@cirus.dhz.hr

Jimei Quan
China Meteorological Administration
National Center for Meteo. Met.
No.46, Zhongguancun Nandajie
100081 Beijing
China
phone: 0086 0106 8406936
fax: 0086 0106 68406936
e-mail: quanjm@cma.gov.cn

Ibrahim Reda
Nat. Renewable Energy Laborat.
1617 Cole Boulevard
80401 Golden CO
USA
phone: 001 303 384 6385
fax: 001 303 384 6391
e-mail: ibrahim.reda@nrel.gov

David Riveros Rosas
Instituto de Geofisica
Cd. Universitaria # 3000
4510 Mexico - Distrito Federal
Mexico
e-mail: driveros@geofisica.unam.mx

Israel Rodriguez Outon
CIEMAT
Av. Complutense 22
28040 Madrid
Spain
phone: 0034 9 1496 2509
fax: 0034 9 1346 6037
e-mail: israel.rodriguez@ciemat.es

Ellen Røed
Ovre Stadionveien 82
5161 Laksevag
Norway
phone: 0047 97 549 761
e-mail: ellen.roed@khib.no

Isabelle Rüedi
WMO
7bis, avenue de la Paix
Case Postale 2300
1211 Geneve 2
Switzerland
phone: 0041 22 730 8278
fax: 0041 22 730 8021
e-mail: iruedi@wmo.int

Tony Sample
European Commission DG JRC ISPRA
Institute for Env. and Sustainability
TP 450, Via Fermi 1
21020 Ispra Varese
Italy
phone: 0039 0332 789 062
fax: 0039 0332 789268
e-mail: tony.sample@jrc.it

Rajendra Kumar Sharma
Central Radiation Laboratory
Instrument Division
India Meteorological Department
411005 Pune, Maharashtra
India
phone: 0091 20 25893415
fax: 0091 20 25882353
e-mail: rajendra_radiation@yahoo.com

Peter Sira
Kenya Meteorological Dept.
P.O.Box 30259-00100
100 Nairobi
Kenya
phone: 00254 722 845907
fax: 00254 203 876955
e-mail: mungaipn@engineer.com

Ilja Staupe
Kipp & Zonen
Delftechpark 36
2628 XG Delft
The Netherlands
phone: 0031 15 2755 210
fax: 0031 15 2620 351
e-mail: ilja.staupe@kippzonen.com

Thomas Stoffel
Nat. Renewable Energy Laboratory
Mail Stop 1612
1617 Cole Blvd.
Golden, CO 80401-3393
USA
phone: 001 303 384 6395
fax: 001 303 384 6391
e-mail: thomas.stoffel@nrel.gov

Watcharapol Subwat
Thai Meteorological Department
4353 Sukhumvit Rd.
10260 Bangkok Banga District
Thailand

Szilvia Varga-Fogarasi
Hungarian Met. Service
Gilice tér 39.
1181 Budapest
Hungary
phone: 0036 1 3464 853
fax: 0036 1 3464 849
e-mail: fogarasi.sz@met.hu

Cor van Oort
KNMI
PO Box 201
3730 AE De Bilt
The Netherlands
phone: 0031 30 2206 417
fax: 0031 30 2210 407
e-mail: oortvan@knmi.nl

Kees van den Bos
Hukseflux Thermal Sensors
Electronikaweg 25
2628 XH Delft
The Netherlands
phone: 0031 15 2142 669
fax: 0031 15 2574 949
e-mail: info@hukseflux.com

Esequiel Villegas Paredes
SENAMHI-PERU
Jr. Cahuide 785, Jesus Maria
Lima 11
Peru
phone: 0051 1 6141414
fax: 00511 471 7287
e-mail: evillegas@senamhi.gob.pe

Yu Peng Wang
CIOMP
Dong Nanhu Road 3888
No.46, Zhongguancun Nandajie
130033 Changchun, Jilin
China
phone: 0086 0431 86708089
fax: 0086 0431 86176883
e-mail: wangyu_peng@sina.com

Rungrat Wattan
Solar Energy Research Lab.
Silpakorn University
6 Rajamankha Nai Road
Muang - Nakhon Pathom 73000
Thailand
phone: 0066 342 707 61
fax: 0066 34 271189
e-mail: rungrat@su.ac.th

Craig Webb
ACRF
309600 EW28
74630 Billings, Oklahoma
USA
phone: 001 580 388 4053
fax: 001 580 388 4052
e-mail: craigw@ops.sgp.arm.gov

Jim Wendell
NOAA/ESRL/GMD
325 Broadway
Boulder, CO 80305
USA
phone: 001 303 497 6994
e-mail: jim.wendell@noaa.gov

Ed Worrell
EKO Instruments Europe B.V.
Middelstegracht 87H
2312 TT Leiden
The Netherlands
phone: 0031 71 5141 300
fax: 0031 71 5126 222
e-mail: ed.worrell@eko-eu.com

Yun Yang
China Meteorological Administration
National Center for Meteo. Met.
No.46, Zhongguancun Nandajie
100081 Beijing
China
phone: 0086 1068 406936
fax: 0086 1068 400936
e-mail: yyaoc@cma.gov.cn

Dong Jun Yang
CIOMP
Dong Nanhu Road 3888
No.46, Zhongguancun Nandajie
130033 Changchun, Jilin
China
phone: 0086 0431 86708089
fax: 086-0431-86176883
e-mail: djyang0827@163.com

Xin Ye
CIOMP
Dong Nanhu Road 3888
No.46, Zhongguancun Nandajie
130033 Changchun, Jilin
China
phone: 0086 0431 86708089
fax: 0086 0431 86176883
e-mail: newsyears@ustc.edu

Willem J. Zaaiman
European Commission-DG JRC
Via Fermi, 2749
21020 Ispra Varese
Italy
phone: 0039 0332 785 750
fax: 0039 0332 789 268
e-mail: willem.zaaiman@jrc.ec.europa.eu